TRACE ELEMENTS IN THREE SOIL MONOSEQUENCES AND IRON-MANGANESE CONCRETIONS FROM WESTLAND AND CANTERBURY NEW ZEALAND.

A thesis presented in partial fulfilment of the requirements for the Degree

of

Doctor of Philosophy in Chemistry

by

Bernard S.W. Dawson

University of Canterbury

1982

ABSTRACT

This work is a study of the first row transition metals Ti, V, Cr, Mn, Fe, Co, Ni, Cu and Zn in three soil monosequences and iron-manganese concretions. Three wet chemical decomposition techniques, to be used for the dissolution of soil samples, were assessed. Analysis of the resulting solutions for the transition metals, except Ti, by atomic absorption spectroscopy was compared with the analysis of solid samples by X-ray fluorescence. The transition elements were also determined in three International Rock Standards, and spiking experiments were used to determine recovery of these elements after sample decomposition and analysis.

The three monosequences studied were selected in order to examine separately, time, the biotic factor and topography as soil forming factors as soil development proceeded. The soils studied were from the Reefton area and Bealy catchment of the South Island of New Zealand. Data for the chronosequence soils were presented on both a mass per mass and mass per volume basis to facilitate a meaningful comparison of the trace elements, in soils of widely varying properties.

Both chemical and mineralogical studies were carried out on iron-manganese concretions from an Irwell pasture in Canterbury, New Zealand. This data, together with data obtained from electron microprobe analyses, was used to demonstrate trace element enrichment in the concretions. It was found that Co and Zn were the trace elements most strongly enriched, and that generally, the transition metals were enriched more strongly in the Mn phases of the concretions than in the Fe

phases. An analysis of possible explanations for this leads to the suggestion that sorption of trace elements on to Mn and Fe oxides is probably the major factor.

Dedicated to my parents

ACKNOWLEDGEMENTS

I wish to sincerely thank my supervisor, Dr J.E. Fergusson, for his help and guidance. Also I thank Dr A.S. Campbell and Mr A.W. Young, of the Soil Science Department of Lincoln College for their assistance in the soil-related aspects of this work. I would also like to thank the technical staff of the Chemistry Department for assistance given, and the Mechanical Engineering Department for use of their electron microprobe which was made easier with the enthusiastic support of the electron microprobe technician, Mr M.J. Flaws. I am also very appreciative for the assistance of various members of the Geology Department, especially Mr Ted Hoggarth, Mr N. Newman and Dr S.D. Weaver.

My thanks are due to Mrs C. Haughey for her competent typing of the manuscript and my wife who has been extraordinarily supportive during the course of this work.

I acknowledge finally the support given to me, by the University of Canterbury , in the form of a Teaching Fellowship.

CONTENTS

PART ONE

LIST OF TABLES

LIST OF FIGURES

PART ONE

CHAPTER 1

INTRODUCTION

Of the many elements necessary for plant growth, only a few are required in large quantities. Deficiencies of the elements required in small amounts (trace elements present at the $\mu g\ g^{-1}$ level) are often found in certain crops or some types of soil. However, more intensive cropping practices generally can result in a change in trace element availability to plants, and a faster depletion of elements not added to the soils in fertilizers[1]. As the demand for higher yields increases, and the plant's need for major elements is more effectively satisfied, trace elements are more likely to become a limiting factor in plant growth.

Many trace elements have been classified as essential trace elements required by plants for normal and healthy growth, and include the transition metals Mn, Fe, Cu and Zn, as well as B and Mo[2]. Cobalt is also reported to be essential for leguminous plants[3], while chlorine is needed by plants in very low concentrations[4]. Mammals need all of these elements, except possibly B, although ruminants have a much higher demand for Co than do plants. Mammals also require I, and some species at least, require trace amounts of Se and Cr[2].

In Table 1.1 the trace elements essential for healthy plant growth are shown. The present work involved a study of the first row transition metals.

TABLE 1.1 Trace Elements Essential for Plants

Mo	Mn	Fe	Co	Cu	Zn	B	Cl

The trace elements essential to plants must be present in the soil solution in a form which plants can use, and at suitable concentrations for plant growth. Essential trace elements are usually involved in specific processes related to plant growth, for instance Mo and Co are thought to be involved in nitrogen fixation[3], Zn is thought to be involved in the formation of growth hormones in plants[5], and Cu with the respiration process[6].

If the concentration of essential trace elements is too low, deficiency results, while if levels are too high, the elements can be toxic to plants. For example, soils derived from ultrabasic rocks, such as serpentine, are likely to be infertile due to high levels of Ni and Cr in the soil solution[7]. This toxicity may be reduced by liming if the soils are acidic.

The principal source of many of these trace elements in the soil is as impurities in compounds of other elements[1]. Thus, many of them have isomorphously replaced a very small proportion of the major ions constituting rock and clay silicates, and others are absorbed when precipitates such as Fe and Mn oxides[8] are being formed. Therefore, much of the soil Co occurs in association with Mn precipitates, and much of the Mo, and probably V, with ferric oxide precipitates[10]; hence soil factors which control the dissolution or formation of these precipitates, or alter their surface properties, affect the pool of active Co and Mo. Some elements have their availability affected by the presence of soil organic matter for there are many organic compounds present in low concentrations in the soil solution which form chelation compounds with

them. In general, poor drainage usually increases the solubility of Mn, Co, Ni, Cu, Zn and Mo[11,12], while liming usually reduces the concentration of Mn, Co, Ni, Cu and Zn in crops and increases Mo.

1. Studying trace elements in the soil

The soil is a very complex system, involving organic and inorganic components. A soil in the field can have great variations in elemental concentrations within very short distances due to factors such as different drainage patterns, and different parent material. It is therefore necessary for care to be taken in selecting sampling sites. Having obtained a soil sample, organic matter and clay contents, pH and bulk density will be recorded for each horizon samples from the soil profile. The concentrations of elements in each horizon are determined from chemical analysis of the soil. It is also useful to estimate, with certain solutions, the amount of the elements that can be selectively dissolved from the soil sample, since this yields information on trace element availability and mobilization, often highlighting the movement of elements within a profile, as a result of the soil forming factors such as time or topography.

Usually it is difficult to be definitive on the cause of the observed trends in concentrations of elements or other soil properties, since many factors are likely to be involved in producing a soil. Correlation analysis of the concentrations or properties of elements is often used in an attempt to indicate relationships between different soil factors, such as elemental concentrations, clay contents, etc., as is an

investigation of trends in concentrations down a profile or within the sand, silt and clay fractions of the soil. In some cases, techniques can be used to directly analyze soils or soil bodies to demonstrate interelemental associations, rather than relying on correlation analysis. For example, the electron microprobe can be used to show elemental associations in iron-manganese concretions.

2. Monosequences in soil studies

In the investigation of soil processes it is advantageous to study monosequences - soil sequences where only one of the factors influencing soil formation has varied effectively. Such sequences are invaluable since they allow quantitative investigation of the most important processes in soil development. Jenny[13] noted that such monosequences are rare, and so suggested that a useful approximation to a monosequence, within a given area, could be made when the degree of change in a specified soil property, as affected by one soil-forming factor, greatly exceeded the changes caused in that soil property by the remaining soil-forming factors.

In the present study, the three monosequences investigated were a chronosequence (with time as the dominant soil forming factor), a biosequence (the biotic factor being dominand), and a toposequence (topography the dominating feature).

SOIL FORMATION

Attempts have been made to produce a mathematical model relating soil properties to the various soil forming factors[14,15]. Jenny's fundamental equation relating soil-

forming factors is[14];

$$s = f(cl, o, r, p, t, \ldots)$$

in which s is any soil property. The five soil-forming factors are climate (cl), the biotic factor (o), topography (r), parent material (p), and time (t). These are independent variables and are said to define the soil system. The incomplete nature of the function shows that other soil-forming factors could also be involved in some circumstances.

1. Time

Time is one of the prime factors of soil formation; many changes in soil properties are directly proportional to the length of time that the soil-forming factors have operated[14]. The attributes and properties of soils as they now appear in different soil types have apparently been conditioned to a large extent by the length of time it took for soil development. Raeside[16] considered that time in itself has no effect on the soil system, but that it governs the extent or duration of process whose nature is determined by other soil-forming factors. Rode[17] considered that soil development results in a continual change in the composition and properties of soil with time. In this change, a series of stages following each other in succession can be identified. For instance, consecutive members of a chronosequence have at one time passed through and been equivalently developed as the stages of development represented by all members preceding them in the sequence.

2. Biotic factor[18]

Organisms affect the soil in many ways. For convenience they can be classified under vegetation, animals and microorganisms. Generally there is a close relationship between the natural vegetation and the soil. This results from the influence of the soil on the vegetation and the influence of the vegetation on the soil. Animals influence the soil indirectly through their effect on the vegetation and directly through their physical effects on the soil and through the part they play in the decomposition of organic material. Some of the soil dwelling animals are worms, snails, beetles, ants, rats and rabbits. By their burrowing, soil animals make channels for air and water to penetrate through the soil, help to break up massive horizons, and provide passages for roots to penetrate. Most groups of soil microorganisms cannot be seen with the naked eye, but their effects in the soil are observable. Often the friability of soils is a product of the microbial degradation of plant remains and their conversion to decomposition products. For example the smell of sulphide in waterlogged soils is due to the presence of sulphate reducing bacteria.

3. Topography

Topography is the shape of the landsurface. Two aspects of topography are important in soil development. Firstly, the relief of the land, whether on a hillside or valley floor for example, and secondly, the drainage patterns afforded by the relief. A toposequence of soils is likely to comprise soils situated at positions of different relief, and therefore different drainage patterns, within a given area.

The basic process producing a toposequence of soils is the movement of water from slopes into the ground water or into the river draining the catchment[2].

SOIL TERMINOLOGY

The following is an introduction to the soil terminology used in this thesis.

1. Horizon designations

The soil profile consists of distinct layers, called horizons, which result from soil development. The main horizons, labelled O, A, B and C (Figure 1.1) may also be subdivided further.

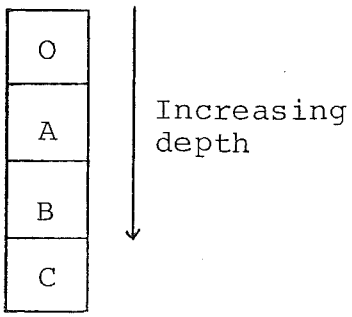

Figure 1.1.
The position of horizons in the soil profile.

The O horizon is organic, forming above the mineral soil, as a result of contributions of organic matter from vegetation, animals and microorganisms. The A horizon, which is eluvial (a region of loss of elements), lies near to the surface of the soil, while the B horizon, deeper down profile, is illuvial (a region of accumulation of sesquioxides and clay). At greater depths still, there is the C horizon, which consists of unconsolidated material.

The characteristics of each horizon are described by letters (Table 1.2) following the general horizon designation as O, A, B or C[19].

As an example of the horizon designations, Bhs refers to an illuvial B horizon, in which sesquioxides and organic

TABLE 1.2 Horizon Designations

Designation	Description of features of horizon
g	mottling
h	accumulation of organic matter
p	disturbed by ploughing
r	strongly reduced
s	accumulation of sesquioxides
u	unspecified
w	alteration in situ

matter have accumulated. If a number precedes the horizon designation, for example 2Bs, the number 2 means there is a lithic discontinuity - that is, the material the horizon is composed of originated from a different material to the horizons above it. Such lithic discontinuities can arise due to wind blown loess deposits, or a glacier removing upper horizons thereby exposing lower horizons, which may be covered by glacier debris or material transported to the site at a later stage.

2. Profile abbreviations

The profiles of the soils studied in this work are abbreviated according to the details given in Table 1.3. This is a local system of nomenclature and is not an international system as is the case for the designation of soil horizons.

MONOSEQUENCE SOILS SELECTED FOR PRESENT STUDY

1. Chronosequence

Campbell[20] reported the Reefton monosequence as a

TABLE 1.3 Soil Type and Abbreviations for Horizons and Profiles Used in this Thesis

Sequence	Soil Type	Profile Abbreviation	Horizons
Chronosequence	Hokitika sandy loam	Ho	Au1,Au2,C
	Hari Hari sandy loam	Ha	Ag,ACg,Cr,Cs,D
	Ikamatua fine sandy loam (older variant)	Io	OA,A,Bs1,Bs2,C1, C2
	Ikamatua fine sandy loam (wetter variant)	Iw	OA,A,Ar,Br1,Br2, Cr1,Cr2
	Ahaura silt loam	Ah	A,AB,B21,Bs2,Bs3, C1,C2
	Kumara silt loam	Ku	A,Er,Br1,Br2,Br3, Cr
	Okarito	Ok	A,Ag,Br1,Br2,Br3, Bs,C
Biosequence	Ahaura silt loam	Ah	A,AB,Bs1,Bs2,Bs3, C1,C2
	Podzolized Ahaura silt loam	Pod Ah	O,E,Bs,C
Toposequence	Lower Footslope gleyed humus podzol	L.F.S.	Ar,Er,Brs,Bhrs, Br,Cr
	Crest podzolozed brown earth	Crest	E,EB,Bhs,2Bs,2Bw

chronosequence suitable for study of the effect of time as a soil forming factor. The greater part of the Grey Inangahua Depression, which contains the Reefton chronosequence, is covered by the outwash gravel fans derived mainly from granite and indurated sandstone, formed during the three major periods of late Pleistocene glaciations. During the long warm inter-glacial and post-glacial periods, the outwash gravels lying in the Grey-Inangahua Depression were terraced by rivers, giving rise to a series of terraces of different heights. These

terraces, from lowest to highest, correspond to a chrono-sequence from the youngest to oldest in terms of soil development.

The glaciations involved, in order of occurrence and of decreasing magnitude, are: the Piedmont glaciation, First Valley and Second Valley glaciations[21] (Table 1.4). In a subsequent study of glacial deposits and outwash fans in Nelson and Westland, Suggate[22] produced revised correlations of glaciations in the Inangahua Depression with Quaternary formations in Nelson and North Westland (Table 1.4).

TABLE 1.4 Correlation of Glaciations in the Inangahua Depression with Formations at Reefton, Nelson and North Westland

Glaciation	Formation			Chrono-sequence Terraces
	Reefton	Nelson	N. Westland	
Otira	Second Valley glaciation deposits	Speargrass	Later Ku-3 Earlier Ku-3 Ku-2	Io Ah
Waimea	First Valley glaciation deposits	Tophouse	Ku-1	Ku
Waimaunga	Piedmont glaciation deposits	Manuka	Hohonu	Ok

Suggate and Moar[23] suggested that the Ku-2 glacier advance occurred during the period 18,600-22,300 years B.P. (before the present) - as determined by radiocarbon dating. They also considered that since pollen analysis results[23] indicated a barren treeless landscape in the Grey Valley during this period, conditions would probably have been

similar in the nearby Inangahua Valley. Therefore, it is assumed that the development of the Ahaura (Ah) soils - those formed on the outwash terrace from the Ku-2 advance - began about 18,000 years ago[20].

It has also been assumed that the Io soils have formed on degradational terraces following the retreat of the earlier Ku-3 advance[20]. Radiocarbon dating has been used to estimate the age of the Io soil as 16,000 years B.P.[23]. Campbell[20] indicated that the Hokitika (Ho) and Hari Hari (Ha) soils of the present flood plain are 1000 years old, consistent with the observation that these soils have not yet developed B horizons.

There has been difficulty in attempting to date the beginning of soil formation for the soils of the Tophouse and Manuka Formations. Nathan and Moar[24] found that a sample from the Tophouse Formation was beyond the range of carbon dating (greater than 47,500 years B.P.). Campbell[20], using results of climatic variation studies suggests 70,000 years B.P. for the age of the Tophouse Formation, and 130,000 years B.P. as the age of the Manuka Formation, corresponding to the ages of the Kumara and Okarito soils of the present study, respectively.

The soil type, horizon and profile abbreviations and type of monosequence are given in Table 1.3 for the soil sequences of this study. The five member chronosequence is the most complete of the soil sequences studied in this work. Profile descriptions for each profile sampled are given in Appendix 2. Information on the chronosequence is also presented in Table 1.5.

2. Biosequence

The two member biosequence comprises the Ah profile, also a member of the chronosequence, and the Pod Ah profile, adjacent to a large beech tree stump. The biotic factor under investigation is the effect of the beech tree on soil development. It was thought likely that there would be significant variations in trace elements between the two sites in light of the previous study on the biosequence[20].

3. Toposequence

The L.F.S. and Crest profiles (Table 1.3) were the end members of a toposequence study carried out by Young[25]; just the end members were studied here as it was anticipated the differences in trace elements would be more marked between them, rather than at intermediate sites. As indicated by the profile names, the Crest profile was at the top of a slope, and the L.F.S. near the bottom, thereby facilitating the study of topography as a soil forming factor.

SITE SELECTION

Site selection was not carried out randomly on each terrace of the chronosequence, as on any terrace, local features such as trees or slope can result in a soil development not typical of the terrace. The effect of trees on site selection was examined in this study.

1. Effect of trees on site selection

Some beech forest remains on the terraces that the Ho, Ha, Io and Ah profiles were selected from in the chronosequence. Wherever beech forest is present, the soils show vary-

ing degrees of soil development in the form of podzolization[20,25]. An exploratory survey[20] showed that the intensity of podzolization is closely related to living beech trees or decaying tree stumps, and is greatest the larger the tree, and the closer to the tree. However, the podzolization does not normally extend beyond 7 m from the tree.

Within this 7 m radius, and increasing in intensity towards the tree, acid leaching (pH 3.0-4.5) of water soluble organic chelates, the mobilization of Al and Fe, and the destruction of clay minerals, happen simultaneously.

Each terrace in the chronosequence therefore has soils at different stages of soil development, ranging from strongly podzolized immediately surrounding beech trees to weakly podzolized at greater than 7 m from any tree. The soils on the Ahaura terrace exhibit the greatest range of podzolization, with strongest and weakest podzolization occurring at the Pod Ah and Ah sites respectively. There is no such differentiation of the soils on the terraces containing the Ku and Ok soils, for in these cases soil development has progressed through podzolization already, and are at the stage of development described as gley podzols. The remaining chronosequence soils, at the Ho and Io sites (as well as the Ha and Iw sites) were deliberately selected to be more than 7 m from the nearest beech tree. On each terrace, any drainage irregularity or any other factor likely to affect the soil development were also noted, and such places avoided as sampling sites. This procedure results in the youngest, least developed soils from each terrace being sampled, and provides samples for the chronosequence in which time is the main soil-forming factor.

2. The sampling sites

(i) *Chronosequence*. Details of the sites, samples and the soils of the chronosequence are given in Tables 1.3, 1.5 and 1.6. In order to investigate time as a soil-forming

TABLE 1.6 Summary of Site Selection Details

Sequence	Soil Forming Factor Studied	Site	Site Characteristics
Chronosequence	Time	Ho, Ha, Io, Iw, Ah Ku, Ok	>7.0 m from nearest beech tree. Each site is on successively older terraces.
Biosequence	Biotic factor	Ah	>7.0 m from nearest beech tree.
		Pod Ah	<0.1 m from nearest beech tree.
Toposequence	Topography	Crest, L.F.S.	1.0 m from nearest beech tree.
Waterton soils	Topography		A pasture; set of profiles across a shallow gully.

factor, site selection was made with a view to minimize variations in the other soil-forming factors. The criteria used to ascertain site suitability for the chronosequence are as follows[20]; 1) the parent material should be of constant composition, and in this case was composed of river alluvium, outwash gravels, sands, and silts originating from granite and indurated sandstone. Following the commencement of soil genesis, there should not have been any additions of loess, alluvium or nutrients. Deepest soil profiles and finest textured soil are preferred. 2) If the area is vegetated, the site should be situated in beech dominated forest, since

beech or beech-podocarp forest has been the dominant biotic factor in the genesis of the chronosequence soils. 3) The area of the site should be typical of the area, and the site should not be situated near the edge of a terrace or in a depression. 4) The influence of man and animals should have been minimal, and 5) it should be possible to estimate the age of the soils of each site.

To assist in establishing the relationship between drainage and soil development, two poorly drained variants, Ha and Iw, were sampled for comparison with the freely drained, and otherwise comparable, Ho and Io profiles. These sites may also assist in understanding the different properties of the younger freely drained soils (Ho, Io, Ah) and the waterlogged gley podzols on the two oldest terraces (Ku and Ok).

The sites samples for the chronosequence soils are shown in Figure 1.2.

(ii) *Biosequence*. An assessment of the biotic factor on soil development (Table 1.6) is made by comparing the properties of the Ah and Pod Ah soil profiles. The Pod Ah profile was sampled at the base of a large decaying beech stump, on the low glacial outwash terrace (Table 1.5). The site of the Ah profile, a member of the chronosequence, was 7 m away.

(iii) *Toposequence*. The toposequence site is on an ice truncated spur which provides a variety of drainage characteristics, ranging from shallow (0.4 m) well-drained soils, through varying degrees of drainage, to gley podzols and peat. Since the area studied was under beech forest, the

Crest and L.F.S. profiles were both sampled 1 m from similar sized beech trees in an attempt to obtain soil samples from sites of comparable development (Table 1.6). The Crest profile is freely drained, while the L.F.S. is poorly drained; the two profiles are 150 m apart.

(iv) *Waterton soils*. Another aspect of this work involved the investigation of the trace element content and distribution in iron-manganese concretions. While a topographic feature, a small gully, is important in the formation of these concretions, this section of the work was primarily concerned with the concretions themselves, rather than the soil forming factor.

The main feature of the Waterton clay loam in which the concretions were formed, is slow drainage, which results in the soil lying wet in the winter and becoming dry in the summer.

The sampling sites were selected in an earlier study[26], and comprise four sets of three profiles, with each profile set spanning 20 to 30 m across a shallow gully of less than 0.5 m in depth. In the present study, four horizons were selected from these profiles. The horizons selected were chosen because they contained the largest percentage of weight of concretions[26].

The soil forming factors of climate, time, biotic factor and parent material do not vary significantly from one profile to the next, leaving topography as the major soil-forming factor responsible for concretion formation (Table 1.6).

AIMS OF THE PRESENT STUDY

There were three broad aims in the present study. Firstly, it was necessary to investigate several chemical methods of decomposition for soils and rocks in preparation for the analysis of the samples for trace elements. A comparison of different instrumental analytical techniques available was also made to find the technique most suitable for the soil analysis.

Secondly, the behaviour of trace elements in soils, as a function of soil development was considered. Three monosequences, as considered above, were chosen and the trace element content related to the processes occurring in soil development.

Thirdly, it was proposed to use an electron microprobe to analyse some iron-manganese concretions, in order to establish trace element associations. This information, together with chemical and mineralogical analyses, would assist in clarifying the behaviour of trace elements in these concretions.

FORMAT OF THESIS

In Chapter 2 results are given for analysis on soil pH, organic matter and particle size fractionation. The presentation of results on a mass per mass or mass per volume basis is introduced along with the reasons for doing so. A review of literature on trace elements in soils is given in Chapter 3, and is intended as a background for a discussion of results found in this work. In Chapters 4 and 6, the results and discussion of the analysis of soil sequences and iron-manganese concretions are presented respectively. A

review of selected decomposition methods used in soil analysis is given in Chapter 5, together with an analysis of the results of the methods used. Chapter 7 contains a description of the experimental techniques together with relevant background theory, while in Chapter 8 the significance of the results is considered. As a great number of tables and figures of results have been produced, these are given in Appendix 1, although representative data are incorporated within the text. Appendix 2 contains profile descriptions of the soils of this study, and Appendix 3 is a glossary of soil related terms.

CHAPTER 2

SOIL pH, ORGANIC MATTER, AND THE PARTICLE SIZE ANALYSIS OF SOILS

In order to interpret analytical data on trace elements in the three soil sequences studied, it is necessary to know the variations in soil pH and organic matter content. In this chapter, the results on the measurement of soil pH and soil organic matter are presented. The expression of the results on a percentage basis, and as the total amount of soil constituents in a soil profile is discussed. The results of the fractionation of soil samples into sand, silt, and clay are given, and some aspects of the fractionation of soils are also discussed.

SOIL pH

1. Introduction

The pH of a solution refers to the hydronium ion concentration arising from the partial or complete dissociation of species in solution. This concept of pH is satisfactory when the volume is large compared with molecular dimensions, for then the molecules and ions of the solution are uniformly dispersed. The pH of a solution containing a soil dispersed in water is not so clearly defined[2]. Soil particles, which carry ions attached to them, are very large compared with molecular dimensions, and consequently there is not a uniform distribution of the ions throughout the solution. The concept of the pH of a soil suspension can therefore only be discussed in relation to the soil properties

of the ionic particles bound to the soil particles.

Almost all soils have pH values in the range 3.0 - 9.0. The pH value of a soil may exceed 9.0 when a significant amount of Na_2CO_3 exists in the soil. The hydrolysis of sodium carbonate produces OH^- ions;

$$Na_2CO_3 + H_2O \rightleftharpoons HCO_3^- + OH^- + 2Na^+$$

resulting in an alkaline solution. The lower pH limit of 3.0 for a soil is probably controlled by organic acids and polyphenols washed off leaves and vegetation.

The two cations H^+ and Al^{3+} are largely responsible for soil acidity. Adsorbed H^+ ions contribute directly to the H^+ ion concentration in the soil, while Al^{3+} ions do so indirectly through hydrolysis[2,27];

$$Al(OH_2)_6^{3+} + H_2O \rightleftharpoons Al(OH_2)_5(OH)^{2+} + H_3O^+$$

$$Al(OH_2)_5(OH)^{2+} + H_2O \rightleftharpoons Al(OH_2)_4(OH)_2^+ + H_3O^+$$

$$Al(OH_2)_4(OH)_2^+ + H_2O \rightleftharpoons Al(OH_2)_3(OH)_3 + H_3O^+$$

Other sources of protons in the soil are -SiOH (pH 7) and -AlOH groups at the surfaces of silicate clays, and carboxyl (-COOH) and phenol (phenyl-OH) groups on the humus colloids. These groups contain covalently bonded hydrogen, which is not dissociated at low pH. As the pH increases, however, the proton dissociates leaving a negative charge on the colloid. The H^+ ions that have dissociated are replaced by other metallic cations.

During the decomposition of soil organic matter, both inorganic and organic acids are formed. The oxidisable

fractions of organic matter are composed mainly of carbon, hydrogen and oxygen, and the overall decomposition reaction is;

$$[CH_2O] + O_2 \rightarrow CO_2 + H_2O + \text{energy}$$

Also $CO_{2(aq)} + H_2O \rightleftharpoons H_2CO_3 \qquad k_{H_2CO_3} = 2 \times 10^{-3} (25^oC)$

Many organic intermediate products are formed, such as short chain fatty acids, hydroxy-carboxylic and polycarboxylic acids, alcohols, aldehydes, and ketones. Since the equilibrium above involving CO_2, H_2O and H_2CO_3 lies largely to the left, it is unlikely to account for the low pH values found in many soils.

Inorganic mineral acids, such as H_2SO_4 and HNO_3, along with the stronger organic acids, such as oxalic acid, fumaric acid and malic acid, account for the development of strongly acidic conditions. Some of the reactions, and the bacteria involved in the production of H_2SO_4 and HNO_3 following organic matter decomposition are[2,27];

$$NH_4^+ + \tfrac{3}{2}O_2 \rightarrow NO_2^- + 2H^+ + H_2O + \text{energy} \quad \text{(Nitrosomonas)}$$

$$NO_2^- + \tfrac{1}{2}O_2 \rightarrow NO_3^- + \text{energy} \quad \text{(Nitrobacter)}$$

$$S + \tfrac{3}{2}O_2 + H_2O \rightarrow H_2SO_4 + \text{energy} \quad \text{(Thiobacillus)}$$

2. Soil pH values

The pH value determined for a soil-water suspension will be influenced by the relative amounts of the various soil constituents and the soil-water ratio. Since soils always contain soluble salts, such as nitrates and bicarbonates, the pH measured will depend on the amount of water

added to give a soil-water suspension; a soil-water ratio of 1:2.5 is usually used[28].

The amount of salt, which varies with soil type, influences the pH of a soil-water suspension. This influence can be reduced by carrying out all the pH measurements in a salt solution, that is concentrated sufficiently to make the changes due to the different salt concentrations of the soils negligible. Cation exchange will inevitably occur when a salt solution is added to a soil, causing a liberation of some H^+ ions and a lowering of the soil pH value.

The pH of a soil is usually measured in one of three ways, 1) in a soil-water suspension, 2) in a 1.0 M KCl solution[29] (which is assumed to approach the pH at the soil particle surfaces), and 3) in a 0.01 M $CaCl_2$ solution[30] (which is assumed to approach the ionic strength of soil solutions). Bache[31], however, has observed that for soil with pH values between 5.0 - 6.0, when placed in a 0.01 M $CaCl_2$ solution, the pH values slowly rise, possibly due to polymeric aluminium species taking up protons from the solution.

3. Effect of tree species on soil pH values

Organic matter can have a pronounced effect on soil pH values. Several authors[20,32,33] have observed that soil pH values of upper horizons decrease as tree stems are approached.

Kaurichev et al.[34] studied the organic acids in some forest gleyed and podzolic soils of Russia. They found that the level of low molecular weight organic acids, which included oxalic, tartaric, citric, fumaric, malic and glycolic acids, ranged from 4 to 65% of the carbon in the water soluble organic matter of the soil solutions. In these

forest soils, the soil solutions of the A horizons were more acidic than similar non-forest soils. This was attributed to the production of carbonic acid and water soluble acidic compounds derived from organic matter decomposition. With time, these compounds leach exchangeable bases.

Moisture accumulation by beech trees has been studied[32,33]. Much of the rainwater falling on the crown of the trees is concentrated by the foliage, branches and stem, and is delivered to the soil in a narrow band around the base of the tree. The stem-flow is normally acidic[33] and contains higher levels of C, Ca, K, Mg, S, Cl, P and N than the canopy drip, which itself has higher concentrations of these elements than the rain. For beech trees, the soil at the base of the stem receives 2.5 times the rainwater falling in the open. The greater water flow around the tree trunk also leads to its further penetration of the soil. The penetration is assisted by the annual decay of roots under trees[35], leaving channels in the soil that can serve as routes for rapid water movement, and for more effective leaching of dissolved elements.

As a consequence of the stem-flow from beech trees being enriched in organic and inorganic substances, there is an intensification of podzolization processes in the soils near the stems of beech trees. In one study[33], for example, it was found that the soil pH (H_2O) value was lowest next to the stem of a beech tree, with a pH (H_2O) of 4.5 being measured in the soil adjacent to and under the stem, while a value of 6.0 was found 2 m away. The change in pH was most marked in the A horizon.

It has been shown[20,33] that the very low pH values close to beech trees are not due to KCl-extractable $Al(H_2O)_6^{3+}$ ions, nor to acid conditions resulting from the oxidation of FeS_2 or S. It is also unlikely that the low pH values are derived from chelation, as a result of the dissolution of aluminosilicate minerals in chelating solutions[36], according to the equation;

$$H_3Y + Al^{3+} \rightarrow AlY + 3H^+.$$

RESULTS AND DISCUSSION - SOIL pH

1. Chronosequence soils

The $pH(H_2O)$ values, measured on a soil-distilled water suspension (1:2.5) and given in Table 2.1, show an increase with depth for all chronosequence profiles, and are all low to very low (4.5 - 5.4). The Io and Ah profiles have similar $pH(H_2O)$ values, while at similar depths, the $pH(H_2O)$ values are decreasing in the Ku and Ok profiles. The strong leaching of the Ku and Ok profiles, and the formation of gley podzols,have meant a loss of Group I and II metal cations from these profiles. Decay of the tree litter, at earlier stages of soil development, producing strong inorganic and organic acids probably also contributes to the lower $pH(H_2O)$ values.

The $pH(H_2O)$ values of the two Ho A horizons are very low for a recently formed soil. However, the more poorly drained recent soil of the Ha profile has a higher pH, in the range expected for a young soil. It is likely that the low pH of the Ho profile A horizons is due to the oxidation

of S^{2-} or S, or that the material has been pre-weathered. The Ho profile is located on the floodplain of the Waitahu River and S^{2-} or S could be derived from nearby coal mining operations, or the weathering of sulphide minerals, deposited during flooding.

The oxidation of sulphur can produce very acid conditions as occurs for acid mine waters[27,28,37]. During periods of flooding, and therefore anaerobic conditions, sulphates are reduced to sulphides by a number of anaerobic bacteria such as Desulfovibro and Desulfotomaculum[27]. These bacteria use the combined oxygen in the sulphate to oxidize organic material.

$$2(R\text{-}CH_2OH) + SO_4^{2-} \rightarrow 2(R\text{-}COOH) + 2H_2O + S^{2-}$$

The sulphide formed may either react with the ferrous iron, which is the major iron species present in anaerobic conditions, forming FeS

$$Fe^{2+}_{(aq)} + S^{2-}_{(aq)} \rightarrow FeS_{(s)} ,$$

or be present in the soil as H_2S. As floodwaters subside, there may be some oxidation of the sulphides, to produce elemental sulphur. When the floodplain is drained completely, the sulphides and elemental sulphur are then oxidized to sulphate, with an accumulation of protons, thereby lowering the pH[6]. The following reactions summarize this situation;

$$H_2S + 4H_2O - 8e \rightarrow SO_4^{2-} + 10H^+$$
$$O_2 + 4H^+ + 4e \rightarrow 2H_2O$$
$$\overline{H_2S + 2O_2 \rightarrow SO_4^{2-} + 2H^+}$$

and $S + 4H_2O - 6e \rightarrow SO_4^{2-} + 8H^+$

$O_2 + 4H^+ + 4e \rightarrow 2H_2O$

$2S + 3O_2 + 2H_2O \rightarrow 2SO_4^{2-} + 4H^+$

2. Biosequence soils

A comparison of the pH(H_2O) values of the biosequence Ah and Pod Ah profiles, given in Table 2.2, reveals a large difference of up to 1.0 pH unit between the upper horizons of these profiles, even though they are only 7.3 m apart. These results are expected in the light of previous workers results and the discussion given above.

3. Toposequence soils

The pH(H_2O) values of the two toposequence profiles are similar (Table 2.3). This is because both sampling sites were one metre from similar sized beech trees, which are the dominant factor in controlling the pH of these profiles. The range of pH(H_2O) values found, as well as the trends observed, are similar to those of the Pod Ah profile of the biosequence, and the same explanations are appropriate.

TOTAL AMOUNT OF SOIL CONSTITUENTS IN A SOIL PROFILE

Analytical data for the trace element composition of the horizons of the chronosequence, biosequence, toposequence and Waterton soils, and for the concretions (Waterton soil) are all given on a percentage composition basis. The data for the chronosequence soils are also expressed on the basis of the total amount of an element present in the profile horizons. The amount of an element present in the various chronosequence profiles is also presented as the total amount

to depths of 0.38 or 0.68 m. The former depth was chosen to minimize the effect of stones - only the Ho profile had stones within the upper 0.38 m of the profile, while 0.68 m was chosen because stones occurred below this level in the Ah and Ku profiles.

The weights of the <2 mm and >2 mm sized soil particles, and bulk densities are given in Table 2.4. In this Table a distinction is made between the actual and an estimated total weight of soil down to 0.68 m, when stones are present in the profile (Ho, Ha and Io). If stones were present in the sample, an estimated total weight was obtained by calculating the volume occupied by the >2 mm particles[20] (their weight and density being known), and replacing it with an equivalent volume of soil particles <2 mm.

Since the changes occurring in the soils will be most intense in the top 0.38 m of the profile, and since there are few complications arising from the presence of stones in the top 0.38 m of each profile, the comparison of the total amounts of the constituents in the chronosequence profiles is carried out in detail only for the upper 0.38 m of the profile.

The volume of soil samples to 0.38 m is the same for all chronosequence soils[20]. However, soil development has led to an initial expansion (up to the Ah profile), followed by compaction of the initial soil volume (up to Ok profile). This is illustrated in Figure 2.1. This expansion and contraction of soil volumes correspond to the development of soil structure resulting from the incorporation of organic matter (Ah profile), and to a destruction of soil structure

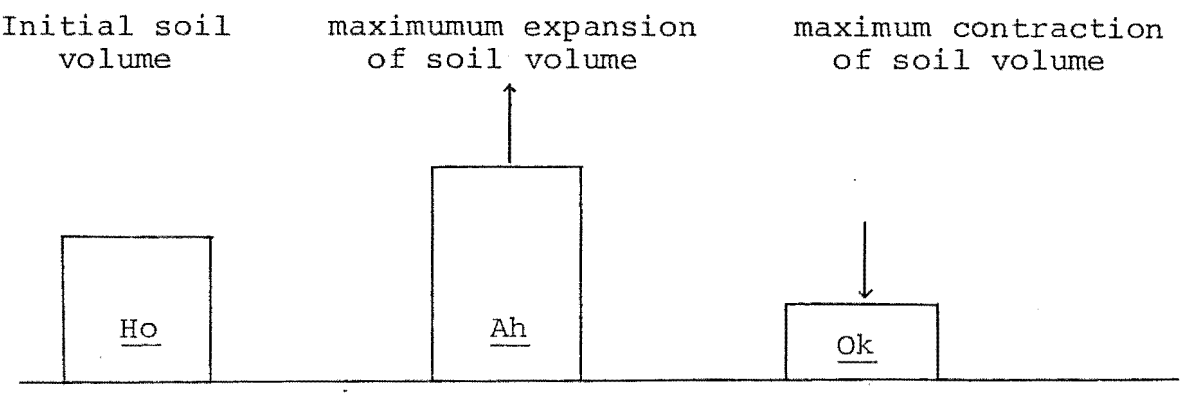

Figure 2.1. The Change of an initial soil volume with soil age.

due to loss of organic matter, hydrous oxides of Fe and Al, and aluminosilicate gels[20] (allophane) (Ku and Ok profiles).

For the younger soils of the Ho, Ha, Io and Ah profiles, it can be seen from Table 2.4A (data from Table 2.4) that the amount of inorganic matter, in a fixed volume, decreases with the age of the soil, from 466 x 10^4 kg ha^{-1} in

TABLE 2.4A The Amounts of Inorganic and Organic Material to 0.38 m

Profile	Ho	Ha	Io	Iw	Ah	Ku	Ok
Inorganic material to 0.38 m (kg ha^{-1} x 10^4)	466	393	320	396	226	246	506
Organic material to 0.38 m (kg ha^{-1} x 10^4)	9.3	13.1	26.4	28.1	33.3	26.2	18.9

the Ho profile to 226 x 10^4 kg ha^{-1} in the Ah profile. This is due to an increase in the presence of organic matter and the sesquioxides of Al and Fe, and has resulted in a loose granular structure for the Ah profile. Similar results have been found elsewhere[38]. The lowest bulk density values and the lowest amount of inorganic material (Table 2.4) are found

for the Ah profile.

In the older soil of the Ku profile, the amount of inorganic material has increased to 246 x 10^4 kg ha^{-1}, which is greater than the amount in the Ah profile, but less than in the Ho profile. In the Ok profile (the oldest soil), the amount of inorganic material has risen to 506 x 10^4 kg ha^{-1} (9% higher than in the Ho profile). The Ok soil has lost a great deal of its organic matter and, as for the Ku profile, has lost most of the Al and Fe sesquioxides, resulting in a compacted soil of higher bulk density (Table 2.4).

The poorly drained Ha profile contains slightly less inorganic material than the freely drained comparable Ho profile, while the poorly drained Iw profile contains slightly more inorganic material than the freely drained Io profile. These variations reflect slight differences in bulk densities (Table 2.4).

SOIL ORGANIC MATTER

Soil organic matter embraces the non-mineral fraction of the soil. The total organic matter content of a soil is estimated from either a knowledge of the total organic carbon content or from the weight loss when the organic matter is destroyed by ignition at a temperature between 350 - 800°C.

1. Total organic carbon

Total organic carbon can be determined by either wet or dry combustion, or by partial oxidation with chromic acid.

(i) *Wet and dry combustion.* Dry combustion of organic matter is carried out in a stream of oxygen at 1200°C, and

the CO_2 evolved is collected and measured[29,39]. Inorganic carbonates are either determined separately or destroyed with acids before combustion.

In a wet combustion of organic matter, the soil is treated with an oxidizing agent such as dichromate, and a strong acid, to convert all forms of carbon into CO_2. Jackson[39] used a mixture of sulphuric, phosphoric and chromic acids for combustion, and then determined the CO_2 content volumetrically after absorbing it in standard alkali.

The total organic carbon determined by combustion can be expressed as total organic matter by use of a multiplicative factor (1/total organic carbon). Conventionally, it is assumed that organic matter contains 58% carbon[28], and so the factor is 1.72 (=1/0.58). However, different soils can contain different organic materials, and therefore the factor will vary.

(ii) *Oxidative organic carbon.* The method of determining oxidizable organic carbon involves the partial oxidation of organic matter with chromic acid[40]. Carbonates do not interfere.

To express oxidizable carbon as total organic carbon, a conversion of 1.3 is commonly used[41]. This figure was obtained by calculating the amount of oxidizable carbon in soils determined by partial oxidation with chromic acid, compared with the total organic carbon determined by the dry combustion method. It was found that the oxidizable carbon was 77% of the total organic carbon, and that multiplication of oxidizable carbon values by 1.3 (= 77% of 1.72) gives the total amount of organic carbon.

2. Total organic matter by weight loss

In this method the soil organic matter is determined by the weight loss of the soil sample on ignition at temperatures between 350-800°C. In the present study, weights of organic matter (Tables 2.1 to 2.3) have been calculated on the assumption that loss on ignition equals organic matter. Campbell[20], however, presented differential thermograms showing that at temperatures between 105°C and 500°C, some of the weight loss was caused by loss of water from clay minerals. To reduce such errors the use of lower ignition temperatures in the range 350-420°C has been advocated[42]. Poorly ordered hydroxy-alumina and gibbsite, which lose about 35% of their weight around 300°C, would still be affected by these temperatures, but errors introduced from this source will not exceed 4% of the weight loss on ignition for the soils of the present study[20,25].

3. Choice of method for organic matter analysis

Campbell[20] obtained a highly significant positive correlation (0.1% level) between organic matter determined by the weight loss on ignition and organic matter determined by oxidizable carbon. He found that a relationship existed between the values for oxidizable carbon and the values for the weight loss on ignition which gave the oxidizable carbon content as being equal to 39% of the weight loss on ignition. Making use of the conversion factor of 1.3 for estimating organic carbon from oxidizable carbon gives the organic content as equal to 51% of the loss on ignition values.

Campbell's work illustrates that comparable results from soil organic matter can be obtained by either the method

of combustion or the method of weight loss on ignition, and that it is therefore reasonable to assume weight loss on ignition values correspond to organic matter values.

RESULTS AND DISCUSSION - SOIL ORGANIC MATTER

1. Soil organic matter on a percentage weight basis

Soil organic matter, as obtained by measuring the weight loss on ignition, shows a decrease with depth in all of the chronosequence and biosequence soils (Tables 2.1 and 2.2).

In the soils surrounding trees, there are variations in the amount and the distribution of tree litter[33,43]. In the biosequence soils, the surface litter horizon of the Pod Ah profile has greater levels of organic matter than does the Ah profile.

Weight loss on ignition values in the toposequence soils decrease down the profiles to the illuvial horizons where the values rise again, demonstrating the accumulation of organic matter in these horizons (Table 2.3). The Crest profile has a more strongly developed soil structure than the LFS soil, due to better incorporation of organic matter[25]. The development of the soil structure of the LFS soils has been hindered by the wet condition of the soil.

2. The total amount of organic matter in a soil profile

The weights of organic matter in each of the chronosequence profiles, to depths 0.38 and 0.68 m, are listed in Table 2.4. The amount of organic material, to 0.68 m, in each profile increases with soil age from the Ho profile to a maximum in the Ah profile. This is followed by a decrease,

at an approximate rate of 2 kg ha^{-1} $year^{-1}$, to the minimum value in the oldest chronosequence soil of the Ok profile. The proportion of organic matter that is present in the top 0.38 m of each profile decreases with time from 86% in the Ho and Ha soils, to 63% in the Ku profile.

The two poorly drained Ha and Iw profiles both contain more organic matter than the similar aged, but freely drained soils of the Ho and Io profiles, demonstrating that organic matter accumulation can occur under restricted drainage and reduced biological activity. This is also seen in Figure 2.2.

3. Variation in the amount of organic matter with depth

In Figure 2.2 the amount of organic matter, per centimetre of horizon, in each chronosequence soil is plotted against the depth of the profile. The distribution of organic matter is controlled by two factors - the percentage weight of organic matter in the soil and the bulk density. The Hokitika, Hari Hari, and Ikamatua soils show a decrease in organic matter levels with depth. The Ah profile has a decrease with depth but has an increase in the Bs3 horizon. Similar trends occur for the Ku and Ok soils with the increases in the Br3 and C horizons respectively. The higher organic matter level of the Ah Bs3 horizon results from the increased density of the horizon, while that of the Ku Br3 is due to increases in both organic matter content and the bulk density of the horizon. The increase in the Ok C horizon is due to a higher organic matter content.

It is evident from Figure 2.2 that the organic matter content per centimetre depth of horizon per hectare is

considerably higher in the upper horizons of the poorly drained Ha and Iw profiles compared with their freely drained counterparts, Ho and Io.

FRACTIONATION OF SOILS

The fractionation of a soil into the three particle size groups of sand, silt and clay is necessary before a study of the silt and clay fractions is undertaken.

1. Percentage of clay in soil horizons

The data on the particle size analysis on the chronosequence, biosequence and toposequence soils is given in Tables 2.1 to 2.3. The data were calculated on an inorganic basis, using weight loss on ignition data.

There is a decrease in the percentage of clay with depth in the biosequence and chronosequence soils, except for the Ku profile where the maximum percentage of clay occurs in the Br3 horizon, and the Ok profile, where the clay content increases with depth to reach a maximum in the Br3 horizon. In the upper horizons of the Ku and Ok, the lower clay percentages are probably due to the destruction of clay below pH 4.5.

The toposequence soils have an increase in the percentage of clay with depth to the Bhs horizons. This is most likely due to an eluviation of clay with percolating waters from the upper horizons to the Bhs horizons.

2. Variation in the amount of clay with depth

The amounts of clay in the horizons of the chronosequence soils are given in Table 2.4 (these data were cal-

culated using the data from Tables 2.1 and 2.4). On a percentage basis (Table 2.1), the clay composition in the Ah profile shows a maximum in the A horizons, as is also the case in the Ho, Ha, Iw and Io profiles. However, it can be seen from the data in Table 2.5 and in Figure 2.3, that the clay content, in kg ha^{-1} cm^{-1} horizon x 10^3, of the Ah profile is now at a maximum in the Bs3 horizon, and similarly for the older gley podzols of the Ku and Ok profiles. The reason for the apparently different clay distribution when the total amounts per horizon are considered, is that bulk densities become a major contributor to the distribution of clay, as well as the percentage of clay per horizon.

3. Total amount of clay in soil profiles

The amount of each size fraction for each horizon of the chronosequence soils is given in kg ha^{-1} x 10^4 in Table 2.5. The amount of clay, to a depth of 0.68 m, increases with soil age from 41.3 kg ha^{-1} x 10^4 in the Ho profile to 126.8 kg ha^{-1} x 10^4 in the Ah profile. The amount of clay decreases in the Ku and Ok profiles compared with the Ah profile, despite the higher bulk densities in the Ku and Oh profiles.

Since an increasing clay content is usually associated with increasing soil development, the decline in clay content after the Ah profile needs explaining. Because the surface horizons of the Ah, Ku and Ok profiles have lower amounts of clay than the underlying horizons this should be considered also.

An explanation for the freely drained Ah profile could be the eluviation of clay, leading to an increased clay

content with depth. In the poorly drained gley podzols however, a more likely explanation of the reduced clay content is the destruction of clay. This could be caused by the action of organic chelates and low pH conditions over a long period of time, during which the rate of clay destruction has exceeded the rate of clay formation from comminution.

4. Total amount of sand and silt in soil profiles

The silt content increases with the age of the soil while the sand content decreases (Table 2.5). The sand content of the Ok profile is higher than that of the Ku profile due to the presence of disintegrating weathered stones. The increase in the silt and clay fractions with soil age results from more extensive weathering of the larger particles, thereby producing a smaller weight of sand.

5. Some of the factors involved in particle size analysis

The process of separating a soil into its component particles, and then estimating the proportion of particles in the various size ranges, is called particle size analysis. Two conditions must be achieved for soil dispersion: a) a breakdown of soil aggregates, and b) peptization of the soil particles.

The breaking up of soil aggregates is carried out in water, and involves separating particles that have a relatively strong attraction for each other when separated by a few hundred picometers, and then keeping them separated. The break-up of soil aggregates is achieved using sufficient mechanical force, such as generated from passing ultrasonic vibrations through water, to pull the aggregates apart. Dispersion can also be achieved chemically, by altering the

surface properties of the individual particles so that they repel each other - as can be done by replacing the exchangeable Ca, Mg and Al ions with sodium. In some soils, it is necessary only to shake a soil with a suitable sodium saturated exchange resin, but for many soils, the negative charge on the soil surfaces must be increased, by shaking the soil in a solution containing, for example, sodium hexametaphosphate[2].

Barkoff[44] reported that the dispersion achieved by a 15 or 60 minute period of ultrasonic vibration of soils suspended in sodium hexametaphosphate-sodium carbonate solution was more complete than that obtained by shaking these suspensions for five hours. Edwards and Bremner[45] confirmed this, but found that it is not necessary to use a dispersing reagent to effectively separate soil particles using ultrasonic vibration. Studies using soils of widely different textures and organic matter contents[45] showed that dispersion, caused by ultrasonic vibration and evaluated for <2 μm material by pipette analysis, was similar to that obtained by chemical methods (such as a 30% H_2O_2 treatment of soil to decompose organic material and use of sodium hexametaphosphate as a dispersant, followed by shaking).

Edwards and Bremner[45] compared four methods of dispersion: a) ultrasonic vibration of a water containing soil, b) a peroxide treatment of a soil, followed by use of sodium hexametaphosphate as a dispersing agent, with shaking for 10 hours, c) use of a sodium-saturated Amberlite IRC-50 resin in water, with shaking for 10 hours, and d) shaking with sodium hypobromite. They found the four methods

generally gave similar results, but on average, the vibration method gave the lowest percentage sand, and the resin method the highest percentage clay. Use of a longer vibration time in the ultrasonic method, and use of less water in the resin method, gave percentage clay values higher than the other methods. However, there is no absolute index of complete dispersion.

The ideal method of fractionating different size soil particles is one which will not result in comminution of the particles in achieving complete dispersion. Edwards and Bremner[45] presented evidence that even primary minerals such as dolomite, quartz and microcline, which are not considered fragile minerals, suffer some abrasion when shaken with water for ten hours. Ultrasonic vibration of these minerals for 30-60 minutes is less abrasive than shaking with water for ten hours, and is significantly less damaging to fine particle size samples than is a treatment with 6% H_2O_2 followed by shaking with sodium hexametaphosphate for ten hours. However, the fragile mineral, biotite, is abraded more by ultrasonic vibration than by shaking with water. The wide range of behaviour of materials encountered in soils, and the difficulty in choosing a single treatment to achieve complete dispersion, are also illustrated by the data of Pritchard[46].

Edwards and Bremner[47] reported that particles which are difficult to disperse are likely to have formed micro-aggregates (<250 μm in diameter), and consist largely of clay and humified organic material, linked by polyvalent metal ions. In such cases, the bonding within the microaggregates can be weakened by chemical treatment, such as H_2O_2 peroxidation to destroy organic material.

In general, the method of dispersion used should be determined by the nature of the soil and where possible, a check should be made on the effectiveness of the dispersion by microscopic or sedigraph testing.

Once dispersed, it is necessary to maintain a stable dispersion in solution. This depends on complete hydration of the clay particles together with the establishment of a high negative potential by the addition of a suitable peptizing agent[48], such as sodium hexametaphosphate or sodium carbonate. Organic matter can make soils difficult to disperse initially, but once the particles are in suspension, it can increase the stability of the soil suspensions[49].

CHAPTER 3

TRACE ELEMENTS IN SOILS

This chapter, a review of trace elements in soils, is a preface to chapters 4 and 6, in which the results and discussion of the present work are given. In the review, emphasis will be given to the location, the form and behaviour of trace elements in the soil.

THE TOTAL TRACE ELEMENT CONTENT OF SOILS

The total trace element content of a soil relates to the relative abundance of the elements, but does not provide information on the chemical form of the elements in the soil. Because of the variety of parent materials, the concentrations of trace elements can vary 10 to 1000 fold[50], while the concentrations of the major elements such as K, Ca, Mg or P normally have less than a 5 fold variation. The wider range of concentrations of trace elements means that their levels can be more significant indicators of soil status than is the case for the major elements.

The trace elements considered in this thesis are the first row transition metals, many of which are essential micronutrients for plants and animals. An average level of the trace elements in the earth's crust, and a typical range of values found in soils, are listed in Table 3.1[51].

In a study of trace elements in soils, the chemical form, as well as the amount present, is important, particularly as an element can exist in more than one chemical form.

TABLE 3.1 Levels of Trace Elements in the Earth's Crust and Soils

Element	Earth's Crust[a] ($\mu g\ g^{-1}$)	Soil[b] ($\mu g\ g^{-1}$)
Ti	4,400	1,000 - 20,000
V	110	50 - 500
Cr	200	8 - 500
Mn	1,000	100 - 2,000
Fe	50,000	10,000 - 50,000
Co	25	2 - 80
Ni	80	8 - 300
Cu	45	3 - 100
Zn	65	10 - 300

[a] Average value for earth's crust
[b] Typical range of levels in soils

A significant proportion of the trace elements in a soil is contained within the crystal lattice of non-weathered minerals. This portion is immobile until released by weathering processes (Table 3.2).

WEATHERING

The principal source of trace elements in soils is the primary minerals in the parent material. Many of these minerals were originally formed, and are stable under conditions different from those in present day soil environments. For example, minerals that crystallized from the magma at high temperatures do not necessarily remain stable at the ambient conditions in a soil. As a result, many primary minerals slowly change through the process of chemical

TABLE 3.2 Some of the Features of the Location and the Behaviour of Trace Elements in soils

Soil Characteristic	Trace Element Location/Behaviour
Age	Young soils contain trace elements mainly in primary minerals. As soils age, they contain greater amounts of secondary minerals, such as clay minerals, and iron oxide, which often contain significant amount of trace elements.
Iron and manganese oxides and hydroxides	Often occur as concretions or pans; can concentrate trace elements, especially Co and Zn.
Organic matter	Organic ligand complexes formed especially For Al(III), Fe(III) and Cu(II) ions.
Waterlogged soils	Reduction reactions occur in soil; mobilization of Fe and Mn as divalent cations can occur, although sulphide formation can immobilise trace elements.
Podzolization	Results in an intensely weathered A horizon, with accumulation of organic matter, clay, iron and aluminium hydroxides, and other trace elements, in the B horizon.
Topography	Topography can affect water flow on a slope; results in transport of some trace elements, especially Mn, downslope; sometimes Fe-Mn concretions form in foot slope

weathering. The new materials formed - the secondary minerals - such as the clay minerals and sesquioxides, are more stable within the soil environment. Throughout the weathering process, material is also leached from the soil profile. Some trace elements, released in weathering, are nutrient elements which support plant and microbial populations. These materials, on decay, add organic acids and debris, which participate in further weathering.

The prominent pedological processes involved in soil genesis are summarized as follows: 1) surface enrichment of trace elements utilized by plants, 2) leaching of mobilized elements, such as Fe and Mn, down a profile, 3) movement of trace elements organic ligand complexes, 4) trace element mobilization, as a result of a breakdown of soil minerals, caused by gleying, 5) movement of clay particles enriched in many trace elements, and 6) microbial activity causing mobilization or immobilization of trace elements.

THE BINDING OF TRACE ELEMENTS BY A SOIL

Trace elements released from primary minerals by weathering processes can be considered as being mobilized, and they are classified into several forms[52]. 1) A small proportion are in the soil solution, either in an ionic or a coordinated form. This is the form most readily available to plants, and it is water extractable in the laboratory. 2) A greater portion of the mobilized trace elements, in particular those in cation form, are adsorbed with varying tenacity onto ion-exchange surfaces of clay minerals or organic material. Some part of the sorbed elements are

available to plants and, in soil analysis, these can be extracted with ammonium acetate or dilute acetic acid. The alkali metals, Mn, Fe, Co, Ni, Cu and Zn, occur in this form, as well as the oxyanions of B and Mo. 3) Some elements, notably Cu, and to a lesser extent Zn, are involved in metal chelates. In the laboratory, these elements can be extracted with strong complexing agents, such as ethylene-diaminetetra-acetic acid. 4) Some of the mobilized trace elements become incorporated in the oxides and hydroxides of Al, Fe and Mn. For example, the fixation of Co in Mn minerals has been reported[53]. 5) Trace elements can become immobilized again by being incorporated into stable secondary minerals.

THE LOCATION OF TRACE ELEMENTS IN SOILS

1. Distribution of trace elements with respect to soil particle size

(i) *Introduction.* The particle size fractions normally considered are sand (2-0.02 mm), silt (0.020-0.002 mm), and clay (<2 μm). The distribution of trace elements, as a function of particle size, is dependent on a number of factors, including the mineralogy of the soil, the parent material, the time and intensity of weathering, the ionic radius, and preferred coordination number of the elements. The concentrations of the elements Ti, V, Cr, Mn, Fe, Co, Cu, Ni, and Zn, generally increase, with a fall in particle size from sand to clay.

Some of these trace elements are discussed below to illustrate the effect of particle size on their distribution, and also to show some of the causes for the distributions.

ii) *Iron, titanium and vanadium.* Berrow et al.[54], in a study of the A and B horizons of some Scottish podzols, found an increase in the contents of Ti and V with decreasing particle size. In the case of Fe, no increase in concentration occurred with a decrease in particle size in the A horizons, but there was a four-fold enrichment in the clay, compared with the sand, in the B_2 horizons. This suggests that Fe had been translocated from the A horizon, and had accumulated in the clay fraction of the B_2 horizon. On the basis of evidence obtained with a scanning electron microscope, Berrow et al. suggested that the accumulation of Ti in the clay fraction was achieved by physical disintegration of the anatase and ilmenite present, with subsequent dissolution and then reprecipitation as clay sized anatase.

Unlike Ti and Fe, vanadium is not usually present in soils in a distinct mineral form, but usually occurs either substituting for Fe in iron oxides and ferromagnesian minerals (for example, in pyroxenes and biotites), or it is adsorbed on to clay particles[55]. In the Scottish soils studied by Berrow et al., the mobilized V is probably not adsorbed by the secondary oxides of Fe, because Fe released by weathering in the A_2 horizons of these podzols would be leached to a lower horizon, and adsorbed onto clay particles, rather than precipitated as secondary oxides. A greater proportion of V can be extracted from the clay fraction with acetic acid, than for Ti, which is consistent with the adsorption of V onto clay minerals as an exchangeable cation.

In terms of the redox potential and the acidity of the Scottish podzols, where the pH is often <4.5, the vanadyl cation VO^{2+} is probably the stable form of V[54]. Humic acids

in the soil could also play a role in the reduction of meta-vanadate, VO_3^-, to the vanadyl ion, VO^{2+}. Results of an electron paramagnetic resonance study of E.D.T.A. soil extracts suggest that V released in weathering is present in the vanadyl form, sorbed to the exchange sites of the clay[56].

(iii) *Manganese*. In three catenas in Israel, on basalt, dolomite and limestone[57], the Mn concentration was found to decrease with particle size; this was most pronounced in the toeslopes. In contrast, other catenas on granite rocks and derived soils, had a high Mn concentration in the clay fraction, compared with the sand[54,55]. To investigate this difference in behaviour, Yaalon et al.[57] studied the mafic minerals present in the parent basalt rocks - augite and olivine - which are host minerals for Mn[58]. They found a high Mn content in the basalt and non-clay fractions of the soil. Precipitation of mobilized Mn in concretions further decreases the concentration of Mn in the clay fractions[59]. The granite rocks of the other catenas weather more readily, producing a well drained, quartz-rich soil, poor in Mn, but the mobilized Mn can become immobilized in the clay and organic matter fractions.

In yet another study, Mn concentrations were found to decrease with decreasing particle size[60]. This was attributed to the formation of hydrated Mn oxide precipitates on coarser particles. Manganese will not precipitate on the moist acid surfaces of the finer particles because of its sensitivity to decreases in reduction potential and soil acidity.

(iv) *Mineralogy*. In a study of a Canadian soil by Dudas and Pawluk[61], aspects of soil mineralogy were used to explain trace element enrichment in clays. It was suggested that the various elements show different preferences for substitution sites in crystalline silicates. The distribution of mica (especially biotite) in the three particle size fractions, was found to be highly correlated with the distribution of Zn, which is able to substitute for Fe in the biotite lattice, both these ions having similar ionic radii (Zn(II), 74 pm, and Fe(III), 64 pm). The distribution of Fe is also determined by biotite because no other ferromagnesian minerals were detected. The distribution of Cu was found to be related to the distribution of both feldspar and mica in the three size fractions. Copper (72 pm) can substitute for Fe in ferromagnesian minerals, and Ca^{2+} in plagioclase feldspars. Finally, Co(II)(74 pm) can substitute for Fe(III) and Mg^{2+}, and is therefore concentrated in the early phase ferromagnesian minerals, such as biotite and hornblende.

(v) *Ionic radius*. The ionic radius of trace elements is of significance in explaining their enrichment in clay fractions. Andersson found a linear correlation between octahedrally coordinated trace metals and the clay content, and as the ionic radius decreased, the correlation became more significant[62]. Andersson found that Cr(III), Mn(II), Co(II), Ni(II), Cu(II) and Zn(II) ions are able to occupy the same octahedral positions as Al, Fe and Mg. As soil development occurs, these ions become trapped and fixed in these positions, with the smaller ions being fixed more effectively. Larger ions, such as Pb(II) and Cd(II), are less likely to occur in

octahedral coordination.

2. Trace element adsorption by clay minerals

The clay minerals, which are the major inorganic ion-exchange materials in soils, include montmorillonite, illite, kaolinite, and to a lesser extent vermiculite. Their cation exchange capacity varies from 1 meq g^{-1} for montmorillonite to less than 0.1 meq g^{-1} for some kaolins[58]. The cation exchange capacity is due, in part, to excess negative charge, resulting from substitution around the tetrahedrally coordinated silicon and octahedrally coordinated aluminium in the layer lattices of the clay minerals, and partly from negative charges on the terminal oxygen atoms at the edges of the lattice. The strength of binding of different ions at these sites varies.

The main interaction of trace elements with soils and clay minerals is one of surface adsorption. An order of difficulty of displacement of trace elements from clay is: $Cu^{2+} > Pb^{2+} > Ni^{2+} > Co^{2+} > Zn^{2+}$ [58]. However, the order will depend on the concentration of the ions in solution, and the presence of organic acids, such as fulvic acid, which may act as complexing agents.

Norrish[51] reported high concentrations of Fe, Ni and Zn in clay. During weathering, Fe released from minerals may be removed from the soil, but much of it can be held in clay minerals, by adsorption or substituting for Al. Micas often contain several percent Fe, and many black soils formed from basalt contain the majority of the Fe in the clay mineral montmorillonite. High Zn concentrations in clays is due to the Zn entering the silicate layer lattice structure; for

example, the montmorillonite mineral sauconite contains up to 30% ZnO [51].

3. Trace elements in hydrous Mn and Fe oxides

(i) *Introduction.* The oxides and hydroxides of Mn and Fe, which are ubiquitous in soils, are formed by the chemical weathering of igneous rocks, and by the metamorphic alteration of primary oxides. The Mn and Fe species control the concentrations of many elements in soil solutions, especially the first row transition metals, by coprecipitation, substitution and surface adsorption[63-65].

Jenne[63] proposed that the hydrous oxides of Mn and Fe act as a sink for trace elements in soils (see Table 3.2). These oxides occur as coatings on soil particles, and as fine discrete particles, in clusters and aggregates of colloidal size. Because of the large surface area of the Mn and Fe species, they exert a chemical influence, on other elements and compounds, far out of proportion to their concentration. The surface areas of ferromanganese concretions and minerals, such as birnessite can be up to 350 $m^2\ g^{-1}$ [65].

Iron oxides occur in soils as hematite (Fe_2O_3), goethite (FeOOH), lepidocrocite (α FeOOH), maghemite (γ Fe_3O_4), magnetite (Fe_3O_4), and hydrated amorphous ferric hydroxide ($Fe(OH)_3 \cdot nH_2O$) [64]. Manganese oxides occur in a wider variety of minerals, the main ones being birnessite ($(Ca,Mg,Na_2,k_2)_x Mn(IV)Mn(II)(O,OH)_2$), lithiophorite ($Li_2Al_8(Mn(II),Co,Ni)_2Mn(IV)_{10}O_{35} \cdot 14H_2O$), todorokite ($(Mn(II),Mg,Ca)Mn(IV)_6O_{13} \cdot 3\text{-}4H_2O$), hollandite ($Ba(Mn(IV),Fe(III))O_{16}$), pyrolusite ($MnO_2$), and amorphous

oxyhydroxides[66].

(ii) *Trace elements in the hydrous oxides of Mn and Fe.* The proportion of trace elements associated with the hydrous oxides of Mn and Fe has been considered by many workers[8,67-71]. In a study of surface and illuvial horizons of podzolic soils, Le Riche[8,67] dissolved amorphous Fe oxides and associated trace elements, with an ammonium oxalate solution. While the extract contained about 5% of the soil by weight, it contained 20-80% of the total V, Cr, Mn, Fe, Co, Ni and Cu in the soil. In a study on Zn in soils, White[68] examined several soil samples from Tennessee. He concluded that 30-60% of the total Zn in these soils was associated with Fe oxides, that 20-45% of the Zn is held in the lattice positions of clay minerals, and that 1-7% is in base-exchange positions on the clay minerals.

Ng and Bloomfield[69] studied trace elements dissolved by the action of anaerobically fermenting plant material. Although the resulting solutions were stable to atmospheric oxidation, the presence of ferrous ions and aeration caused coprecipitation of trace elements with ferric oxide. Molybdenum and V were almost completely coprecipitated, as were substantial amounts of Cu and Zn, but only 5% of the Mn, Co and Ni were coprecipitated. Ng and Bloomfield also considered the extent to which sorption on ferric oxide was involved in the coprecipitation process. They found that sorption was more pronounced at higher pH, and that the amount sorbed was greater for Cu and Zn, than for Co and Ni.

There is evidence that Mn oxides are better trace element scavengers than Fe oxides. For instance, McLaren and

Crawford[72] found that the strength of sorption of Cu onto various soil components was in the order: Mn oxides > organic matter > Fe oxides > clay minerals.

Cobalt is an element which several authors have claimed is concentrated by Fe oxides in soils[70,71,73] but it is now generally accepted that Co in soils is mostly concentrated by the less abundant Mn oxides[51,53,66,74]. Nickel, Cu and Zn are often concentrated in Mn oxides as well[51,53,63,66]. The association of Co with Mn minerals has been extensively studied because of its importance in agriculture. Adams et al.[75] examined the effect of adsorption of Co on Mn oxide surfaces, on the availability of Co. They found that the uptake, by clover, of Co applied to pastures, was inversely related to the total Mn content of the soil. They concluded that soils with Mn contents from 100-1000 μg g^{-1}, required higher than normal dressings of Co salts for relief from Co deficiency, and that for soils containing more than 1000 μg Mn g^{-1}, the use of Co salts as a fertilizer was not a practical solution for Co deficiency.

Another example of the importance of Mn and Fe oxides as scavengers for trace elements, has been demonstrated from a study of the site used for the disposal of radioactive liquid waste in Oak Ridge, Tennessee[65]. River sediments, extracted with a dithionite solution, contained ^{60}Co, from which it was concluded that ^{60}Co was mainly associated with Mn oxides, and to a lesser extent, with Fe oxides. Deliberate addition of Mn oxides to disposal pits may be a method to concentrate some radioactive metals, such as ^{60}Co and actinides.

(iii) *Ferromanganese concretions.*

(a) Introduction. Ferromanganese concretions have been studied extensively[51,53,59,63,66,71,74] because soil and marine concretions are known to concentrate trace elements such as Mn, Fe, Co, Ni, Cu and Zn. Marine concretions in particular, are regarded as a potential economic source of Co and Ni. Marine concretions generally contain more Mn than soil concretions, and have lower Al and Si contents[59]. Since basically the same minerals are involved in marine and soil concretions, mechanisms suggested for the sorption and fixation of trace elements in marine concretions are considered applicable to soil concretions. However, one distinct difference between the two types of concretions, which may well affect their chemistry, is that in the soil there is often an alternation between wet and dry environments while marine concretions are always in contact with water.

Some trace elements often associate with either Mn or Fe. In an examination of interelemental relationships in ferromanganese concretions, Childs[76] found a significant positive correlation between Fe and Ti, P, Mo, V, S and Cu, and between Mn and Co, Ni and Zn. Iron did not correlate with Mn. In general, these differences can be attributed to the dissimilar surface charges of Mn and Fe oxides[77] at the pH values (4.0 - 9.0) in soils. Hydrous Fe oxides are positively charged or near neutral, and will attract oxyanions, while hydrous Mn oxides are negatively charged, and will therefore attract cationic species. Means et al.[65] considered the surface charge of Mn oxides in detail. They found the surface charge of freshly precipitated birnessite is unusually high,

exceeding 100 μC cm^{-2} at pH 8. The zero point of charge (or the pH at zero net surface charge) for fresh birnessite and amorphous Mn(IV) oxides is about pH 2. Therefore, the Mn oxides have a negative charge and a high cation exchange capacity over the pH range of most soils.

(b) Factors controlling the hydrous Mn and Fe oxides, and trace elements in soils and concretions. The concentrations of trace elements in the soil water are controlled by the factors which influence the sorption and desorption of the trace elements by the hydrous oxides of Mn and Fe. The principal factors affecting the availability of trace elements in soils are the redox potential (Eh), soil acidity (pH), the concentrations of the metals, and the concentrations of other ions capable of forming inorganic complexes and organic chelates. The most significant of these factors are likely to be Eh and pH[63]. A serious limitation in any study of this sort, is the lack of reliable data on the Eh of the pore water of sediments and soils, and how this is affected by liming, fertilization and irrigation.

On the other hand, it is well documented that in the soil there are microorganisms which oxidize Mn and Fe salts to insoluble oxides[78], and it has been suggested that the formation and deposition of Mn and Fe oxides in nature is due generally to biological activity[79]. Ehrlich isolated bacteria from Mn concretions collected from the Atlantic Ocean, and suggested that these microorganisms played a role in the formation of the concretions[80]. However, because of the long times involved and the conditions of low temperature and high pressure, relatively little is known about the mechanisms of

concretion formation in the sea, and the role that microorganisms play in the process, or the possible utilization of the energy obtained from the oxidation of Mn(II) by the microorganisms[78]. It is only recently that bacteria of a similar nature have been isolated from soil concretions, although the question of their role remains unanswered[78,79].

It is likely that both chemical factors (such as Eh, pH) and biological factors (microorganisms) are involved in influencing trace elements in soils and in concretion formation. In an indirect way, microorganisms may oxidize or reduce Mn and Fe compounds without enzymatic interaction. For example, they may cause the oxidation and precipitation of Mn or Fe by generating an oxidizing environment through oxygen production or carbon dioxide useage. In addition, microorganisms may produce a reducing environment by forming metabolic end products which can act as reductants of Mn or Fe oxides.

In this thesis, emphasis will be given to the chemical aspects of concretion formation.

(iv) *Fixation of Co in ferromanganese concretions.* A number of mechanisms have been proposed to explain the accumulation of certain trace elements in terrestrial and marine ferromanganese concretions. It has been mentioned earlier in this chapter how the Mn and Fe phases of ferromanganese concretions can carry a positive or negative charge which is dependent on the pH of the medium, and that anions or cations can be attracted to such surfaces[59,65,81]. McKenzie[82] carried out sorption studies of Co(II), Ni(II), Cu(II) and Zn(II) on to the surfaces of terrestrial Mn concretions. He found that although more Co was sorbed than

Ni, even greater amounts of Cu were sorbed. Thus, sorption alone does not account for the marked accumulation of Co in the Mn oxides of soils. In an experiment to assess the effect of aging on the non-extractable (in 2.5% acetic acid) fraction of sorbed Co, Ni, Cu or Mn oxides, McKenzie found that the amount of non-extractable Co increased sharply with time until, after 6 months, 86% of the Co originally sorbed was non-extractable. Non-extractable Ni and Cu, in contrast, showed only a slight increase with time.

In sorption studies on synthetic Mn oxides minerals it was found that the amount of metal ion sorbed was balanced by the total amount of Mn(II), K^+ and H^+ released into the solution[53]. Cobalt replaced less K^+ and H^+, but more Mn(II) ions, than did Cu or Ni, and the uptake of Co with time was greater than that of Ni or Cu.

It would appear from the above experimental data that there is a specific interaction taking place between Co and the Mn minerals, and that the mechanism is not simply adsorption of Co onto the surface. A number of mechanisms have been proposed, and these are listed in Table 3.3, along with some of the relevant factors for each mechanism. McKenzie[53] proposed a mechanism for the preferential fixation of Co in Mn oxides, whereby the Co(II) ions are rapidly adsorbed onto the surface of the minerals, while exchangeable Mn(II), K^+ and H^+ ions are displaced. Sorbed Co(II) ions are then said to diffuse into the surface layers of the crystal lattice, where, it is claimed, they are oxidized by Mn(III) ions, which are then replaced by the Co(III) ions.

The electrode potential for the oxidation of Co(II) by Mn(III) is negative;

$$Co^{3+} + e \rightarrow Co^{2+} \qquad E^{o} = +1.84\ V$$

$$\underline{Mn^{3+} + e \rightarrow Mn^{2+} \qquad E^{o} = +1.51\ V}$$

$$Co^{2+} + Mn^{3+} \rightarrow Co^{3+} + Mn^{2+} \qquad E^{o} = -0.33\ V$$

Consequently, the free energy change $\Delta G(= -nFE)$ of the reaction is positive (+32 kJ mol^{-1}), and so the reaction is not favoured thermodynamically. (While these calculations refer to aqueous conditions, they are a guide to the energy changes involved.) The reaction however has a gain in crystal field stabilization energy. In Table 3.4, details of the crystal field stabilization of metal ions in an octahedral crystal field are given for an octahedrally coordinated water environment, where Δ_o is the energy difference between the t_{2g} and e_g orbitals (Figure 3.1). The crystal field stabilization energy (C.F.S.E.) is a function of both Δ_o and the electronic configuration of the

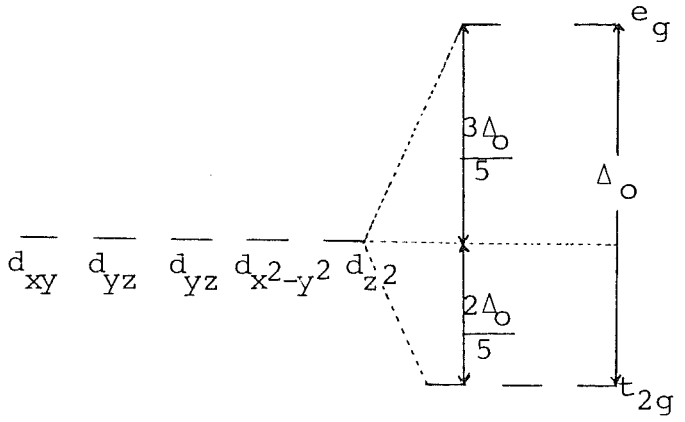

Figure 3.1. Relative energy levels of d orbitals of a transition metal ion in octahedral coordination

TABLE 3.3 Proposed Mechanisms for the Incorporation of Co into Manganese Oxides

Mechanism	ΔG (kJ mol^{-1})	Δ C.F.S.E. (kJ mol^{-1})	Ionic Radius (pm)
$Co(II)_{(aq)} + Mn(III)_{(s)} \rightarrow Co(III)_{(s)} + Mn(II)_{(aq)}$	+32	+311	Mn(II) = 80 Mn(III) = 66
$Co(II)_{(aq)} + Fe(III)_{(s)} \rightarrow Co(III)_{(s)} + Fe(II)_{(aq)}$	+103	+512	Fe(III) = 64
$2Co(II)_{(aq)} + Mn(IV)_{(s)} \rightarrow Co(III)_{(s)} + Mn(II)_{(aq)}$	-60	+132	Mn(IV) = 54

TABLE 3.4 Crystal Field Stabilization in an Octahedral Crystal Field[87]

Ion	D Electron	Electronic Configuration	C.F.S.E. (kJ mol^{-1})	$M(H_2O)_6^{n+}$ Δ_o (kJ mol^{-1})	$M(H_2O)_6^{n+}$ CFSE (kJ mol^{-1})
Mn(IV)	3	t_{2g}^3	$6\Delta_{o/5}$	275	330
Mn(III)	4	$t_{2g}^3 e_g^1$	$3\Delta_{o/5}$	250	151
Mn(II)	5	$t_{2g}^3 e_g^2$	0	-	0
Fe(III)	5	$t_{2g}^3 e_g^2$	0	-	0
Fe(II)	6	$t_{2g}^4 e_g^2$	$2\Delta_{o/5}$	124	50
Co(III)	6	t_{2g}^6	$12\Delta_{o/5}$	222	534
Co(II)	7	$t_{2g}^5 e_g^2$	$4\Delta_{o/5}$	89	72
Ni(II)	8	$t_{2g}^6 e_g^2$	$6\Delta_{o/5}$	102	123
Cu(II)	9	$t_{2g}^6 e_g^3$	$3\Delta_{o/5}$	155	93
Zn(II)	10	$t_{2g}^6 e_g^4$	0	0	0

metal ion (Table 3.4). In the oxidation of Co(II)(t_{2g}^5 e_g^2) which has an octahedral C.F.S.E. of 72 kJ mol^{-1}, to Co(III) (t_{2g}^6), with a C.F.S.E. of 534 kJ mol^{-1}, there is a gain in stabilization of 462 kJ mol^{-1}. The reduction of Mn(III) to Mn(II) is accompanied by a loss of C.F.S.E. of 151 kJ mol^{-1} (Table 3.4), hence the overall C.F.S.E. change for the reaction is +311 kJ mol^{-1}. Since Mn(II), Co(II), Cu(II), Ni(II) and Zn(II) all have lower octahedral C.F.S.E.'s than Mn(III), this energy will not be a driving force for the replacement of Mn(III) by the divalent metal ions.

Glasby[83] has criticised this application of crystal field theory to the interpretation of a mechanism for the accumulation of Co in Mn oxide phases of concretions. Glasby advocates a consideration of the total free energy change of the reactions in any mechanism, and not merely a consideration of the C.F.S.E., which is a minor part (<10%) of the overall free energy. In reply to Glasby's criticism, McKenzie[84] has pointed out that for the non-stoichiometic Mn oxides being considered, there is a lack of accurate thermodynamic data available, and even more so with respect to the inclusion of Co(II) ions in the surface of such oxides, which makes a consideration of the overall free energy for these processes difficult.

Glasby[83] also claimed that the Mn(III) ion is unlikely to be stable in manganese minerals, as suggested by McKenzie[53], and Loganathan and Burau[85]. To illustrate this point, Glasby used the free energy data[86] for the compounds in the reaction;

$$2Mn(OH)_{3(s)} \rightarrow Mn(OH)_{2(s)} + MnO_{2(s)} + 2H_2O_{(aq)}$$

ΔG°(kJ mol^{-1}): 2 x -757.3 -616.5 -464.8 2 x -237.2

to show that the free energy change is -41.1 kJ mol^{-1}. On this basis, Glasby claimed that a mechanism for the accumulation of Co by Mn oxides is unlikely, in terms of a replacement of Mn(III) by Co(III).

McKenzie[53,84] maintained that Mn(III) does occur in manganese minerals (such as hausmannite (Mn_3O_4)) in octahedral sites. McKenzie considered that thermodynamic arguments are inconclusive in the present context, for although $Mn(OH)_3$ may be unstable with respect to disproportionation, the free energy change for the reaction;

$$Mn_2O_{3(s)} + H_2O_{(aq)} \rightarrow MnO_{2(s)} + Mn(OH)_{2(s)},$$

G^o(kJ mol^{-1})	-888.3	-237.2	-464.8	-616.5

is +44.2 kJ mol^{-1}, and therefore Mn(III) is stable in this form.

It should be pointed out that all of the free energy changes discussed above are small, and cannot be taken as an adequate guide to thermodynamic stability. Also investigators appear to have not discussed the major energy factor for solids, which is the lattice energy.

McKenzie's mechanism[53] of Co(III) replacing Mn(III) does not explain the correlations between Co and Fe which have been found in concretions by several workers[69-71]. Burns and Fuerstenau[71] found that Co was correlated with Fe in marine concretions, and that Ni, Cu and Zn correlated with Mn. They suggested that divalent Ni, Cu and Zn replaced Mn(II), and the Co(III) substituted for Fe(III), in the hydrated iron oxide phase, $FeOOH \cdot nH_2O$, of ferromanganese concretions. If the oxidation of Co(II) is by Fe(III)

ions in the concretion, this process is not favoured thermodynamically, but does have a gain in C.F.S.E. (Table 3.3) to overcome this.

In a later study, Burns[87] rejected his former proposal, as he now claimed it is unlikely that Co(III) ions will enter into isomorphous substitution with Fe(III) ions in the $FeOOH \cdot nH_2O$ phase, or with high spin Mn(II) or Mn(III) ions in the Mn oxide phase of the concretions (mainly high spin Fe(III), Mn(II) and Mn(III) oxides are found in minerals[87]). This is because of, firstly, the ionic radii of Fe(III)(64 pm), Mn(II) (80 pm) and Mn(III)(66 pm) are larger than that of the low spin Co(III)(53 pm) ion. The differences, 17, 34 and 19% respectively, are, for Fe(III) and Mn(III), just outside that normally expected (±15%) between the ionic radii of the host and substituent ions[87], and therefore there may be some doubt in this argument for these cases. Secondly, the small Co(III) cation is said to be the reason why CoOOH has a different crystal structure from any of the FeOOH and MnOOH polymorphs[74].

The closeness of the ionic radii of Co(III)(53 pm) and Mn(IV)(54 pm) suggests that Co(III) could substitute for Mn(IV) ions. Burns[74] proposed that hydrated cations, including Co(II), are initially adsorbed on to the surfaces of certain Mn(IV) oxides, near vacancies found in the chains or sheets of edge-shared $[MnO_6]$ octahedra. Then, fixation of Co occurs as a result of the oxidation of the adsorbed Co(II) ions by Mn(IV) ions, and replacement of the resulting Mn(II) ions by low spin Co(III) ions in the octahedral environment. Such a process is;

$$2Co^{2+}_{(aq)} + 2OH^{-}_{(aq)} + 2H_2O_{(aq)} + \delta\text{-}MnO_2 \rightarrow 2Co(OH)_{3(s)} + Mn^{2+}_{(aq)}$$

ΔG^{o}(kJ mol^{-1})	2x-53.6	2x-157.3	2x-237.2	-464.8	2x-596.6	-227.6

and the overall free energy change is -59.8 kJ mol^{-1}.

This mechanism has a favourable crystal field stabilization energy, because the C.F.S.E.'s for Co(III) and Mn(II) are 534 and 0 kJ mol^{-1} respectively, while the reactants species Co(II) and Mn(IV) have C.F.S.E.'s of 72 and 330 kJ mol^{-1}, so that the net gain in C.F.S.E. is 132 kJ mol^{-1}. The C.F.S.E. of the Mn(IV) ion in an oxide structure is not known[53], and the values for Mn(IV) in Table 3.4 are approximate values calculated from parameters given by Figgis[88]. It is also likely that there would be a loss of lattice energy due to the replacement of Mn(IV) by Co(III), although the Co(III) ion could occupy a previously vacant position in the lattice[74].

Burns[74] offers an explanation of the Fe-Co correlations that some workers have observed in ferromanganese concretions. Ferric ions are randomly distributed in the octahedral sites of δ-MnO_2. The structural similarities between δ-MnO_2 and $FeOOH \cdot nH_2O$ make them amenable to epitaxial intergrowths, which probably initiate nucleations, and lead to the intimate association of Mn and Fe oxide phases in ferromanganese concretions. Therefore, an apparent Fe-Co correlation could actually be a Mn-Co correlation, with the δ-MnO_2 phase epitaxially intergrown with $FeOOH \cdot nH_2O$.

Murray and Dillard[89], using X-ray photoelectron spectroscopy, showed the presence of Co(III) adsorbed on to MnO_2. The manganese spectra were characteristic of Mn(IV). This

evidence supports Burns[74] proposal of a Co(III)-Mn(IV) mechanism, and confirms that an important factor of Co accumulation in Mn oxides is its ability to be oxidized from Co(II) to Co(III), in the process gaining C.F.S.E.

4. Trace element associations with organic matter

(i) *Types of organic matter.* Organic matter in soil is arbitrarily divided into two categories - humic and non-humic substances[90]. The non-humic substances include compounds still possessing recognizable chemical characteristics. This group includes carbohydrates, proteins, peptides, amino acids, fats, waxes, and various low molecular weight organic substances such as fumaric and oxalic acids. Usually these substances have short lifetimes, as they are rapidly attacked by soil microorganisms.

Most soil organic matter falls into the category of humic substances. They are amorphous, brown or black, hydrophilic, acidic, and in the molecular weight range from hundreds to tens of thousands. Humic substances are divided into three groups: 1) humic acids, which are soluble in dilute alkali, but acid insoluble, 2) fulvic acids, which are soluble in both acid and alkali, and 3) humin, which is insoluble in both acid and alkali. Fulvic acids tend to have lower molecular weights and a higher content of oxygen-containing functional groups per unit weight, than do humic acids and humin. Humic fractions are resistant to microbial degradation, and can form stable water-soluble and water-insoluble salts and complexes with metal ions and hydrous oxides. They can also react with clay minerals.

(ii) *Organic complexes.* In a study of the concentrat-

ions and forms of trace elements in soil solutions, Hodgson et al.[91] found that the concentrations of Co, Cu and Zn extracted in water from surface horizons were less than 1 μm, while the concentration of Mn ranged from 0.02 to 68 μm. In acid soils, the dominant inorganic species is M^{2+}(Mn, Co, Cu and Zn), while in neutral and alkaline soils the monovalent hydroxy cation, $M(OH)^{+}$, becomes more important. Hodgson et al. also found significant portions of the trace elements tied up in complexes, about 25% of the Co in the extracted solution being complexed, and 50% of the Zn, 90% of the Mn, and up to 99% of the Cu extracted also being complexed. Although the chemical nature of these complexes is not clear, they are probably anionic[92], and involve organic ligands, since the amount of Cu and Zn complexed correlates with the organic matter content of the soils[91].

Geering et al.[93] found that in the solution extracted with water from one soil, there were at least two groups of organic containing compounds present, with weakly acidic properties, which were associated with Cu and Zn. One of the groups separated was relatively inert and non-dialyzable, and the other was dialyzable, and had acidic characteristics, attributable to aliphatic and amino acid residues.

(iii) *The interaction of trace elements and soil organic matter.* Humic compounds form very stable complexes with a number of metallic ions. There are several types of interaction possible: 1) a simple salt formation by the neutralization of the negative charge on the humic acid, 2) the interaction of a polar humic group with the waters of hydration around the metal ion, and 3) a coordination

compound, in which the carboxylate group of the humic acid is directly bonded with a metal ion. It is likely that for divalent cations, the interactions will be through H-bonding between the waters of hydration and the carboxylate group of the humus, but for the trivalent cations, such as Al^{3+} and Fe^{3+}, coordination will be with the cation itself[2]. The functional groups in the organic matter, which are bonded to the metal ions, are probably carboxylate (COO^-), phenolic -OH, carbonyl groups (C=O), and $-NH_2$ groups[94].

Fulvic, and other humic acids in the soil, probably preferentially complex Al^{3+} and Fe^{3+} ions, due to their greater abundance. Humic polymers will also complex other trace element ions, and in particular, they complex Cu^{2+} strongly. A measure of the strength of the metal ion-organic matter interaction can be gauged by the drop in the pH of a solution, when the chloride or sulphate of the ion is added to a solution of organic acids[95]. Experiments showed that the order of the strength of interaction of the trace element ions and organic matter, is as given below. The ionic potentials (charge/radius) are also listed.

	Fe^{3+}	> Al^{3+}	> Cu^{2+}	>> Zn^{2+}	> Ni^{2+}	> Co^{2+}	> Mn^{2+}
Ionic potentials:	4.7	6.0	2.8	2.7	2.8	2.7	2.5

It is apparent that the interaction is determined, to a large extent, by the charge density of the metal ion.

The stabilities of the metal-organic complexes increase with pH, and then sharply fall, as insoluble hydroxides form. Schnitzer and Skinner[96] found that complexes of fulvic acid with Al^{3+} ions broke up at pH 8, and with Fe^{3+} ions at pH 9, but those with Cu^{2+} ions did not break up until pH 10.

(iv) *Stability constants of metal-fulvic acid complexes.* Schnitzer[97] determined the stability constants of water soluble complexes formed between fulvic acid and some metal ions, at pH 3.5 and 5.0. The stability constants were greater at pH 5.0, possibly due to increased acid dissociation of the functional groups, especially carboxylate groups;

$$R\text{-}COOH + H_2O \rightleftharpoons R\text{-}COO^- + H_3O^+$$

The order of stability of the metal ion-fulvic acid complexes, at pH 3.5 is;

$$Al^{3+} > Cu^{2+} > Fe^{2+} > Ni^{2+} > Co^{2+} > Zn^{2+} > Mn^{2+},$$

and at pH 5.0;

$$Fe^{3+} > Cu^{2+} > Fe^{2+} > Ni^{2+} > Mn^{2+} > Co^{2+} > Zn^{2+}.$$

The order deviates significantly from the Irving-Williams order $Mn^{2+} < Fe^{2+} < Co^{2+} < Ni^{2+} < Cu^{2+} < Zn^{2+}$. Two notable features of the order of stability of the fulvic acid complexes, are the high stability of the Fe^{2+} complex and the low stability for the Zn^{2+} complex. The formation of the Cu^{2+}-fulvic acid complex, at pH 5.0, may be represented by the equation;

$$Cu(H_2O)_6^{2+} + 2 \left[\begin{array}{c} COO^- \\ \diagup \\ \diagdown \\ OH \end{array}\right] \rightleftharpoons \left[\begin{array}{c} COO \\ \diagup \\ O \end{array}\right] Cu \left[\begin{array}{c} OOC \\ \diagdown \\ O \end{array}\right] + 2H^+$$

The stability constants measured for the metal ion-organic matter complexes are an average value for sites of varying bonding strengths[94]. The constants have been determined at high concentrations of trace elements whereas at the

low metal concentrations which exist in the soil solution, the situation could well be different, and specific sites with higher bonding strengths may assume a dominant role.

The bonding of several trace metal ions to organic matter is sufficiently strong for the organic material to compete with the hydrous oxides of Mn and Fe. Fulvic acid, added to goethite, gibbsite or soil, formed complexes with Al or Fe [96]. A mixture of fulvic and other humic acids, also removed Mn from hydrous Mn oxides [98] as complexes. Such reactions may be important in maintaining these metals in solution in alkaline soils.

THE BEHAVIOUR OF TRACE ELEMENTS IN SOILS

1. The chemistry of waterlogged soils

In this section, the redox potential and soil acidity are considered as parameters which play a significant role in the chemical form that the elements take in the soil. In the following discussion on the chemistry of waterlogged soils, reference is made to Eh-pH diagrams, which are described, and their limitations noted. The effect of the loss of oxygen from the soil, on waterlogging, is also discussed, as is the major role that Mn and Fe have in determining the redox potential and soil acidity.

(i) *Redox potential (Eh) and soil acidity (pH).*

(a) Definition of Eh. For every redox system, the potential of the half reaction;

$$aA + bB + ne \rightleftharpoons cC + dD,$$

at 25°C is; $$Eh = E^{o} - \frac{RT}{nF} \ln \frac{[C]^{c}[D]^{d}}{[A]^{a}[B]^{b}} .$$

Eh is the half-cell potential relative to the standard hydrogen electrode, E^o is the standard half-cell potential, R is the gas constant, n is the number of electrons transferred in the reaction, and F is the Faraday constant. Often, the equation involves H_3O^+ ions, and so it is possible to relate Eh with pH. Eh-pH diagrams are often calculated over the Eh and pH ranges of the natural environment. Limits of pH in soils are about 4 and 9. The upper and lower limits of the redox potential, Eh, are defined by the stability of water[86]. The oxidation of water, written as a reduction reaction, is given by;

$$\tfrac{1}{2}O_{2(g)} + 2H^+_{(aq)} + 2e \rightleftharpoons H_2O_{(aq)} \qquad E^o = 1.23\ V$$

which gives $Eh = 1.23 - 0.059\ pH$,

assuming that P_{O_2} is unity. The lower limit of the redox potential, and the reduction of H^+ (which comes from water) is given by;

$$2H^+_{(aq)} + 2e \rightleftharpoons H_{2(g)} \qquad E^o = 0\ V$$

resulting in $Eh = -0.059\ pH$,

assuming that P_{H_2} is unity. These equations are drawn in Figure 3.2, and define the normal limits of the Eh and pH values found in soils.

(b) Limitations to the use of Eh-Ph diagrams. An Eh-pH diagram is a quantitative summary of redox and pH data, which can be used to predict areas of stability of species, both in the solid state and in solution. The use of Eh-pH diagrams, however, is limited, when applied to the complex

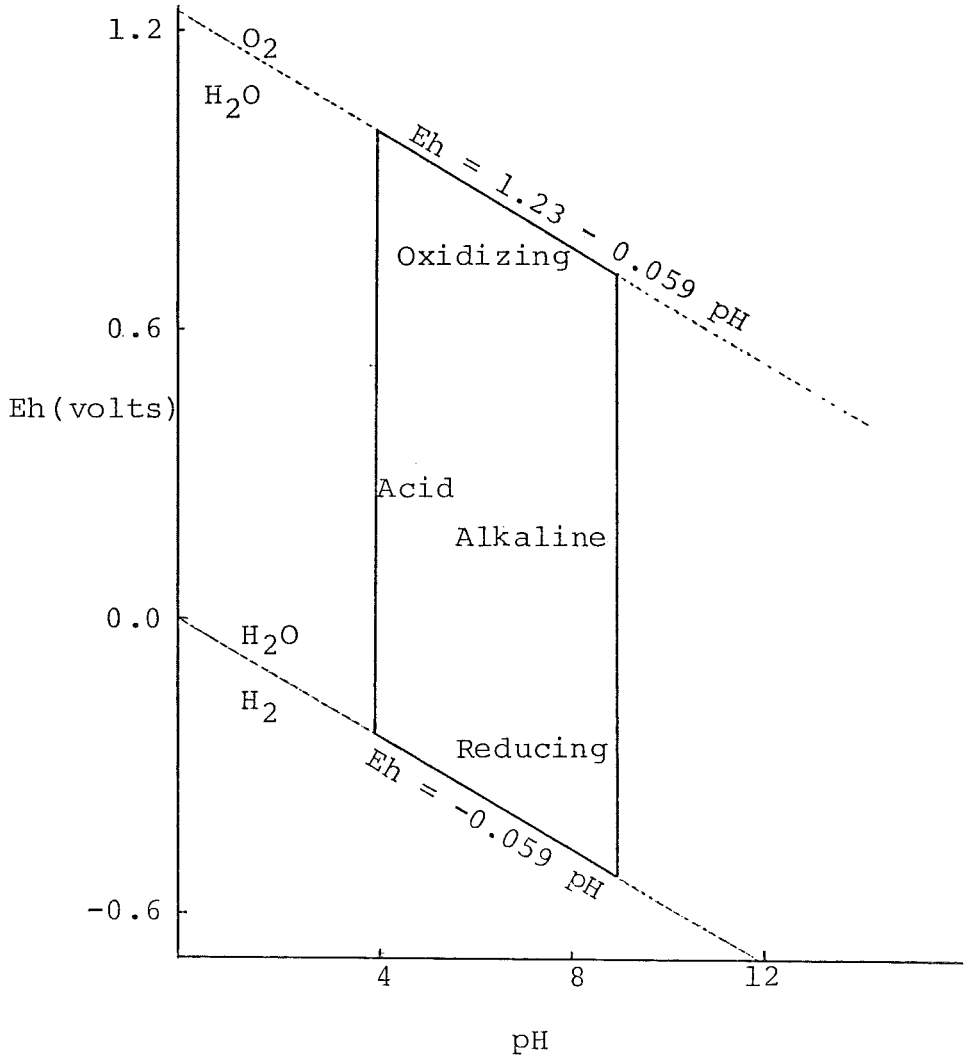

Figure 3.2. Framework for Eh-pH diagrams. The parallelogram outlines the usual limits of Eh and pH found in soil.

systems met in geology and soil science. For example, in a soil there are more variables than allowed for in an Eh-pH diagram and the diagrams are calculated assuming pure compounds, which are rarely the case in soils.

Other limitations to the use of Eh-pH diagrams include the fact that calculations are made for T = 25°C and P = 101.3 kPa. Also, it is assumed that equilibrium has been attained; in flooded soils, this is not so. Irreversible

reactions, such as the loss of gaseous products (N_2, NH_3), hinder further the attainment of true equilibrium conditions. Finally, complex formation in soils may alter redox potentials and redox equilibria between inorganic ions.

Irrespective of these limitations, Eh-pH diagrams do have a useful contribution to make in summarizing soil redox reactions.

(ii) *Chemical changes in waterlogged soils*[2,99,100]. Saturation of a soil with water causes marked changes in the normal chemical and biological reactions in soils, principally because of the oxygen deficiency. Soil bacteria use up any free oxygen dissolved in the soil water, faster than oxygen can diffuse into the wet soil. This shortage of oxygen means that anaerobic or partially anaerobic bacteria obtain their energy from biological electron transfer reactions.

The most efficient energy yielding reaction is aerobic respiration, where oxygen acts as an electron acceptor, to form water;

$$O_{2(g)} + 4e + 4H^+_{(aq)} \rightarrow 2H_2O_{(aq)}$$

However, in the absence of oxygen, other compounds in the soil such as nitrates, sulphate, manganese-oxy species and ferric ions are the oxidizing agents, for example;

$$NO^-_{3(aq)} + 2H^+_{(aq)} + 2e \rightarrow NO^-_{2(aq)} + H_2O_{(aq)}$$

$$2NO^-_{2(aq)} + 8H^+_{(aq)} + 6e \rightarrow N_{2(g)} + 4H_2O_{(aq)}$$

Also, in oxygen deficient conditions, organic matter is no longer fully oxidized to CO_2 and H_2O, but is partially oxidized to fatty acids, hydroxy-carboxylic acids, alcohols and

ketones. Some of these products can reduce ferric ions, producing soluble ferrous species[2]. Anaerobic bacteria also produce sulphides, hydrogen and methane, as products of relatively inefficient respiration processes.

Takai and Kamura[99] found that the reduction processes occurred in sequence, namely reduction of oxygen, nitrates, Mn(IV) and Fe(III). Turner and Patrick[100] also found that the reduction process was sequential. However, they showed that there is an overlapping of the various reductive steps, with reduction of Fe(III) oxides commencing before complete reduction of the Mn(IV) oxides, as is predicted by the Eh values (Table 3.5), of a typical soil[101]. This overlap may in fact, be as result of the release of coprecipitated materials; that is, reduction of insoluble ferric oxide to more soluble ferrous hydroxide, could release entrapped Mn species, coprecipitated with the ferric oxide.

TABLE 3.5 Redox Potentials for Some Processes Occurring in Soils

	Eh(mV)	
	pH 5	pH 7
$O_2 + 4H^+ + 4e \rightleftharpoons 2H_2O$	930	820
$NO_3^- + 2H^+ + 2e \rightleftharpoons NO_2^- + H_2O$	530	420
$MnO_2 + 4H^+ + 2e \rightleftharpoons Mn^{2+} + 2H_2O$	640	410
$Fe(OH)_3 + 3H^+ + e \rightleftharpoons Fe^{2+} + 3H_2O$	170	-180
$2H^+ + 2e \rightleftharpoons H_2$	-295	-413

(iii) *Manganese and iron.* As nitrate disappears rapidly in flooded soils, and as soils normally contain much more

Fe than Mn, the dominant redox species in reduced soils are the hydrous Fe systems. Ponnamperuma et al.[102] showed that the solid species involved in Fe(III)-Fe(II) hydroxide equilibria in flooded soils are the metastable substances $Fe(OH)_3$ and ferrosoferric hydroxide $Fe_3(OH)_8$. The main redox systems operating are $Fe(OH)_3$-Fe^{2+}, $Fe_3(OH)_8$-Fe^{2+} and $Fe(OH)_3$-$Fe_3(OH)_8$. The total system is portrayed in the Eh-pH diagram in Figure 3.3; for reduced soils the limits are pH = 6.5 - 7.0 and Eh = 0.1 V to -0.1 V.

Ponnemperuma et al.[103] also studied the behaviour of Mn oxide systems in flooded soils. They concluded that six manganese redox systems are involved, each system dominant at a different time. Their results show that initially, MnO_2 is reduced, partly to Mn^{2+} and partly to Mn_2O_3, and later, Mn_2O_3 and any Mn_3O_4 are reduced to Mn^{2+} (Figure 3.4). However, the redox potentials are all lower (at a given concentration of Mn^{2+} ions) than is theoretically predicted, presumably due to the contamination of the oxides with ferric and other ions. The Mn ions involved in redox equilibria in a soil are complex, non-stoichiometric oxides, and they have standard free energies of formation which are said to be less than those of more stoichiometric compounds.

The reduction reactions that occur in the soil depend on the environmental Eh and pH values. The effect of change of pH, by one unit, on Eh is not the same for all reduction reactions, as can be seen from the different slopes of lines in Eh-pH diagrams. Hence, some species are more easily reduced than others, as for instance, Mn relative to Fe. This results in Mn being more easily mobilized[57,73,104,105] than Fe in a soil.

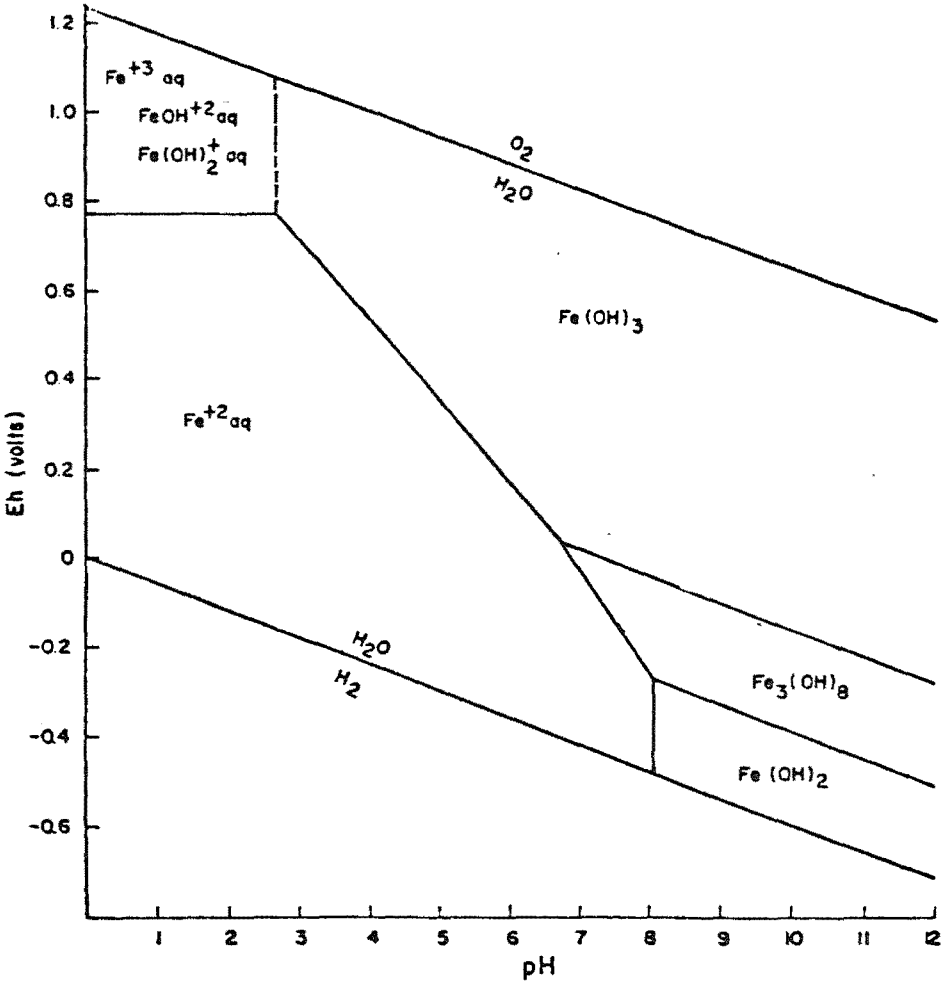

Figure 3.3. Stability areas of ferric, ferrosoferric, and ferrous hydroxides relative to Eh, pH, and an aqueous Fe^{++} activity of one millimole at 25°C.

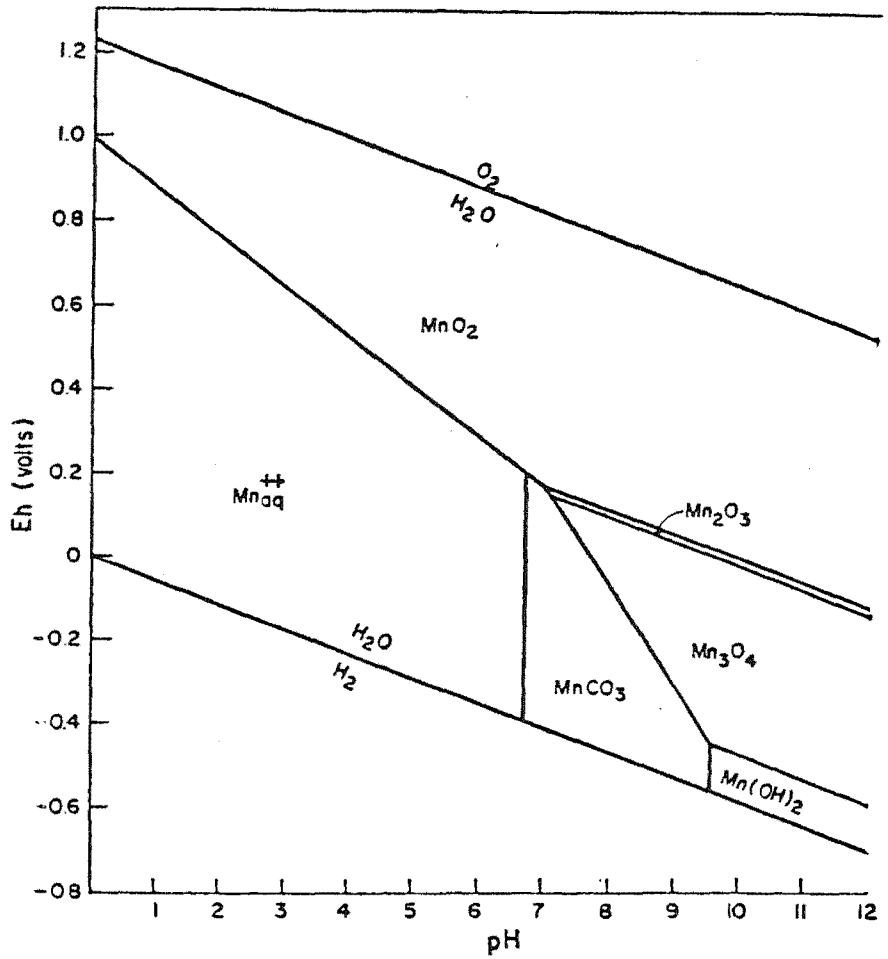

Figure 3.4. Stability areas of the hypothetical manganese oxides, $Mn(OH)_2$, and $MnCO_3$, relative to an Mn^{++}_{aq} activity of 10^{-4}, and a P_{CO_2} of 0.1 atm, at a total pressure of 1 atm, at 25°C, for flooded soils high in manganese.

The trends in the distribution of Fe and Mn in soils, and in ferromanganese concretions are well documented. In soils where ion movement is downward, concentrations of Mn are usually located lower in the profile than those of Fe, due to the greater mobility of Mn at higher Eh and pH. The reverse situation occurs in soils of restricted drainage, where ion movement is upwards. Here, as oxidizing conditions set in from above, Fe precipitates first, leaving Mn in solution, to eventually precipitate higher in the profile[105,106]. Similar segregation of Fe and Mn is also observed in Fe-Mn concretions, where successive rings of Fe and Mn deposits, reflect alternation in the Eh and pH conditions of the environment.

The earlier precipitation of Fe, relative to Mn, can be explained by reference to Figures 3.3 and 3.4. At a pH value of about 6.0-7.0, for example, Fe(III) will precipitate as $Fe(OH)_3$ and $Fe_3(OH)_8$, at a lower Eh than Mn(II) will be oxidized and precipitate to form MnO_2, Mn_2O_3, Mn_3O_4 and, if P_{CO_2} is sufficient, as $MnCO_3$. Consequently, as a waterlogged soil is beginning to dry out, and oxygen diffuses into the soil, a more oxidizing environment occurs, with a rise in the Eh value, which results in the precipitation of Fe(III). At the same Eh values, Mn(II) is still in the soil solution.

(iv) *Behaviour of other trace elements in reduced soils.* The distributions of Cu and Zn, within the soil, are also influenced to some extent, by Eh and pH, even though Cu and Zn are not themselves involved in redox reactions. Experimental data indicate that Cu and Zn, precipitated and occluded as oxides and hydroxides, were solubilized by low pH and Eh[105]. Kee and Bloomfield explain the effect of drainage on trace

element solubility as due to the influence of anaerobic conditions on the microbial decomposition of organic matter[107]. Under reducing conditions, soluble organic products from plant material decomposition, are more effective in solubilizing trace elements, than the corresponding products found under aerobic conditions. It is likely that Co(III), incorporated into hydrous Mn oxides, is also reduced and solubilized by soil reduction processes. In contrast, Reddy and Patrick[108] reported that under intensely reduced soil conditions, sulphate bacteria, utilizing sulphate ions as electron acceptors, produce sulphide, which fixes Cu and Zn, and other metal ions, that were originally in solution as organic ligand complexes.

2. The effect of impeded drainage

One of the most important factors affecting the mobilization, or otherwise, of trace elements in soil, is drainage[1]. The effect of soil aeration on the chemistry of Fe and Mn is well documented. In well drained, agricultural soils, there is normally a decrease in extractable trace elements (extracted by acetic acid or ammonium acetate) from surface horizons downwards. In poorly drained soils, greater amounts of trace elements are extracted, especially in the gleyed horizons at considerable depth. In some poorly drained soils on olivine gabbro, it was found that there was an increased extraction of V, Mn, Fe, Co, Ni, Cu and Zn, compared with similar freely drained soils[11]. Since the total Co and Ni in these lower horizons showed no increase over the levels in higher horizons, the amounts extracted could be due to Co and Ni being released, in situ, by a breakdown of the ferromagnesian minerals in which they are initially bound. In the same

study it was also reported that areas of Ni toxicity of plants in Scotland are associated with areas of restricted drainage.

3. Podzolization

Podzolic soils usually occur at well drained sites. The A_2 horizon of a podzol has been subjected to intense weathering, and consequently, the minerals remaining in this horizon are normally resistant to further weathering, or are at advanced stages of weathering. The other characteristic of a podzol is the B horizon, which is enriched with material that has been washed out of the A horizons, namely organic matter, clay and iron and aluminium hydroxides, together with their associated trace elements. In an iron podzol, the zone of accumulation occurs at the top of the B horizon[2]. Some of the features of podzolization are recorded in Table 3.2.

Mitchell[58] reported data for a Scottish podzol. The B1 horizon contained large amounts of extractable (in acetic acid) Fe and Al, as well as increased amounts of Ti, V, Cr, Mn and Cu. It was also noted that the higher amounts of extractable Ti, V, Cr and Al in the lower A2 horizon, may be evidence of mobilization and imminent translocation. After the trace elements have accumulated in the B horizon, with possible fixation by sesquioxides,oxides or as organic ligand complexes, they are not as readily extracted by dilute acid.

It is likely that most of the Fe and Al accumulated in the B horizons of podzols, were initially associated with organic matter[2]. Originally it was thought that humic acids from the humus layer, on top of the mineral soil, dissolved Fe and Al from the A2 horizons, as they leached down the

profile. However, it has been shown that humic acids from the humus layer do not dissolve iron hydroxide[2]. Instead, it appears that soluble organic compounds washed off living, or recently dead vegetation could be mobilizing the elements. Leaf drip from oak and pine trees has been shown to contain up to 1 kg ha^{-1} of polyphenols[109]. These polyphenols, which can reduce ferric ions under acid conditions, could mobilize, as water-soluble complexes, comparable amounts of Fe and Al. Polyphenols involved in these complexes are probably in the form of a polymer, after binding with other organic compounds, such as amino acids from the vegetation.

Podzolization processes are important in the genesis of the chronosequence, biosequence and toposequence soils.

4. Toposequence soils

A toposequence is a sequence of soils formed in a changing topography, in an area of constant parent material. In general, the distribution of elements depends on the way water moves in the soil, and on how dissolved compounds behave. Since drainage in a toposequence depends on the topography, so does the resulting distribution of elements.

The basic process producing a toposequence of soils, is the movement of water from the slopes of a hillside, into ground water or a river draining the area[2]. Rainwater, having fallen on the hillside, has a lateral flow, which carries the soil solution and soil particles downslope. As the ground water downslope may be near to the soil surface, there can develop a gleyed horizon, which is most pronounced in the footslope (see Table 3.2).

Percolating water removes soluble weathering products

from soils on the upper slopes, while laterally moving water carries some of these species to lower slope profiles[2]. Consequently, upper slope soils become more acidic. Lower slope profiles, on the other hand, are partially illuvial, have a higher pH, and display lesser effects due to eluviation.

Yaalon et al.[104] reported that in a toposequence of soils on basalt, there was a differentiation in elemental distributions, due to the drainage effects of the slope. The Mn concentrations increased downslope, whereas Sr, Ba and Ti decreased. They gave a mobility sequence for these elements as Sr > Ba > Mn > Co ~ Ni ~ Cr ~ V ~ Cu > Ti. It can be seen therefore, that Ti is immobile, while the decrease of Sr and Ba downslope is due to a higher mobility of these elements, resulting in their being washed out of the toposequence.

In an earlier paper, Yaalon et al.[57] showed that Mn is more mobile than Fe in three Mediterranean toposequences. Total Mn increased downslope by 50-80% through lateral transport. Although Mn is mobilized in reducing conditions, it was accumulated in the poorly drained downslope profiles, forming Mn-rich concretions.

Childs and Leslie[76] studied a toposequence of yellow grey earths, finding that compact subsoils with impeded drainage resulted in a mobilization of many elements. For two groups of elements, it was found that Fe correlated well with Ti, V, Mo and Cu, while Mn correlated well with Co, Ni, Zn and Ba.

EXTRACTION OF TRACE ELEMENTS IN SOILS

It is useful, from the point of view of soil classif-

ication and soil genesis, to differentiate between the free oxides of Fe, Al, Mn and Si, formed as secondary products of recent weathering, and those inherited (primary) from the parent material. Different extraction techniques have been developed to differentiate the types of weathering products found in soils. Some of the extractants used for this purpose are listed in Table 3.6, and a few of these will be discussed in this section.

1. The amorphous and crystalline iron oxides

McKeague and Day[110] outlined an extraction procedure which allows an approximate differentiation to be made between the amorphous forms of Fe, and finely divided crystalline Fe oxides. They used a selective extraction of soils with acid ammonium oxalate (in darkness) and a dithionite-citrate-bicarbonate solution[111], respectively. Since there is no sharp division between amorphous and crystalline material, the results from the extraction can only be an approximate guide to the different materials. The selectivity of the extractants is based on the fact that rates of dissolution are controlled by the surface area, structural order, and bonding within the oxides. The rate is greatest for amorphous material.

Le Riche and Weir[8] also determined the total free Fe oxides using acid ammonium oxalate under ultraviolet radiation, and found that the photolytic procedure extracted greater amounts of the free oxide than did the dithionite-citrate-bicarbonate method. The dithionite method is the method normally used now for free oxide determinations.

McKeague et al.[116] reported a complication which can

TABLE 3.6 Some Extractants Used in Soil Analysis

Method	Fraction of Soil Extracted	Reference
Ammonium oxalate (in darkness)	Amorphous Fe oxides	8,110,112
Ammonium oxalate	Amorphous and crystalline Fe oxides	8,110,112
Dithionite-citrate-bicarbonate	Amorphous and crystalline Fe oxides	8,111
Sodium pyrophosphate	Amorphous, organic Fe, Al	113
Ethylenediamine-tetraacetic acid	Transition metal chelates	52,114
Acetic acid, ammonium acetate	Exchangeable cations	52
Hydrochloric acid	Exchange cations	115
Water	Mobilized elements still in the soil solution in an ionic or chelated form	52

arise in the interpretation of oxalate extractable Fe values (extraction in darkness) in soils containing magnetite, due to the ability of ammonium oxalate to dissolve significant amounts of magnetite. However, the more common Fe minerals, goethite and hematite, were relatively unaffected by an oxalate treatment. McKeague and Day[110] tested the ammonium oxalate method as an aid in soil classification, and used it in developing criteria for distinguishing spodic Podzol B horizons, from other horizons enriched in Fe.

Although the distinction between amorphous and more or less crystalline forms of extractable elements is useful, a further division of the amorphous portion would be an advantage, namely inorganic, compared with organic amorphous material. For example, some soils developed in volcanic ash contain high amounts of inorganic Fe, yet they cannot be distinguished, by their oxalate extractable Fe content, from spodic horizons in which the iron is usually associated with

organic matter[116].

2. The amorphous organic fraction in soils

Aleksandrova[113] found that sodium pyrophosphate extracted humus and its complexes with Fe and Al from soils. Bascomb[117] reported that potassium pyrophosphate extracted Fe from organic complexes and amorphous gels, but not from aged amorphous hydrous oxides. McKeague[118] presented evidence that sodium pyrophosphate was reasonably specific for the organic complexed Fe and Al in soils. McKeague et al.[116] estimated organic complexed Fe, amorphous inorganic Fe, and more or less crystalline Fe oxides, by selective extraction of soils using pyrophosphate, oxalate and dithionite-citrate-bicarbonate respectively. They also gave evidence suggesting that, for Fe and Al fulvic acid complexes and Fe and Al hydrous oxides, pyrophosphate is reasonably specific for Fe-organic complexes, but less specific for Al-organic complexes.

McKeague et al.[116] considered that their results, and earlier work[117,118], demonstrated that pyrophosphate-extractable Fe and Al could be used as a basis of a chemical criterion for spodic horizons. For this purpose they considered that pyrophosphate is more specific than pyrophosphate-dithionite mixture[119], and that unlike acid oxalate, it does not dissolve magnetite or other easily weathered Fe minerals such as olivine.

3. The mechanisms of pyrophosphate and oxalate extractions

The two extraction methods used in this work were sodium pyrophosphate for the amorphous organic fraction of Fe and Al, and the ammonium oxalate extraction for the amorphous Fe oxides. Proposed mechanisms for these two extractions are

as follows.

(i) *Sodium pyrophosphate extractions*[120]. In the pyrophosphate extraction, there is an increase in pH, and a saturation with Na^+ ions. At the higher pH, any previously undissociated -COOH and phenol -OH groups lose their protons, with an increase in the charges on the organic species, which are then neutralized by the Na^+ ions. The charges tend to cause repulsion between the organic molecules which produces a breaking of some of the Van der Waals and H-bonds between the organic molecules. Cations bonded to organic ligands tend therefore to be released into solution while this process occurs, and are preferentially complexed to the pyrophosphate anions.

(ii) *Ammonium oxalate extractions*. De Endredy[112] proposed a mechanism for the dissolution of Fe(III) oxides by ammonium oxalate, both in darkness and under ultraviolet irradiation. Firstly, the soil will contain Fe-organic ligand complexes. The bidentate ligand oxalate $C_2O_4^{2-}$, could form a complex with some of this Fe, displacing other organic ligands. Also, suspensions of ferric oxides are positively charged and are likely to adsorb the oxalate anion. Once the ferric oxalate complex has been formed, a redox reaction can occur, more efficiently under ultraviolet radiation, generating the $C_2O_4^-$ radical, which can cause further redox reactions to occur;

$$[Fe^{3+}(C_2O_4)_3]^{3-} + h\nu \rightarrow [Fe^{2+}(C_2O_4)_2]^{2-} + C_2O_4^-$$

$$[Fe^{3+}(C_2O_4)_3]^{3-} + C_2O_4^- \rightarrow [Fe^{2+}(C_2O_4)]^{2-} + C_2O_4^- + 2CO_2$$

The mechanism of dissolution of Fe oxides in ammonium oxalate in darkness is less efficient (extracting 10-20% of the Fe in the photolytic procedure[112]). This could be due to little production of the $C_2O_4^-$ radical, which would make the second reaction above slow. The oxalate ligand can still form complexes with the organic bound Fe in the soil, as De Endredy[112] found that absorption spectra of the extracts indicated the presence of soluble organic matter. Some $C_2O_4^-$ radicals could also be produced owing to a small amount of oxygen present; if some Fe(II) is present, bound to organic matter, it may react with the oxygen;

$$Fe^{2+} + O_2 \rightarrow Fe^{3+} + O_2^-$$

$$O_2^- + H^+ \rightarrow HO_2$$

$$HO_2 + C_2O_4^{2-} \rightarrow HO_2^- + C_2O_4^-$$

The $C_2O_4^-$ formed could then initiate the redox reaction above. This reaction would cease once the oxygen has been used up.

CHAPTER 4

TRACE ELEMENTS IN THREE SOIL SEQUENCES

The separated soils (sand, silt and clay) for the chronosequence, biosequence and toposequence were analysed for the elements Ti, V, Cr, Mn, Fe, Co, Ni, Cu and Zn by digestion in an HF-$HClO_4$ acid mixture and determined by atomic absorption spectroscopy or colorimetrically (Ti). The whole soils of the three sequences were treated with ammonium oxalate and sodium pyrophosphate extraction reagents, and the resulting solutions analysed for Al, Si, Mn, Fe, Cu and Zn by A.A.S. The methods of analysis are outlined in Chapter 7.

The results of the analyses are presented below in two ways; firstly elemental analyses as a concentration based on the ignition weight of the sample, and secondly on the basis of the amount of each element in a given volume of soil - both per horizon, and to depths of 0.38 and 0.68 m in the profile (see Chapter 2 for reasons).

The results are then discussed in light of the review given in Chapter 3.

RESULTS

1. Concentration of trace elements in the soil sequences

The concentration of the trace elements, on an ignition weight basis, in the sand, silt and clay fractions, and of the whole soils (obtained by combining the data for each fraction) of the chronosequence, biosequence and toposequence soils are listed in Tables 4.1 to 4.10, which are listed in

Appendix 1. Tables summarising typical results are presented in the Chapter when necessary.

(i) *Chronosequence soils*. For all the elements measured, their concentrations increase within a soil sample with decreasing particle size (Tables 4.1 to 4.3); typical data are given in Table 4.1A;

TABLE 4.1A Variation in Concentration of Elements With Particle Size

SOIL AND HORIZON		SIZE FRACTION	ELEMENT								
			Ti	V	Cr	Mn	Fe	Co	Ni	Cu	Zn
			(%)	μg g^{-1}			(%)	μg g^{-1}			
Io	Bs1	sand	0.16	17	13	223	1.17	7	6	8	21
		silt	0.47	41	31	325	1.87	8	21	30	40
		clay	0.63	108	73	291	4.34	17	24	49	300
Ah	Bs3	sand	0.18	22	16	286	1.55	8	10	22	34
		silt	0.37	58	37	483	2.56	10	15	17	63
		clay	0.73	172	94	423	7.87	21	33	66	151
Ok	Ag	sand	0.16	3	0	79	0.10	0	9	7	0
		silt	0.36	4	6	111	0.17	0	9	27	11
		clay	1.26	24	20	259	0.44	4	13	19	18

Within any size fraction the concentration of the elements tends to increase with depth down the profile (Table 4.2A) except for Ti and Cu. The Ti concentration remains relatively uniform with increasing depth for sand, silt and clay. The concentration of Cu on the other hand is often high in the sand, silt and clay fractions of surface horizons, decreasing in the lower A horizons, and then increasing again deeper in the profile.

With increasing age of the soil, that is from the Ho (youngest), Io, Ah, Ku to the Ok (oldest) soil profile, there

TABLE 4.2A The Variation in Concentration of Elements in Sand, Silt and Clay Fractions of the Iw Profile with Depth

SOIL AND HORIZON		FRACTION	INCREASING DEPTH	Ti	V	Cr	Mn	Fe	Co	Ni	Cu	Zn
				(%)	μg g^{-1}			(%)	μg g^{-1}			
Iw	A	Sand	↓	0.24	17	13	252	0.89	5	5	11	15
	Br1	Sand	↓	0.22	22	16	268	1.54	6	4	4	27
	Cr1	Sand	↓	0.26	30	21	281	2.14	10	13	17	50
Iw	A	Silt	↓	0.47	20	32	281	1.25	8	22	38	45
	Br1	Silt	↓	0.46	40	31	363	2.22	9	18	16	45
	Cr1	Silt	↓	0.49	85	66	466	4.00	16	25	28	103
Iw	A	Clay	↓	0.71	42	67	153	1.99	13	36	44	86
	Br1	Clay	↓	0.61	98	89	317	5.41	21	39	39	164
	Cr1	Clay	↓	0.56	102	101	408	7.43	22	41	44	223

is a distinct trend in the concentration of the trace elements in the whole soil (i.e. combined data, Table 4.4) to increase to either the Io or Ah profiles and then decrease (in concentration) in the remaining older soils. These trends are illustrated by the data given in Table 4.3A, where the

TABLE 4.3A Variation in Concentration of Elements in the Whole Soils with Soil Age

SOIL AND HORIZON		Ti	V	Cr	Mn	Fe	Co	Ni	Cu	Zn
		(%)	μg g^{-1}			(%)	μg g^{-1}			
Ho	Au2	0.34	52	34	380	2.56	11	17	24	42
Io	Bs2	0.32	47	32	561	2.45	13	15	18	72
Ah	Bs3	0.32	57	35	349	2.94	11	15	29	62
Ku	Br3	0.54	43	22	170	0.44	4	8	10	15
Ok	Br3	0.45	35	12	111	0.25	4	5	5	11

concentrations of elements in the horizon immediately above the C horizon are given for each chronosequence profile (note that the Ha and Iw profiles are excluded as these are wetter variants of the Ho and Io profiles). The observed trend is also apparent for the separated sand and silt fractions. In the case of the clay fractions the concentrations of Ti and V increase with age throughout the whole chronosequence, and the concentration of Cr remains relatively constant, while for the other elements, the observed trends are the same as for the whole soil.

In the wetter variant of the Ikamatua soil, Iw, the Ti concentration in the whole soil is greater than for the drier Io profile. This may be attributed to greater Ti levels in the sand and clay fractions of the upper horizons of the Iw profile. The higher concentrations of Cr in the A and B horizons of the Iw whole soil (compared with Io) are due to higher levels in the clay fraction of the wetter soil. In contrast, the elements Mn, Fe and Zn are at lower concentrations in the upper horizons of the Iw profile.

In the wetter variant of the recent soils (Ha) the concentrations of the elements Mn and Fe are significantly lower than in the freely drained Ho profile. The concentrations of the other elements are similar in both profiles.

(ii) *Biosequence soils.* The concentrations of the trace elements in the biosequence profiles are presented in Tables 4.5 to 4.8. The levels of metals in the whole soil (Table 4.8) and the clay fraction (summarizing data in Table 4.4A) indicate that differences in the concentrations of the metals between the Ah and Pod Ah profiles occur mainly in the

TABLE 4.4A BIOSEQUENCE

Concentration of the Elements Ti, V, Cr, Mn, Fe, Co, Ni, Cu and Zn in the Clay Fraction

SOIL AND HORIZON		Ti	V	Cr	Mn	Fe	Co	Ni	Cu	Zn
		(%)	μg g^{-1}			(%)	μg g^{-1}			
Ah	AB	0.77	115	61	241	5.74	15	22	30	73
Pod Ah	E	1.27	42	47	180	1.12	11	15	37	39

horizon above the Bs horizon (AB in the Ah profile, and E in the Pod Ah). The levels of V, Cr, Mn, Fe and Zn are reduced in the E horizon (Pod Ah) while the levels of Ti, Co, Ni and Cu are generally similar. However, the Ti concentration in the clay fraction of the E horizon (Pod Ah) is higher than for the AB horizon (Ah). Perhaps the most striking feature of the biosequence soils is the 4 to 5 fold reduction of Fe levels in the clay of the Pod Ah E horizon compared with the Ah AB horizon. Similar trends occur for the sand and silt fractions. The greatest change in the Mn levels from the Pod Ah E horizon to the Ah AB horizon occurs in the silt fraction (a 42% reduction).

(iii) *Toposequence soils*. The concentrations of the trace elements in the Lower Footslope and Crest profiles of the toposequence are given in Table 4.9 and 4.10. The levels of the elements in both profiles are similar, with the exceptions of Ti, which is at slightly higher levels in the L.F.S. profile, and Fe, which is at higher concentrations in the Crest profile (Table 4.5A). These trends occur for both the clay fraction and the whole soil.

TABLE 4.5A TOPOSEQUENCE

Concentration of the Elements Ti and Fe in the Clay Fraction

SOIL AND HORIZON		Ti (%)	Fe
L.F.S.	Ar	0.71	0.78
	Er	1.12	1.78
	Brs	1.27	1.78
	Bhs	0.87	1.51
	Br	1.34	2.26
Crest	E	0.98	1.48
	EB	1.00	6.85
	Bhs	0.75	5.76
	2 Bs	0.89	6.77

2. The amount of trace elements in the chronosequence profiles

Expressing the amount of the trace elements in the profiles of the chronosequence (i.e. amount per volume, rather than amount per mass), highlights how the trace elements have been affected by weathering. The values presented in Table 4.11 and 4.12 have been calculated for the clay fraction and the whole soil of each horizon by making use of the data in Tables 2.4, 2.5, 4.3 and 4.4. The total amount of each trace element, in the clay and the whole soil, to a depth of 0.38 m, has also been calculated (Tables 4.13 and 4.14). The change in the amount of an element, in the whole soil and clay fraction of each horizon, with depth are more clearly shown graphically as given in Figures 4.1 to 4.7, and with soil age in Figures 4.9 to 4.12. The Figures are presented in Appendix 1.

The plots have been constructed by graphing the amount

of the element in a profile (as kg ha^{-1} cm^{-1} horizon) against the depth of the midpoint of each horizon (in cm). Expressing the amount per volume as per cm of horizon enables a comparison to be made of horizons of different thicknesses. The use of the midpoints of each horizon is not meant to infer a constant concentration throughout a horizon, but is used for ease of presentation of the data. Only mineral horizons have been considered in calculating the data and therefore the Ikamatua OA horizons are not included.

(i) *Changes in the amount of elements with depth.* The variation with depth in the amount of Ti and Fe, for the whole soils is given in Figures 4.1 and 4.2. For the younger soils, i.e. the Ho, Ha, Io, Iw and Ah profiles, the Ti and Fe data closely resemble each other. The same trends also occur for the elements V, Cr, Mn, Co, Ni, Cu and Zn. In general, the trend in the younger soil is for the amount of an element (per cm of horizon) to increase with depth to the B horizons and then decrease to the C horizon, except for the Ah profile where there is a continual increase with depth.

The amounts of Ti and Fe (per cm of horizon) in the A and B horizons of the youngest soils (Ho and Ha), are greater than in the older Io, Iw and Ah soils (Figures 4.1 and 4.2). Because of the greater weathering of the oldest soils (Ku and Ok), one could expect the amount of an element (per cm of horizon) to be even less, as is the case for Fe (Figure 4.2). Similar trends also occur for the elements Cr, Mn, Co, Ni, Cu and Zn. However, for Ti (Figure 4.1), and to a lesser extent V, the amount of these elements (per cm of horizon) increases significantly with the age of the soil.

The values (kg ha^{-1} cm^{-1} horizon) plotted in Figures 4.1 and 4.2 are influenced by variations in bulk density (Table 2.4) and elemental composition (Table 4.4). Bulk density determines the amount of inorganic material in a volume of soil. A plot of the amount of inorganic material with depth (Figure 4.3) resembles closely that of the plots for Ti and Fe, described above for the Ho, Ha, Io, Iw and Ah profiles, and for Ti and V in the Ku and Ok profiles. This clearly highlights a difference between Ti and V on the one hand,and the remaining elements, as regards resistance to weathering.

For the wetter variants, Ha and Iw, of the more freely drained Ho and Io profiles, the change in the amount of all the elements (except Mn) with depth, is similar to the change in the amount of inorganic material with depth. In the case of Mn, levels per cm of horizon are greater in the Bs2 and C1 horizons of the Io profile than in the Iw profile. Manganese has been lost under the wetter conditions of the Iw profile.

The variation in the amount of Ti, Mn, Fe and Co in the clay fraction with depth is presented in Figures 4.4 to 4.7. The variations are similar for Ti, V, Cr, Fe, Ni and Cu in the Ho, Ha, Io, Iw and Ah profiles, namely an increase in amount,per cm of horizon, to the B horizons followed by a decrease in the C horizons. For the remaining elements (Mn, Co and Zn), a similar pattern is observed in the Ho, Ha, Iw and Ah profiles, but significantly greater values occur in the Io B horizons than found for the other elements. This suggests loss of Mn, Co and Zn from the wetter Iw profile, and a chemical association of Mn, Co and Zn.

The data also indicates (Figure 4.3 to 4.7) that for all elements there is a tendency for the amount of an element, per cm of horizon, to increase with soil age from the youngest Ho and Ha profiles to the older Ah profile. However, the figures obtained for the oldest soils (Ku and Ok) again indicate a difference between two groups of elements. For Ti, there is a continuing increase in weight per cm of horizon with soil age (Figure 4.4) reaching the highest levels in the Ok profile. A similar trend occurs for V and to a lesser extent, Cr. On the other hand, the amounts of the elements Mn, Fe, Co, Ni, Cu and Zn, per cm of horizon, all show a marked depletion from the young to old (Ku and Ok) soils.

(ii) *Changes in the amount of the elements with soil age*. The weights of each element in the whole soil and clay fraction of each horizon are given in Tables 4.11 and 4.12. The amounts of the elements down to a depth of 0.38 m are listed in Tables 4.13 and 4.14. Plots, representative of these data, are given in Figures 4.9 to 4.12, for the elements Ti, Mn, Fe and Zn.

For the whole soil the amount of each element (except Ti and Zn) decreases with soil age to the Ku profile, and then increases slightly to the Ok profile. The decline may be related to weathering while the slight increase in amounts from the Ku to the Ok profile is due to the greater amount of inorganic material in the Ok profile (Table 2.4). The element Zn is different only in that the amount to a depth of 0.38 m is greatest at the Io profile, due to a high concentration of Zn in the clay fraction of that profile, rather than in the Ho profile. For the whole soil, the Ti levels

decrease from the Ho to the Ah profiles, after which they rise in both the Ku and Ok profiles, demonstrating an accumulation of Ti in these older profiles.

The amounts of each element in the clay fraction, to a depth of 0.38 m,increases from the Ho profile to the Ah profile for Ti, V, Cr and Fe, and the Io profile for Mn, Co, Ni, Cu and Zn, due to the increasing development of clay in the soil with age (Figures 4.9 to 4.12). The amount of Ti and V in the clay fraction continues to increase with soil age to a maximum value in the Ok profile, while the amount of Cr, Mn, Fe, Co, Ni, Cu and Zn in the clay fraction decreases with soil age after the Io or Ah profiles.

The amount of each element, to a depth of 0.38 m, in the clay fraction of the wetter Ha and Iw profiles, compared with Ho and Io is greater for each element (except Mn and Zn). This is mainly due to greater amounts of clay to 0.38 m in the Ha and Iw profiles. In the case of Mn and Zn this is offset by losses of these elements in the Iw profile.

(iii) *Real and apparent changes in the amount of elements in soil profiles.* The data for the weights of elements, to a depth of 0.38 m, given in Table 4.13, refer to a constant volume of soil material. As outlined above, these data show that there is a decline in the amount of elements with soil age from the Ho to the Ah profile, but that the elements Ti and V, and also Si^{20}, accumulate in the oldest soils of the chronosequence, while Mn, Fe, Co, Ni, Cu and Zn continue to fall.

In tracing the development of the chronosequence, the amounts of all elements would have been expected to decrease

with time as weathering intensified. One of the difficulties in comparing soils of different ages is establishing a reference point to which all the soils can be related. The differing stages of soil development of the chronosequence soils means that an initial volume would expand in the formation of the Ah profile, and then contract later by the time the Ku and Ok profiles had been produced. That is, sampling to 0.38 m at the Ah and Ok profiles would yield lesser and greater amounts of inorganic material than an initial volume before weathering.

From a consideration of the ratio of the amount of Si to the amount of Ti (Table 4.13) it appears that Si is lost more rapidly than Ti during the period of formation of Ho to Ah, while Ti is lost faster during the formation of the Ok soil. The data in Table 4.15(A) is calculated assuming 1) the amount of Si remains constant from Ah to Ok, and 2) the amount of Ti remains constant from the Ho C horizon to the Ah profile. The Ho C horizon represents the parent material of the soils of the chronosequence[20], and the Ti level of the Ho C horizon (assuming 38 cm thickness) is used for calculations in Table 4.15(A). The remaining elements were adjusted in proportion to the changes calculated for the amount of Si and Ti.

The data in Table 4.15(A) can be used to calculate that over the period of formation of Ah to Ok, Ti was lost at a rate of approximately 0.026 kg ha^{-1} $year^{-1}$. The data in Table 4.15(B) were then calculated assuming that a constant loss of Ti (of 0.026 kg ha^{-1} $year^{-1}$) occurred throughout the entire period of soil development.

As a result of this analysis of the data to 0.38 m, and with reference to the levels of the elements in the parent material Ho C, it may be seen that all elements, including Si, Ti and V have been lost from the profile through soil development. The percentage loss of elements is given in Table 4.15(C). Up to the formation of the Ah soil, 22 to 42% of the total amount of Si, V, Cr, Mn, Fe, Co, Ni and Zn in the unweathered soil has been lost, while only 4% of the Ti has been. The values indicating no loss of Cu up to the formation of the Ah soils (Table 4.15(C)) are due to the low Cu levels in the Ho C horizon. From the formation of the Ah to the Ok soils, the loss of V, Cr, Mn, Fe, Co, Ni and Zn has increased markedly to between 83 to 97%, while only 57% of the Si and 44% of the Ti have been removed, suggesting a greater resistance of the Si and Ti minerals to weathering, or a lower mobility of Si and Ti species.

Though greater loss of the elements has occurred in the oldest profile, the rate of loss probably has been faster in the younger soils. From Table 4.15(C), it can be seen that 22-42% of V, Cr, Mn, Co, Ni and Zn has been lost in 18000 years (to the Ah soil),while the further loss of 41-72% of the amount of the elements has been over a period of 52,000 to 112,000 years - a somewhat slower rate. This would be expected as the more readily weathered materials are removed first.

3. Ammonium oxalate and sodium pyrophosphate extractions

An ammonium oxalate solution was used to estimate the amount of poorly ordered or amorphous forms of Al, Si, Mn, Fe, Cu and Zn[8,110,112] while sodium pyrophosphate was used to

extract the metal-organic portion of the amorphous content of Al, Si, Mn, Fe and Zn in the soils[113,117,118]. The oxalate extraction gives information on secondary weathering products such as the hydrous oxides of Mn and Fe while the significance of organic chelates in binding such secondary products is estimated with sodium pyrophosphate.

(i) *Chronosequence soils*. The levels of elements extracted, on an ignition weight basis, are given in Table 4.16 (ammonium oxalate) and Table 4.22 (sodium pyrophosphate). There are two main features of the concentrations of the elements extracted by these reagents. Firstly, the highest concentration of elements extracted usually occurs in the lower A or upper B horizons, although for Al in the Ku profile, and Al, Si and Fe in the Ok profile, the concentration extracted increases with depth, with the maximum occurring around the Bs iron-pan or C horizon. Pyrophosphate extractable levels fall more quickly than oxalate levels, with depth in the profile, reflecting the lower organic levels with depth. In general, these trends reflect the trends in the amounts of elements in the horizons. Secondly, the levels of Al, Si, Fe and Zn extracted by both reagents increased with the age of the soil, from the Ho to the Ah profiles, and then declined sharply in the older soils (Ku and Ok profiles). In the case of Mn, the initial increase in concentration extracted was from the Ho to the Io profile, followed by a decrease with increasing soil age. Levels of Cu extracted were always very low. The trend with age (Ho to Ah) does not follow the trend in the amount of the elements - there is more poorly ordered material in the older (Ah) soil. The low extraction in the oldest (Ku and Ok) soils is probably due to the lower

levels of elements present.

As regards the wet and dry variants of a soil, high levels of Al, Si, Mn, Fe and Zn were extracted from the upper horizons of the Io profile compared with the wet Iw profile.

The percentages of the total amounts of the elements present that are extracted are a more meaningful figure, and are given in Table 4.20 (oxalate) and 4.26 (pyrophosphate). For Al, Mn and Fe, the percentage extracted decreases with depth except in the Ok profile where there is a maximum percentage of Al and Fe extracted in the Bs and C horizons. For Si, the percentage extracted usually increases with depth to the B or C horizon, with less than 1% of the total Si content being extracted.

The amounts (kg ha^{-1}) of trace elements extracted by the two extractants from the chronosequence soils are given in Tables 4.19 (oxalate) and 4.25 (pyrophosphate). The variation in amounts of extractable material with depth is different for the oxalate and pyrophosphate reagents. Representative plots of the data in Table 4.19 (oxalate) are given in Figures 4.13 to 4.16, and for data in Table 4.25 (pyrophosphate) in Figures 4.19 to 4.22. The main differences are observed for the soils in the Ho to the Ah profiles. For these soils, the variation with depth in the amount (kg ha^{-1} cm^{-1} horizon) of Al, Si and Fe extracted by oxalate, parallels the change in the amount of clay with depth (Figure 4.8). The amounts extracted increase with depth and with age of the soil. For pyrophosphate extractable Al, Si and Fe, the highest amounts removed are from the upper horizons (and parallels the variation in organic matter (Figure

2.2)) followed by a decrease with depth in each profile. The Ku and Ok profiles are relatively depleted of extractable Al, Si and Fe (both oxalate and pyrophosphate extractable). Oxalate and pyrophosphate extractable Mn levels are highest in the Io and Ho profiles respectively, and the levels decrease rapidly with both depth in the profile and with age of the profile (Figures 4.16 and 4.22).

There is a marked depletion in both oxalate and pyrophosphate extractable Mn in the Ha and Iw profiles (wet), and extractable Fe in the Iw profile, compared with the drier Ho and Io profiles. This may be explained by the mobility of both amorphous and organic bound Mn in the wet soils, and by a significant weathering of Fe minerals.

The amount of extractable Al, Si, Mn, Fe and Zn, to a depth of 0.38 m, is given in Table 4.19 (oxalate) and Table 4.25 (pyrophosphate) for each profile. Typical data is graphed in Figures 4.17 and 4.18 (oxalate) and 4.23 and 4.24 (pyrophosphate). All elements showed a similar trend, namely an increase in both oxalate and pyrophosphate extracted levels, with soil age, from the Ho to either the Io or Ah profiles. The amounts extracted then fall to very low levels in the most weathered soil profiles (Ku and Ok).

The percentage of the total amount of elements, to a depth of 0.38 m, extracted by oxalate and pyrophosphate, is given in Table 4.21. The data follow the same trend depicted in Figures 4.17, 4.18, 4.23 and 4.24. Up to 9.0% (Al), 70% (Mn) and 65%(Fe) were extracted by oxalate, and 14% (Al), 17% (Mn) and 51%(Fe) were extracted by pyrophosphate, showing that much of the extractable amorphous material is organic

bound.

In the Iw profile, the percentage of Fe extracted is about two-fold less than in the Io profile. Although this difference is much less than the thirty five-fold decrease of Mn, it does show that amorphous forms of Fe have been removed in significant amounts from the Iw (wet) profile.

(ii) *Biosequence soils*. The concentrations of Mn, Fe, Al and Si extracted from the two biosequence profiles are given in Tables 4.17 (oxalate) and 4.23 (pyrophosphate). The main feature of these results is the marked depletion of extractable Mn, Fe, Al and Si from the Pod Ah E horizon compound with the Ah AB horizon.

(iii) *Toposequence soils*. The concentrations of elements extracted from the toposequence soils are given in Tables 4.18 (oxalate) and 4.24 (pyrophosphate). Trends for both extractants are similar, and horizons in both profiles with highest levels of extractable Al, Si and Fe coincide with horizons of maximum organic matter accumulations (Table 2.3). There is a marked decrease of extractable Fe in the L.F.S. profile compared with the Crest profile, suggesting that poorly ordered forms of Fe have been washed out of the L.F.S. profile.

DISCUSSION

The main features of the results outlined above, and the results of different soil forming processes will be discussed for each of the soil sequences studied.

For the soils of this study, the range of levels of trace elements found are in accord with the range of levels

given in Table 3.1 for typical concentration ranges of elements in soils.

The results found for the soil sequences studied are in agreement with the descriptions of the sequences as a chronosequence, a biosequence and a toposequence.

1. Chronosequence soils

(i) *Mineralogy*. The effect of weathering on a soil is most marked on smaller sized particles, because they have larger surface areas per unit mass. Consequently the effects of weathering should be more evident in the clay fraction of soils, and it could be expected that the mineral composition of the finer and coarser grained fractions of the soil would differ. Also, the duration of weathering will affect the mineral composition of soils, as is seen in the chronosequence.

In the chronosequence the effect of weathering is evident in a change from rock forming minerals, such as quartz, feldspars and micas, found in the coarser fractions of the Ho soil, to minerals such as illite, vermiculite and interlayered hydrous micas (at about 5 to 10% levels), as well as chlorite and amorphous minerals including allophane, in the Ku and Ok profiles[20,21]. The Io and Ah profiles exhibit mineralogy midway in the weathering sequence.

Feldspars, which are present in 30 to 40% quantities in the young chronosequence soils, have weathered in the older soils (Ku and Ok) and constitute less than 5% of the soil. The proportion of quartz on the other hand, a resistant primary mineral, has increased from 30 to 40% in the Ho and Io profiles to 70 to 90% in the Ku and Ok profiles[20,21].

The greater proportion of Ti found in the oldest Ku

and Ok soils may be accounted for by the resistance of the minerals anatase and rutile to weathering[8,122,123]. Both these Ti minerals were detected in the older chronosequence soils in the present study using X-ray diffraction, and also by Campbell[20]. A close correlation (significant at the 0.10% level - Table 4.27) exists between total Ti and total Si in the soils, which would support their continued existence together. Vanadium was also found to accumulate in the older soils, and this element has a high positive correlation coefficient (0.10% level) with Ti in the clay fractions of the soils. This correlation does not extend, however, to a positive correlation between V and Si in the total soil, in fact a highly significant (0.10%) negative correlation occurs and there is no significant correlation (>5% level) between total Si and clay V. The relevant correlation coefficients given below are taken from Table 4.27. It should be pointed out that the correlation coefficients were obtained using concentration data ($\mu g\ g^{-1}$) for each horizon of the chronosequence soils (Ho, Io, Ah, Ku and Ok).

clay Ti	clay Ti			
clay V	0.812	clay V		
total Si	0.749	0.303	total Si	
total Ti	0.705	0.600	0.555	total Ti
total V	-0.201	0.331	-0.657	0.101

The lack of mobility of Ti has been well demonstrated from the results in this work. For example, it was found that within any particle size fraction (Table 4.2A), Ti concentrations were approximately uniform down a profile, whereas a more mobile element would have been leached from upper horizons. It was further shown that increased levels of Ti (and V) in the oldest soils (Ku and Ok)(Tables 4.1 to 4.3) were

due to increased Ti (and V) concentrations in the clay fractions, present as anatase and rutile. Berrow et al.[54] suggested that the accumulation of Ti in the clay fraction of some Scottish soils was achieved by a process of physical disintegration of anatase and ilmenite present, with subsequent dissolution and reprecipitation as clay sized anatase. It could be that a similar process occurred in the chronosequence soils of this study.

Anatase and rutile are two of the minerals that have been proposed as index minerals for evaluating changes that occurred during soil formation[122]. It is generally assumed that these titanium minerals are almost unweatherable due to the low solubility of TiO_2 and its immobility[8,123]. The data presented in Table 4.15(C) shows that in the chronosequence Ti is the most resistant element to weathering of those determined, more so than Si. However, Berrow et al.[54] states that there is good evidence for a limited mobility of Ti in environments characterized by intense leaching over long periods of time. In a study of the use of quartz, Zr and Ti as weathering indices in four Canadian soils, Sudom and St. Arnaud[124] also found that Ti was subject to limited mobilization.

(ii) *Resistance of the transition metals to leaching.* With an increase in soil age there is a distinct tendency for the concentration of elements in the whole soil, sand and silt to increase to the Io or Ah profiles, and then decrease to the Ku and Ok (oldest) profiles (Table 4.3A). In the clay fraction however, although Mn, Fe, Co, Ni, Cu and Zn continue to follow this trend, Ti, V and Cr do not, with Ti and V concentra-

tions rising, and Cr concentrations remaining constant. Both Ti and V, in the clay fractions, correlate negatively with the other elements, suggesting a chemical difference to the other elements. This difference is most likely related to resistance to weathering. The appropriate correlation coefficients, taken from Table 4.27, are;

Clay	[Ti	V	Cr	Mn	Fe	Co	Ni	Cu	Zn]
Clay Ti	1.00	0.812	0.891	-0.380	-0.510	-0.388	-0.523	-0.556	-0.272
Clay V	0.812	1.00	0.608	-0.065	-0.037	0.028	-0.177	-0.259	0.005
Clay Cr	0.891	0.608	1.00	0.549	0.669	0.654	0.533	0.403	0.388

In the whole soil, Ti correlates negatively with the other elements except Si and V. All elements except Ti and Si show strong intercorrelations (Table 4.27). It appears therefore, that of the transition metal ions studied they fall into two groups, one consisting of Ti, V and to a lesser extent Cr, and the other of Mn, Fe, Co, Ni, Cu and Zn.

This segregation is not unexpected as it is typical of the division between the left hand and right hand side of the transition metal series. The elements Ti, V and to a lesser extent Cr, all form relatively strong bonds with oxygen (>600 kJ mol^{-1} for Ti and V), and are much less likely to occur as free ions in the soil than the elements on the right of the transition metal series. Hence, one could expect the Ti, V (and Cr) species in soils to be more resistant to weathering and less mobile. A similar relationship between Ti, V and Cr was discovered in the Fe-Mn concretions discussed in Chapter 6.

While Ti, V and Cr have been considered as relatively

immobile as a soil ages, the other first row transition metals are considered as mobile especially with soil aging. In young unweathered soils (such as Ho) the major part of the total content of many of these trace elements occurs locked up in the crystal lattice of the primary minerals. This is supported by the relatively low percentage of oxalate extractable material in the young Ho soil, but as the soils age and weather, a greater proportion of the trace elements are extracted,having been released from the minerals (up to the Ah soil). The released elements may be taken up by micro-organisms or plants, or remain partly in the soil solution in an ionic or combined form, or bound with differing tenacity to exchange sites of clay particles, or be re-immobilized. For the more mobile elements (Mn, Fe, Co, Ni, Cu and Zn), the low pH and longer duration of exposure to rainfall of the older chronosequence sites tends to destroy the clay particles they bind to, allowing for transport down, and out of, the profile. The great mobility of Mn in wet conditions is clear from the comparison of the levels in the wet and dry variants of the soils.

(iii) *Extractable trace elements*. Extractants such as ammonium oxalate and sodium pyrophosphate are often used to differentiate secondary minerals—products of weathering, and to help in determining soil forming processes which have been important in soil genesis.

The trends found for both oxalate and pyrophosphate extractions show an increase in poorly ordered forms of Al, Si and Fe with soil age from Ho to Ah, followed by a decline in the Ku and Ok soils. This is in agreement with the

extractable Al levels in a chronosequence of soils developed on alluvial and morainic deposits from the Franz Josef Glacier[125], which also has the Ok soil as the oldest member.

The results of oxalate and pyrophosphate extractions are similar in most cases, and from regression analysis involving the oxalate and pyrophosphate values for Al, Si, Fe and Mn, most pairings of these variables have highly significant correlations (Table 4.27);

	pyro Al	pyro Si	pyro Mn	pyro Fe
oxal Al	0.782	0.517	0.309	0.648
oxal Si	0.404	0.090	-0.080	0.237
oxal Mn	0.471	0.751	0.800	0.576
oxal Fe	0.753	0.587	0.405	0.663

The amount of extractable elements Al, Si and Fe (by oxalate and pyrophosphate) increases with age to the Ah profile, and to the Io profile for Mn, reflecting increasing development and breakdown of primary minerals. By the time the Ok soil has developed however, extractable Mn has been virtually removed from the profile (Figure 4.16) as well as much of the extractable Al, Si and Fe. It is notable that there is an increase in extractable Al, Si and Fe with depth in the Ok profile, to maximum values in the Bs and C horizons, and that a significant proportion of the total amounts of the elements (Table 4.26) are pyrophosphate extractable (10% of the Al and 41% of the Fe). It appears therefore, that there has been a movement down the profile, in the older soils, of considerable amounts of Al, Si and Fe as water soluble organic compounds. Presumably at some later stage these extractable levels will drop lower.

It is generally recognised that the clay and organic

matter fractions are responsible for most of the cation exchange capacity[2,6] (C.E.C. - the amount of cations that a soil can hold when a salt solution (ammonium acetate) is leached through a soil). The correlation coefficients of C.E.C. with organic matter (L.O.I.) and % clay are 0.703 and 0.549 respectively, both highly significant.

Correlation of C.E.C. with the concentrations of trace elements in the whole soil and clay fraction (Table 4.27) produced few significant correlations. Total Cu correlated at the 1% level, and this is discussed later. The other significant correlations were with the Ti, V and Cr concentrations in the clay fractions - the correlations were negative and significant at the 5%, 1% and 5% levels respectively. This suggests that the metals Ti, V and Cr in the clay fractions are not in a cation exchangeable form, and are in fact limiting the cation exchange ability of the clay.

The correlation coefficients found between C.E.C. and extractable levels of some elements (Table 4.27) are as follows;

	pyro Al	pyro Si	pyro Mn	pyro Fe	oxal Al	oxal Si	oxal Mn	oxal Fe	oxal Zn
C.E.C.	0.451	0.545	0.884	0.552	0.222	-0.205	0.693	0.357	0.337

The correlation of C.E.C. with oxalate extractable Mn, Fe and Zn are significant at the 0.1%, 5% and 5% levels respectively, while the correlations with pyrophosphate extractable Al, Si, Mn and Fe are significant at the 0.1% level (1% level for Fe).

In a previous study[20] of the chronosequence soils it was shown that the organic matter fraction makes four times the contribution of the clay fraction to the C.E.C. of the Ho, Io

and Ah soils, but that in the gley podzols (Ku and Ok) the contribution of the clay is twice that of the organic fraction. This is probably why the pyrophosphate levels of elements shown above correlate more significantly with C.E.C. than do the oxalate levels, since it is the amorphous organic portion of elements that is extracted by pyrophosphate.

The data in Table 4.16 indicates that a podzolization process is taking place in the Ah profile. The characteristic process in podzolization[2,58] is the dissolution of Fe and Al from the A horizon, and their deposition in a lower horizon, in this case the AB horizon for Fe, and the Bsl horizon for Al. This is also in association with the movement and deposition of organic matter. As was portrayed in Figure 2.2, the maximum organic matter content of the Ah profile, in contrast to the other profiles, is not the surface horizon, but the AB horizon. The greater movement of Al down the profile suggests the Al organic compounds are more mobile than the Fe compounds. Further weathering would continue the podzolization process in the Ah profile, leading to a more eluviated A horizon, and a B horizon more enriched in Fe and Al. Similarly, the Io profile could be expected to develop the characteristics of a podzol by the time its development had reached the stage of the Ah profile.

The present results also suggest that a substantial portion of the organic matter in the chronosequence soils is bound up in metal complex forms (i.e. bound to cations and hydrous oxides of Al, Fe and Mn). The evidence for this is that highly significant correlations (0.10% level) occur between pyrophosphate (organic bound) Al, Fe, Mn and Zn, and

loss on ignition values. It is likely that organic complexes have played a significant role in the removal of Al, Fe and Mn from the eluvial horizons during such soil forming processes as podzolization which is occurring in the Ah profile.

It was noted in the results section that Cu concentrations in the silt and clay fractions of surface horizons are often high. This may be attributed to an association of Cu with organic matter in the surface horizons, especially as there is a significant correlation between total Cu and loss on ignition values. Surprisingly however, levels of pyrophosphate extractable Cu were very low to zero. It has been shown that Cu has a strong interaction with soil organic matter[95,96], and that the Cu-fulvic acid stability constant is high (log of stability constant is 8.7 at pH 5.0)[97]. This is also supported by the significant correlation (1% level) between total Cu and C.E.C. (Table 4.27) since cation exchange capacity depends mainly on the levels of organic matter present. It is possible therefore, that the Cu complexes are too stable to enable pyrophosphate to extract the metal.

Another soil forming process which is important in the chronosequence profiles is gleying, where impeded drainage leads to anaerobic conditions involving the reduction of Fe and Mn oxides to the mobile divalent cation state[2]. Swaine and Mitchell[11], in a study of Scottish soils, found that in poorly drained soils the level of extractable (acetic acid) Mn, Co, Ni, Cu and Zn is markedly higher than in similar freely drained soils, particularly in the soils derived from rocks with high contents of ferromagnesian minerals. They found that impeded drainage may in some cases mobilize up to

50% of the total content of an element, and that the effects of other pedological processes, such as podzolization were minor.

In contrast, data from the present study (Table 4.21) show that in the wetter Ha and Iw profiles, oxalate and pyrophosphate extractable levels of Mn are reduced compared with the more freely drained Ho and Io profiles. Extractable levels of Fe are also lower in the Iw profile, but are higher in the Ha profile. The higher extractable levels of Fe in the Ha profile is probably indicative of mobilization, and imminent translocation, as the young age of the Ha soil has not yet permitted movement of mobilized Fe.

From Table 4.21, it can be seen that 70% of the total Mn, to a depth of 0.38 m, is oxalate extractable from the Io profile, as is 29% from the Ho profile. There are a thirty five-fold and a two-fold reduction in oxalate extractable levels of Mn from the Iw and Ha profiles (less for the younger Ha soil which has had less weathering) illustrating the high mobility of Mn in such profiles. Also, from the Io to the Ah profile there is a five fold decrease in extractable Mn, so that in the chronosequence of the present study, it appears that the effect of podzolization, in the Ah profile, is significant compared with the effect of impeded drainage or gleying. The differences between the extractable levels of elements in the Io and Ah profiles, and the Scottish soils studied by Swaine and Mitchell, are probably due to the different extractants used, and more particularly, the age difference of the soils - the Scottish soils are 12,000 years old, considerably less than the Io and Ah soils, in which

podzolization is probably more advanced. Podzolization of the Ah profile has resulted in the mobilization of 65% of the total Fe (Table 4.21).

The relative mobility of Mn and Fe in gleying conditions has been discussed in detail in Chapter 3. The Iw profile is weakly gleyed, while the Ha profile is even more weakly gleyed. Although the Ah profile does not have gleyed conditions, by the time soil development has progressed to that of the Ku and Ok profiles, gleying has become intense as a result of low pH levels in upper horizons, removal of organic matter and elements, and loss of soil structure resulting in compaction. The resulting reducing conditions have led to mobilization of elements, and so have produced the very low extractable values observed in the oldest soils.

2. Biosequence soils

The most striking feature of the two biosequence profiles, in terms of the concentration of elements, is seen in comparing the two horizons directly above the Bs horizon of each profiles, namely the AB horizon in the Ah profile, and the E horizon in the Pod Ah profile. In the clay fraction (Table 4.7) the significant differences are in the elements V, Mn, Fe and Zn, which all have lower values in the Pod Ah E horizon. The five-fold decrease in Fe levels from the AB to the E horizon is the most notable change. Similar trends occur for the whole soil (Table 4.8).

When oxalate and pyrophosphate extractable levels are considered (Tables 4.17 and 4.23), even more marked differences occur between the AB and E horizons of these profiles. For Mn, Fe, Al and Si, the E horizon has a notable reduction in

the amounts of both oxalate and pyrophosphate extractable elements.

These changes show that the soil of the Pod Ah profile is at a more advanced stage of podzolization compared with that of the Ah profile. Since the only distinguishable difference between the two sites is a beech tree adjacent to the Pod Ah site, it is confirmed that the presence of beech trees speeds up the podzolization process of soils, and that the large beech population of the Reefton area has had a widespread effect in the genesis of podzolized soils there[20]. Since the soils of the Ku and Ok profiles have lost structure, it is likely that beech trees would have been involved in the podzolization of these soils at an earlier stage, though there was no evidence of recent tree growth.

As discussed in Chapter 3, the presence of beech trees reduces surface pH to below 4.5, concentrates rainfall, and increases the supply of organic chelates from both decaying litter, and by leaching from the canopy during rainfall, about individual trees.

3. Toposequence

Data for the two profiles of the toposequence (Tables 4.9 and 4.10) show the concentration difference of Fe in the two profiles is the most marked difference. In the freely drained Crest profiles, podzolization processes have led to a depletion of Fe in the E horizons with an enrichment in the illuvial Bhs horizon. Oxalate and pyrophosphate extractable data (Table 4.18 and 4.24) support this suggestion. In the poorly drained L.F.S. profiles the Fe has also be removed from upper horizons. The extractable data for Fe in this

profile suggest that most of the mobilized Fe has already been removed from the profile. It would appear therefore that soil development is at a more advanced stage in the L.F.S. profile. In the B horizons of both profiles, but especially in the L.F.S. there is an accumulation of humus material (Table 2.3), which has probably been involved in the transport of iron from upper horizons, down the profile. Podzolization of both profiles has also been hastened by the close proximity (1 m) of beech trees to both profile sites (Chapters 1 and 2).

The higher Mn and Fe values for the Cr horizon of the L.F.S. and the Bs and Bw profiles of the Crest profile are due to a lithic discontinuity at these points in each profile, where underlying material is of a different origin (morainic) to the wind blow loess above[25]. The morainic material is coarser and has therefore not weathered at the rate that the upper horizons have.

CHAPTER 5

AN ASSESSMENT OF ANALYTICAL METHODS

An analysis of silicate materials by wet chemical methods is usually carried out in two steps. Firstly, the sample is decomposed, either by acid dissolution or by fusion. In the latter case the melt is leached with water or inorganic acids. Secondly, the concentrations of the elements present in the resulting solution are determined. For this stage, a wide range of methods are available from classical gravimetric and titrimetric methods, to modern instrumental techniques. Alternatively, analysis may be carried out on the dry material making use of instrumental techniques for the solid state.

In this chapter a comparison is made of some methods of wet chemical decomposition of soils for subsequent analysis. Of the three methods studied experimentally (namely hydrofluoric acid-perchloric acid digestion, lithium metaborate fusion, and sodium carbonate fusion), the hydrofluoric acid-perchloric acid digestion was found to be the most suitable for soil decomposition.

Also a comparison is made of atomic absorption spectroscopic analyses on solutions obtained by wet chemical decomposition of soil samples with X-ray fluorescent analyses of solid samples. The relative suitability of these two methods for soil analysis is assessed.

INTRODUCTION

1. Soil composition

(i) *Silicates*. The major silicate components found in a soil include silica (SiO_2), feldspars (for example, orthoclase ($KAlSi_3O_8$)), and clay minerals (such as the mica muscovite ($K_2Al_2Si_6Al_4O_{20}(OH)_4$), and kaolinite ($Al_2Si_2O_5(OH)_4$).

Silicates contain tetrahedral 'SiO_4' groups linked together in a number of ways by oxygen bridges to form chain, sheet, ring, and three dimensional structures. An example is the $[SiO_3^{2-}]_n$ chain structure of the pyroxenes.

In order to decompose these structures it is necessary to break some of the strong covalent Si-O bonds (799 kJ mol^{-1}) and thereby reduce the polymerization which is a reason for the insolubility of silicates. That macromolecular structures exist in the fusion melts is indicated by the high viscosity and the tendency of the melts to form glasses on cooling.

(ii) *Oxides*. In addition to the silicates, oxides such as Fe_2O_3, MnO_2, and TiO_2 exist in soils, and these need to be taken into solution if the metal ion concentrations are to be measured. This is particularly important in trace metal analysis as many metal ions are incorporated into the structure of the major oxides (see p. 49). This may be achieved by attacking the oxide with a reagent that replaces the oxide ion with another ligand, such as the fluoride ion, producing a more soluble material. Alternatively, the metal ions could be oxidized to produce soluble, usually oxy-anion, salts.

WET CHEMICAL ANALYSIS

1. Sodium carbonate fusion

In the breakdown of the macrosilicate structure the oxygen bridges have to be broken; this would be achieved according to the reaction;

$$[\geq Si - O - Si \leq]^{n-} + O^{2-} \overset{\text{melt}}{\rightleftharpoons} 2[- \underset{|}{\overset{|}{Si}} - O]^{\frac{n+2}{2}} -$$

The sodium oxide would be produced at the temperature of the melt (1000 - 1200^{o}C) from the decomposition of sodium carbonate. The sodium oxide would probably dissociate to give free oxide ions;

$$2Na^{+}_{(\ell)} + CO_3^{2-}{}_{(\ell)} \rightleftharpoons 2Na^{+}_{(\ell)} + O^{2-}_{(\ell)} + CO_{2(g)}$$

which, in the melt, exist sufficiently long to react with the silicates. Another source (minor) of the oxide ion is the metal oxides already present in the soil. As a result of the breakdown of the polymeric substances, water or acid soluble species are formed. Trace metal ions incorporated in the silicate structure are also released and go into solution. It is clear, therefore, that it is necessary to achieve complete decomposition if a total analysis is required.

The completeness of decomposition of a sample, using Na_2CO_3 fusion, depends on the size of the particles in the sample, the duration of the fusion, and the temperature used. High temperatures (1000 - 1200^{o}C) are necessary to allow for the reactions between solids and the melt to be rapid. Most silicates rich in Al, and minerals such as beryl ($Be_3Al_2Si_6O_{18}$), zircon ($ZrSiO_4$), and titanite ($CaTiSiO_5$) are decomposed with

difficulty, and some will often remain in the solid melt.

A number of workers[126-128] have used Na_2CO_3 fusions to decompose soil samples. Boratynski et al.[127] determined Mn, Cu and Zn in solutions obtained by the decomposition of a soil by a) HF digestion, b) Na_2CO_3 fusion, and c) aqua regia digestion. They obtained similar analytical results when using HF digestion or Na_2CO_3 fusion. Aqua regia apparently did not completely remove Mn and Cu from the soils. On the other hand, Terashima[128] investigated the analysis of manganese concretions for Mn, Fe, Co, Ni, Cu and Zn, using the same methods, and established that A.A.S. analysis gave a satisfactory recovery of the elements.

A number of authors[39,130-133] do not recommend Na_2CO_3 fusions for soil decomposition when analyzing for Co, Ni, Cu and Zn. Jeffery[130] considers that the large amount of Na_2CO_3 required is excessive, and can lead to contamination problems. Jeffery, and others[39,130-133], have instead suggested a scheme for transition metal analysis using HF digestions.

Bosch et al.[131] used HF - H_2SO_4 digestions and Na_2CO_3 fusions for decomposition, followed by atomic absorption analysis for Fe, Mn, Ca, Mg, Na, K, and Al. They found that the excess alkali metal introduced in the fusion reduced the analytical precision for Ca and Mg. The results for Mn were similar by both methods, but they preferred the acid digestion for the remaining elements.

Platinum crucibles are commonly used for soil decomposition procedures. During a Na_2CO_3 fusion, the crucible is corroded[130,132] to some extent by the Na_2O produced from the thermal dissociation of the Na_2CO_3;

$$Na_2CO_{3(s)} \rightarrow Na_2O_{(\ell)} + CO_{2(g)}$$

The corrosion is more pronounced for materials containing Fe, particularly Fe(II). Staining of the platinum crucibles by Fe occurs, suggesting reduction to metallic Fe with subsequent alloying to the platinum. The iron can be removed by either repeated extractions with hot concentrated HCl or by fusion with sodium pyrosulphate. Up to 10 mg of platinum[132] may be removed from a crucible in a single Na_2CO_3 fusion of a sample containing iron. The amount of platinum lost for fusions with $LiBO_2$ on similar samples, was around 0.01 mg per fusion, while for a $HF-HClO_4$ digestion, even less platinum was removed.

Nickel, copper, and zinc have been detected[132] on the internal surface of platinum crucibles by X-ray fluorescent analysis, after Na_2CO_3 fusion of soil samples. These metals may also alloy with the platinum, or isomorphously replace alloyed Fe. The metallic radii of these elements are all similar (126, 125, 125, 128 and 137 pm for Fe, Co, Ni, Cu and Zn respectively) and lie within 15% of the radius of Pt metal (139 pm). Also, these elements have some chemical similarity to Pt, as they all occur to the right hand side of the transition metal period.

2. Lithium metaborate fusion

A principal goal of the analysis of silicate minerals is the development of a procedure which allows for the rapid analysis of major elements, including Si, in a wide range of samples. To this end, several groups[134-137] have developed a $LiBO_2$ fusion followed by the A.A.S. method of analysis. The procedure involves, as for Na_2CO_3, routine fusion

followed by dissolution of the melt. In the $LiBO_2$ fusion method there is no need to filter the silica at any stage; this is an advantage over the Na_2CO_3 fusion method. The $LiBO_2$ fusion has also been used in the preparation of constant background discs for X-ray fluorescence[133].

The fusions, normally carried out in platinum crucibles, require free access to oxygen, otherwise Fe, Co, Ni, Cu and Zn, and possibly other metals, are likely to be reduced and alloy with the platinum[132].

The analytical determinations should be carried out as soon after preparation as possible, because on standing, silicate species precipitate and these may remove trace metals from solution by co-precipitation or absorption[136].

Barredo and Diez[138] decomposed silicate rock samples by fusion with a 1:1 mixture of lithium carbonate and boric oxide, and analyzed for major elements, and Mn, Fe and Ti by A.A.S. Some authors[139,140] have used strontium metaborate as the fusion material for rock, soil and ore samples. In another report[141], after the initial fusion of silicate rock samples the melt was dissolved in fluoroboric acid (HBF_4) instead of the usual dilute HCl or HNO_3.

3. Hydrofluoric acid digestion

The alternative to decomposition by fusion is acid digestion. Hydrofluoric acid is the most commonly used acid for the dissolution of silicate minerals. Hydrofluoric acid is a weak acid (pK = 2.9 in 0.5M $NaClO_4$) and its use as a solvent is related to the coordination properties of the fluoride ion. The fluoride ion forms a number of stable

complexes, especially with elements in high oxidation states, such as Zr^{4+}, Ti^{4+}, Al^{3+} and Fe^{3+}.

The reaction between HF and silicates produces initially, hexafluorosilicic acid, H_2SiF_6, which decomposes to SiF_4 above 200°C.

$$SiO_{2(s)} + 6HF_{(aq)} \rightarrow H_2SiF_{6(aq)} + 2H_2O_{(aq)}$$

$$H_2SiF_{6(aq)} \xrightarrow{200^{\circ}C} SiF_{4(g)} + 2HF_{(g)}$$

Hydrofluoric acid is the only acid that achieves this type of decomposition of silicates. The removal of the gaseous SiF_4 leaves the solutions free of silicon.

Hydrofluoric acid can be used alone for sample dissolution or in admixture with strong acids such as $HClO_4$, H_2SO_4, HCl, HNO_3, and aqua regia[133]. These acid mixtures achieve simultaneous destruction of the crystal lattices of silicate and non-silicate minerals, thereby releasing trace elements into solution. The strong acid added to the HF also aids in the removal of excess HF from the reaction by fuming.

During the HF digestion of alumino-silicates, insoluble fluoride complexes (such as $NaAlF_4.xH_2O$ and $MgAlF_5.xH_2O$) can precipitate. The use of a strong acid (such as $HClO_4$ or H_2SO_4) with HF helps to remove the fluoride from such complexes, which can cause interference in subsequent A.A.S. determinations of many metal ions[142] including Ti(IV), Al(III), and Fe(III). Often however, these complexes cannot be destroyed even after repeated evaporations using $HClO_4$ or H_2SO_4. In a digestion of a German rock standard (Slate TB) with a HF-$HClO_4$ mixture, a complex fluoride, very similar

in structure to the mineral ralstonite $Na(Mg,Al)_6(F,OH)_{18}.3H_2O$ was isolated from the residue[133]. Chemical analysis of the residue, which contained negligible amounts of the original rock, yielded fluoride levels up to 48%, and Al levels up to 20%. Other major elements present in the residue were Fe, Mg, Na, and K. It has been shown[143] that sparingly soluble complex fluorides dissolve in concentrated solutions of aluminium salts or boric acid solutions.

During the decomposition of samples with HF there is the possibility of a loss of certain elements by the formation of volatile fluorides. For example GeF_4 and SiF_4 sublime at -37 and -95°C respectively, and BF_3 and AsF_5 have boiling points of -100 and -53°C respectively. The volatility of SiF_4 and its removal is a major reason for the use of HF digestions of silicate samples. However, it is important to maintain a low temperature when fuming off SiF_4 and HF, in order to minimize the loss of other elements. A closed system avoids this problem and can be used for the determination of silicon[144].

Extensive use has been made of the HF digestion in soil and rock analyses[127,128,133,139,144-146]. Langmyhr and Paus[144] discussed the application of HF digestions, followed by A.A.S. analysis, to inorganic siliceous materials of geological origin. One investigation[146] of the relative efficiencies of three digestion methods for geological samples, advocated the use of $HF-HNO_3$ digestion, followed by A.A.S. analysis, when analyzing for Co, Ni, Cu, and Zn.

Use of a closed system enables higher temperatures and pressures to be used[133,147]. Under these conditions the

reactivity of the acids increases and resistant solid phases are dissolved, while the whole procedure is speeded up.

4. Other decomposition techniques

The three wet chemical decomposition methods discussed above have been studied in the present work. However, there is a diversity of decomposition methods in the literature and some of these are listed in Table 5.1. The choice of a particular method depends to some extent on the samples themselves and the type of analyses required. In this section brief comments are made on some of the methods.

The almost universal solubility of perchlorates (except perchlorates of K, Rb, and Cs) is an advantage in using perchloric acid for decomposition. However, contact of the boiling, concentrated acid, or hot vapour, with either organic matter or easily oxidized inorganic matter, can lead to explosions[148].

The technique of sintering[149,150] Na_2CO_3 has many advantages, and overcomes some of the drawbacks of the fusion method. The smaller flux to sample ratio (about 1.5:1) in sintering reduces the volumes of acids and other reagents added at subsequent stages, reduces the amount of sodium salts that have to be washed from precipitates, and results in a lower loss of platinum from the crucible and less contamination from impurities in the Na_2CO_3. On the other hand silica must still be filtered off, and the lower tempeature and shorter heating time[150] in sintering may make sintering less effective at decomposing some minerals.

Bernas[143] developed the fluoroboric acid (HBF_4) matrix to decompose silicates. When boric acid is added to HF,

TABLE 5.1 Some Decomposition Methods Used in Soil and Mineral Analysis

Method	Description	Comment	Reference
HF	Digestion	Open system, 200°C	133,142
HF	High pressure digestion	300°C, over 10130 kPa pressure	130,133, 152
HF/strong acid[a]	Digestion	Suitable for soil samples	130,142
HCl	Digestion	Suitable for carbonates	130,133
HNO_3	Digestion	Suitable for carbonates and sulphides	130,133
$HClO_4$	Digestion	Forms soluble perchlorate salts	130,133, 148
Na_2CO_3	Fusion	Excessive salts added	130,133
$K_2S_2O_7$	Fusion	Quartz insoluble in $K_2S_2O_7$	130,133
$K_2S_2O_8$	Fusion	Not recommended because of spitting	130,133
Na_2CO_3	Sintering	Less contamination than fusion	149,150
NaOH,KOH	Fusion	Attacks platinum	130,133
$LiBO_2$	Fusion	Quick decomposition of soils	134,136, 137
H_3BO_3, B_2O_3	Fusion	Efficient flux; cannot analyze for B	130,133
HBF_4	Digestion	Limits interference in A.A.S.	141,143, 151

[a] Strong acids used include $HClO_4$, H_2SO_4, HCl, HNO_3

fluoroboric acid is produced according to the reaction;

$$H_3BO_3 + 4HF \rightleftharpoons HBF_4 + 3H_2O$$

Excess fluoride in the solution is complexed by the boric acid, and insoluble fluorides are dissolved. Bernas was able to use glassware, over short periods of time without contamination, in handling solutions because the hydrolysis of HBF_4 is slow. Bernas did not attempt to prevent interference in A.A.S. by the addition of releasing agents, claiming his fluoroborate system eliminates interference effects. While this may be true for many silicates, it is unlikely to hold for the full range of silicate minerals that may be encountered. La Brecque[151] analyzed for Al and Si in some Venezuelan laterites using fluoroboric acid, and found the analysis was free from interelemental interference. He also showed that good correlation existed between the results obtained from A.A.S. and from X.R.F. analyses. Saavedra et al.[141] used the same method on some silicate rocks and analyzed for the major and minor trace elements. The solutions were stable and ionization effects were largely removed. Precision in the measurement of Ti (at 0.5% TiO_2) was low.

RESULTS AND DISCUSSION

A selection of soils studied in this work were analyzed by three wet chemical methods, namely Na_2CO_3 fusion, $LiBO_2$ fusion, and HF-$HClO_4$ digestion. Two methods were used to evaluate and compare the three wet chemical methods. These were, a method similar to standard addition, and the analysis of International Rock Standards.

1. Evaluation experiments

(i) *Standard additions.* The results of the method of standard additions to assess the $HF-HClO_4$ digestion, and Na_2CO_3 and $LiBO_2$ fusions, as methods for soil decomposition are given in Table 5.2. Two experiments were carried out; the first, denoted So, involved the addition of known amounts of trace elements to five equal weight samples of the same clay in platinum crucibles. The samples were then digested with acid or fused, and subsequently A.A.S. was used to analyze the resulting solutions. One of the five clay samples just mentioned had no trace elements added. It was assumed that the A.A.S. signals obtained for each of the elements analyzed in the solution from this sample would also contribute to the signal obtained for each of the other four samples, to which known amounts of trace elements had been added. Hence the A.A.S. signal for each element obtained from the non-spiked sample was subtracted from the A.A.S. signal of each element in the four spiked samples, to give the absorption corresponding to the amount of each element in each spike. The amount of each element added was then determined with reference to standard solutions. The results reported in Table 5.2 are expressed as the percentage recovered.

In the second experiment, denoted Sp, no soil component was used. Known amounts of trace elements were added to platinum crucibles, followed by acid digestion or fusion. The A.A.S. results were treated as above, and percentage recovery is given in Table 5.2.

The values listed in Table 5.2 are the mean (n=4) of the percentage recovery of each element added in the four

TABLE 5.2 Evaluation of Wet Chemical Decomposition Methods

	Percentage of Added Trace Elements Recovered[a]						
Method	V	Cr	Mn	Co	Ni	Cu	Zn
$HF-HClO_4$-AAS							
So[b]	102±9	101±5	79±4	92±2	93±4	94±7	97±6
Sp[c]	72±2	54±5	105±4	99±4	102±2	102±2	105±3
$LiBO_2$-AAS							
So	89±10	103±4	83±4	86±5	67±2	52±1	94±1
So(2% La)	86±7	104±4	97±6	93±4	78±1	79±8	94±1
Sp	79±11	97±6	97±2	104±11	99±7	94±1	101±2
Na_2CO_3-AAS							
So(1M HCl)[d]	92±2	94±11	72±5	42±16	25±6	41±66	32±23
So(6M HCl)[e]	104±7	100±5	84±6	46±49	34±41	7±14	57±32
Sp	106±7	104±6	87±7	87±25	74±11	56±47	103±16

a The uncertainty is the standard deviation of the mean of the percentage of material added in four spikes.

b So = soil sample + spike

c Sp = spike with no soil

d (1M HCl) = 1M HCl was used to wash the silica when filtering

e (6M HCl) = 6M HCl was used to wash the silica when filtering

spiked samples, and the standard deviation (σ_{n-1}) of the mean. The elements analyzed for were V, Cr, Mn, Co, Ni, Cu and Zn.

(a) Hydrofluoric acid digestion. The HF digestion, followed by A.A.S. analysis, achieves good recovery of Mn, Co, Ni, Cu and Zn for the Sp series of standard additions. Only partial recovery was achieved for V and Cr (Table 5.2). However, when the standard additions were made to a soil (that is, the So series), good recovery was achieved for V and Cr. Added Co, Ni, Cu, and Zn are also recovered in the So series but only 79% of the Mn was.

Since there is no silicon remaining in the solutions of the So series, the major contribution to the solutions from the soil sample is most likely aluminium. Aluminium may, therefore, be the cause for the improved recovery of V and Cr in the So series. To test this proposition solutions containing V (10, 20, and 30 μg ml^{-1}) and Cr(3, 5, and 7 μg ml^{-1}) in 3 M HCl, with and without added aluminium (200 μg Al ml^{-1}), were analyzed. The absorption signals for V and Cr were higher by 37 and 12%, respectively, in the solutions containing Al, suggesting that the results for V and Cr in the Sp series are low because of the absence of Al. An adjustment of 37% to the V results raises the recovery to 100%, but for Cr the adjustment only raises the figure to 60% recovery. Since, in the So series, all the Cr was recovered, it appears that a further factor is affecting the absorbance. This latter effect was not determined.

In order to explain the low A.A.S. signals for V and Cr, one can consider ionization suppression or the formation of stable species in the flame, and how Al may remove these

interferences. The sum of the 1st, 2nd and 3rd ionization potentials for Al, V and Cr are 5140, 4892 and 5301 kJ mol^{-1} respectively, suggesting that the influence of Al is not as an ionization suppressant for Cr and only marginally so for V.

A more fruitful explanation is in terms of the stability of the metal oxides (M_2O_3) in the flame. It is quite possible that in the nitrous oxide-acetylene flame, the oxides V_2O_3 and Cr_2O_3 have sufficient stability to reduce the metal atom population. One way of investigating this and to determine if there is an effect by Al is to calculate the lattice energies of the sesquioxides. The lattice energies can be determined using the thermochemical cycle shown in Figure 5.1 where ΔH_f is the standard enthalpy of formation, ΔH_A is the standard enthalpy of atomization, ΔH_D is the standard enthalpy of dissociation, ΔH_I is the standard enthalpy of ionization, ΔH_{EA} is the standard enthalpy of electron affinity, and ΔH_{LE} is the standard enthalpy of the lattice formation.

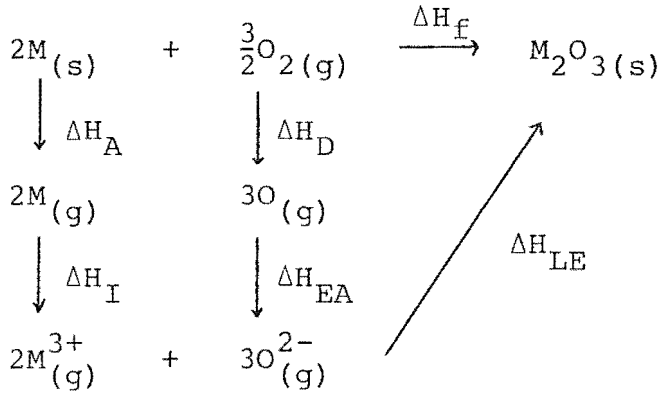

Figure 5.1. The thermochemical cycle for the formation of M_2O_3

The lattice energy is given by

$$\Delta H_{LE} = \Delta H_f - 2\Delta H_A - \tfrac{3}{2}\Delta H_D - 2\Delta H_I - 3\Delta H_{EA}.$$

Numerical values for these terms are given in Table 5.3.

TABLE 5.3 Calculation of Lattice Energies[a,b] for the M_2O_3 Oxides of Al, V, and Cr.

M_2O_3	ΔH_{LE} =	$+\Delta H_f$ -	$2\Delta H_A$ -	$\frac{3}{2}\Delta H_D$ -	$2\Delta H_I$ -	$3\Delta H_{EA}$
Al_2O_3	-15455	-1674	-648	-747	-10280	-2106
V_2O_3	-14893	-1226	-1030	-747	-9784	-2106
Cr_2O_3	-15380	-1131	-794	-747	-10602	-2106

a All values are in kJ mol^{-1}

b Values for ΔH_f from reference 153, all other values from reference 154.

It can be seen from these results that the lattice energy of Al_2O_3 is marginally greater (< 4%) than those for the V and Cr sesquioxides. Aluminium could therefore be acting as an effective releasing agent.

The lattice energies may also be calculated using the Kapustinskii equation[154];

$$L.E. = \frac{N_A A e^2}{4\pi\varepsilon_o} \frac{\nu}{2} \frac{Z_+ Z_-}{r_+ + r_-} \left(1 - \frac{1}{n}\right)$$

where N_A, e, π and ε_o have their usual values, ν is the number of ions in the molecule, Z_+ and Z_- are the numerical values of the charges on the cation and anion, r_+ and r_- are the ionic radii in metres, and A is the Madelung constant.

Since the three sesquioxides have the same corundum structure[155], A will be the same. Taking the ionic radii of Al^{3+}, V^{3+}, Cr^{3+} and O^{2-} as 50, 74, 69 and 140 pm respectively, and assigning n a value of 9[154], the lattice energies, in terms of A, are shown in Table 5.4.

TABLE 5.4 Theoretical Lattice Energy Values Obtained Using the Kapustinskii Equation

M_2O_3	Al_2O_3	V_2O_3	Cr_2O_3
L.E.(kJ mol^{-1})	-9756A	-8661A	-8868A

The trend of these values is similar to that for the experimental data, and shows that the lattice energy of Al_2O_3 is greater than for the other two oxides (by 9-11%). This is because of the smaller ionic radius of the Al^{3+} ion.

(b) Lithium metaborate fusion. When using a $LiBO_2$ fusion followed by A.A.S., there was complete recovery, in the Sp series, for all elements except V ((79±11)%, Table 5.2). The low recovery for V may also reflect the absence of Al in the solutions analyzed. The recovery of the elements Co, Ni and Cu in the So series was low at 86±5, 67±2 and 52±1 % respectively. An improvement was achieved when the solutions contained 2% La[135], a releasing agent, but still 100% recovery for Ni and Cu could not be achieved.

(c) Sodium carbonate fusion. Sodium carbonate fusions followed by A.A.S. analysis, on the Sp series provided good recovery for V, Cr, Mn, Co and Zn, but Ni and Cu were poorly recovered (74±11 and 56±47 % respectively) (Table 5.2). The results for Co and Zn are also suspect due

to the high standard deviations of ±25 and ±16 % respectively. While the percentage recovery of added V, Cr and Mn in the two So series was good, the results for Co, Ni, Cu and Zn were poor with a wide scatter, the standard deviations ranging from 6 to 66%.

The silica filtered off, after taking up the melt in 1M HCl in the So experiments, was taken into solution with HF-$HClO_4$ digestions, and the solutions analyzed for Co, Ni, Cu and Zn by flameless A.A.S. No Co, Ni, Cu, or Zn could be detected. Similar results were obtained for digestions of the silica from the So (6M HCl) experiments, except that the Zn levels were not determined due to significant levels being present in the glass fibre filter paper used.

(ii) *Analysis of International Rock Standards.* Three International Rock Standards were analyzed, and though not strictly the same as soil they do contain the same basic components. The three methods of decomposition were used, followed by A.A.S. analysis, and the results are listed in Table 5.5.

In general, the three decomposition methods produce analytical results in agreement with each other and the reported values[156].

(iii) *The decomposition methods applied to soils.* In addition to the determination of the recovery of added material, and analysis of the International Rock Standards, the three methods of decomposition were used on selected soil samples.

The HF-$HClO_4$ digestion and $LiBO_2$ fusion methods were used for the analysis of the toposequence and Waterton soils,

TABLE 5.5 Evaluation of Wet Chemical Decomposition Methods

Method	Rock Standard[b]	RESULTS ON THE ANALYSIS OF INTERNATIONAL ROCK STANDARDS[a]								
		Ti[c]	V	Cr	Mn	Fe	Co	Ni	Cu	Zn
		(%)	$\mu g\ g^{-1}$			(%)	$\mu g\ g^{-1}$			
$HF-HClO_4$-A.A.S.	BCR-1	1.48±0.10	435±20	13±3	1517±50	9.65±0.30	33±8	8±2	24±6	148±10
	G-2	0.28±0.05	25±6	8±2	272±30	1.90±0.10	4±2	5±2	15±10	94±10
	AGV-1	0.68±0.05	114±10	13±3	790±40	4.99±0.20	14±3	13±3	65±10	99±10
$LiBO_2$-A.A.S.	BCR-1	1.44±0.10	431±10	9±4	1544±50	9.94±0.30	40±8	15±4	n.d.[d]	143±10
	G-2	0.29±0.05	58±10	10±6	242±20	1.79±0.10	n.d.	5±1	15±6	91±6
	AGV-1	0.64±0.05	134±10	16±10	694±40	4.50±0.20	n.d.	13±3	59±8	92±6
Na_2CO_3-A.A.S.	BCR-1	n.m.[e]	n.m.	n.m.	1346±90	8.54±0.30	38±8	n.m.	11±10	136±10
	G-2	n.m.	n.m.	n.m.	212±30	1.32±0.10	21±5	n.m.	n.d.	59±10
	AGV-1	n.m.	n.m.	n.m.	680±50	3.93±0.20	23±6	n.m.	33±10	83±10
Preferred literature values[f]	BCR-1	1.33	410	16	1471	9.46	37	13	19	120
	G-2	0.30	34	9	310	1.87	6	6	11	85
	AGV-1	0.63	125	12	774	4.78	17	17	63	84

a The uncertainty stated is the estimated experimental error.

b BCR-1 is a basalt, G-2 is a granite, and AGV-1 is an andesite.

c Ti concentrations determined colorimetrically.

d n.d. = Not detected.

e n.m. = Not measured.

f See Reference 156.

and the concretions (Waterton samples). The results are listed in Tables 5.6 to 5.9. The analytical results obtained are similar by both methods, although data for V are 30-40% lower using the HF-$HClO_4$ digestion as compared with the $LiBO_2$ fusion. Though less pronounced, V levels in the International Rock Standards G-2 and AGV-1 were also lower using HF-$HClO_4$. The higher values obtained in the $LiBO_2$ fusion method were not explained. The Waterton soils and concretions had previously been analyzed for Mn, Fe, Co, Cu and Zn by Budhia[26], using Na_2CO_3 fusion followed by A.A.S. analysis. The results he obtained (Table 5.10) are in good agreement with those obtained in the present study, using HF-$HClO_4$ digestion and $LiBO_2$ fusion.

The Na_2CO_3 fusion and HF-$HClO_4$ digestion methods were also used on clay samples obtained from fractionation I (p.209), and the results of some representative data are shown in Table 5.11 and 5.12. The analytical data in these tables are in good agreement with each other.

(iv) *Conclusions.*

(a) Standard additions. For the standard addition experiments, the HF-$HClO_4$ method is considered superior, followed by the $LiBO_2$ fusion method. The recovery of added materials (in the presence of a soil component) after decomposition and A.A.S. analysis, tends to be poorest for the elements on the right hand side of the first transition metal series (namely Co, Ni, Cu, and Zn), especially for the Na_2CO_3 decomposition method. The reason could be that these are the elements most likely to alloy with the platinum of the crucible, as discussed on p.116.

TABLE 5.6 TOPOSEQUENCE

Analytical Data for Ti, V, Cr, Mn, Fe, Co, Ni, Cu, and Zn using $HF-HClO_4$ - A.A.S.

SOIL AND HORIZON		Ti[a]	V	Cr	Mn	Fe	Co	Ni	Cu	Zn
		(%)	μg g^{-1}			(%)	μg g^{-1}			
LFS	Ar	0.32	29	18	54	0.40	6	11	14	17
	Er	0.36	32	26	59	0.51	8	5	2	30
	Brs	0.57	65	44	78	0.94	8	5	5	46
	Bhrs	0.48	68	33	81	0.87	9	12	12	41
	Br	0.40	39	35	95	1.00	10	7	1	44
	Cr	0.31	41	30	232	1.83	11	18	4	65
CREST	E	0.22	17	7	35	0.30	5	8	8	14
	EB	0.31	163	21	51	1.67	6	0	3	26
	Bhs	0.41	68	36	69	3.03	7	0	4	34
	2Bs	0.39	52	44	95	2.78	8	11	10	58
	2Bw	0.35	39	34	151	2.66	12	10	6	54

[a] Ti concentrations determined colorimetrically

TABLE 5.7 TOPOSEQUENCE

Analytical Data for Ti, V, Cr, Mn, Fe, Co, Ni, Cu, and Zn using $LiBO_2$ - A.A.S.

SOIL AND HORIZON		Ti[a]	V	Cr	Mn	Fe	Co	Ni	Cu	Zn
		(%)	μg g^{-1}			(%)	μg g^{-1}			
LFS	Ar	0.38	74	5	42	0.40	n.d[b]	9	16	18
	Er	0.41	80	18	55	0.52	n.d	n.d	7	22
	Brs	0.53	105	47	73	0.81	n.d	13	34	55
	Bhrs	0.52	117	22	81	0.86	n.d	5	11	45
	Br	0.40	66	37	90	0.93	n.d	7	18	55
	Cr	0.30	57	25	198	1.65	n.d	19	43	74
CREST	E	0.22	57	5	38	0.25	n.d	25	28	30
	EB	0.32	83	20	39	1.50	n.d	4	15	27
	Bhs	0.42	94	24	70	2.44	29	37	n.m[c]	62
	2Bs	0.41	86	36	105	2.78	n.d	3	15	70
	2Bw	0.40	96	44	155	2.65	n.d	17	35	76

a Ti concentrations determined colorimetrically

b Not detected

c Not measured

TABLE 5.8 WATERTON SAMPLES

Analytical data for Ti, V, Cr, Mn, Fe, Co, Ni, Cu, and Zn in Soils[a] and Concretions Determined using $HF-HClO_4$ - A.A.S.

SOIL AND HORIZON	Ti[b]	V	Cr	Mn	Fe	Co	Ni	Cu	Zn
	(%)	$\mu g\ g^{-1}$		(%)		$\mu g\ g^{-1}$			
SOIL									
1 Brs	0.43	87	39	0.38	4.93	29	n.d[c]	10	91
2 Br	0.47	95	39	0.14	4.30	21	27	23	75
3 Brs1	0.49	92	40	0.62	4.93	26	3	19	137
4 Brs2	0.49	86	26	0.89	4.76	35	25	19	147
CONCRETIONS									
1 Brs	0.34	70	22	5.52	9.59	224	38	18	218
2 Br	0.41	130	36	3.65	8.43	222	162	85	160
3 Brs1[d]	0.31	92	36	7.39	13.4	242	38	45	428
3 Brs1[e]	0.29	92	16	8.10	15.4	229	76	147	543
4 Brs2	0.34	110	30	6.62	10.8	184	52	58	446

a Soils 1, 2, 3, and 4 in this thesis are the same as soils 2-2 B_1, 3-1 B_2G, 3-2 B_1MnC, and 3-2 B_2GMnC in Budhia's work[26].

b Ti concentrations determined colorimetrically

c Not detected

d Concretion size: about 5 mm across

e Concretion size: about 15 mm across

TABLE 5.9 WATERTON SAMPLES

Analytical Data for Ti,V,Cr,Mn,Fe,Co,Ni,Cu and Zn in Soils and Concretions Determined using $LiBO_2$-A.A.S.

SOIL AND HORIZON	Ti	V	Cr	Mn	Fe	Co	Ni	Cu	Zn
	(%)	$\mu g\ g^{-1}$		(%)		$\mu g\ g^{-1}$			
SOIL									
1 Brs	0.44	101	13	0.33	4.10	20	0	27	69
2 Br	0.46	115	34	0.14	3.64	20	6	20	64
3 Brs1	0.51	125	25	0.67	4.66	28	1	4	103
4 Brs2	0.47	113	25	0.80	4.31	37	3	16	113
CONCRETIONS									
1 Brs	0.32	100	nd[b]	5.39	9.78	226	34	23	178
2 Br	0.37	127	39	3.55	7.85	222	212	66	167
3 Brs1[c]	0.31	104	22	7.74	12.7	255	43	19	372
3 Brs1[d]	0.28	94	14	8.87	15.9	199	41	24	482
4 Brs2	0.34	131	39	6.26	10.0	159	68	27	355

[a] Ti concentrations determined colorimetrically.

[b] Not detected.

[c] Concretion size: about 5 mm across.

[d] Concretion size: about 15 mm across.

TABLE 5.10 WATERTON SAMPLES

Analytical Data[a] for Mn,Fe,Co,Cu and Zn in Soils and Concretions - Na_2CO_3-A.A.S.

SOILS AND HORIZON	Mn	Fe	Co	Cu	Zn
	(%)			$\mu g\ g^{-1}$	
SOIL					
1 Br2	0.42	3.72	48	23	105
2 Br	0.13	3.46	21	33	91
3 Brs1	0.58	4.09	46	17	139
4 Brs2	0.73	3.91	44	33	158
CONCRETIONS					
1 Brs	4.79	8.34	258	40	146
2 Br	3.32	7.86	243	77	195
3 Brs1[b]	7.62	11.4	272	63	438
3 Brs1[c]	10.5	14.0	278	52	679
3 Brs2	6.60	9.29	246	56	409

a Data from Budhia[26].

b Concretion size: 5 mm across.

c Concretion size: 15 mm across.

TABLE 5.11 Analytical Data for Some Clays as Determined by the Method of HF-$HClO_4$-Digestion-A.A.S.

SOIL AND HORIZON		Ti[a]	V	Cr	Mn	Fe	Co	Ni	Cu	Zn
		(%)	μg g^{-1}			(%)	μg g^{-1}			
Ho	Aul	0.72	192	100	2300	10.1	44	63	62	251
Ha	Ag	0.54	156	95	1610	7.39	35	47	40	153
Ah	Bs2	1.21	188	65	348	10.1	14	28	24	107
Ah	Bs3	1.27	191	90	410	10.3	16	24	53	118
PodAh	E	1.92	190	73	99	2.08	24	25	47	33
Iw	Cr2	1.09	216	126	347	9.31	17	58	102	193
Io	Bs1	0.97	186	102	1190	10.4	21	29	39	158
Io	Bs2	0.81	146	97	2300	9.77	33	26	64	132
Ku	Cr	1.84	261	75	112	1.41	14	22	36	35
Ok	Br1	3.01	346	90	137	1.02	nd[b]	15	15	21
Ok	Bs	2.41	334	97	114	7.29	nd	30	19	31
Ok	C	2.15	274	156	126	1.89	nd	19	16	32

[a] Ti determined colorimetrically.

[b] nd = not detected.

TABLE 5.12 Analytical Data for some Clays as Determined by the Method of Na_2CO_3 Fusion - A.A.S.

SOIL AND HORIZON		Ti[a]	V	Cr	Mn	Fe	Co	Ni	Cu	Zn
		(%)	$\mu g\ g^{-1}$			(%)	$\mu g\ g^{-1}$			
Ho	Aul	0.68	250	124	2120	9.57	63	93	62	212
Ha	Ag	0.50	227	102	1820	6.42	61	81	40	169
Ah	Bs2	1.08	247	110	318	10.7	48	52	22	112
Ah	Bs3	1.26	239	97	369	9.84	47	53	33	119
PodAh	E	1.59	280	85	93	2.21	24	26	30	34
Iw	Cr2	0.92	236	100	299	7.34	38	61	51	161
Io	Bs1	0.94	241	137	909	10.6	53	52	18	169
Io	Bs2	1.01	189	117	2960	10.2	78	59	30	188
Ku	Cr	1.80	323	100	97	1.21	12	18	28	46
Ok	Br1	2.56	384	106	128	0.93	20	24	21	26
Ok	Cs	2.20	354	93	94	6.50	27	31	26	33
Ok	C	2.12	348	145	104	1.79	17	15	12	32

[a] Ti determined colorimetrically

(b) International Rock Standards and Soils. Good agreement was found for all three decomposition methods. It is surprising that these results do not correlate all that well with the standard addition experiments, particularly for the Na_2CO_3 fusion method. It is possible that there was an artifact in the standard addition experiments. The addition of the spikes on to the bottom of the platinum crucible may have introduced an error. However, this was not the case when the digestions were carried out with $HF-HClO_4$.

(c) The choice of decomposition method. The $HF-HClO_4$ digestion was the decomposition method selected for the analytical study in the present work. A number of reasons led to this decision. The acid treatment gave consistently satisfactory results in the recovery experiments and in the analysis of the International Rock Standards. The other methods of decomposition were not as consistent (especially the Na_2CO_3 fusion). With the acid digestion, excess reagent was fumed off, and Si, a major component, was removed from the solution. The extra steps of dissolution of the melt and filtration, necessary in the fusion methods, were avoided in the acid digestion. As a consequence, the volume of solute can be kept low - an advantage for elements present in small amounts. Finally, decomposition of soil samples with $HF-HClO_4$ is as rapid as the $LiBO_2$ fusion.

A COMPARISON OF ATOMIC ABSORPTION SPECTROSCOPY AND X-RAY FLUORESCENCE

The other major approach to soil and rock analysis is to analyse solid samples. This approach removes the need to

destroy the structure in the sample in order to get the material into solution. It also avoids the problems associated with addition of reagents to the sample with the possibility of contamination. On the other hand, analytical measurements on solid samples have the effect of the matrix to contend with. It was decided, therefore, to compare Atomic Absorption Spectroscopy with X-ray Fluorescence. Both techniques have been developed over the past few decades into standard analytical techniques.

1. X-ray fluorescence

(i) *Introduction.* While X.R.F. can be used to determine elemental concentrations in solid soil or rock samples, it can also be used for solutions. However, a matrix problem as regards background scattering, due to the materials in the solution reagent, occurs. Consequently, X.R.F. analyses of solutions is not the normal procedure.

Around 80 elements (atomic number >8) can be detected using X.R.F., and with special instrumentation, elements with atomic numbers between 2 and 8 can also be detected. The sensitivity of the X.R.F. analyses is less than 1 $\mu g\ g^{-1}$ for the first row transition metals[157]. On a routine basis, the lower limits of detection in X.R.F., for a 20 second counting period, are shown in Table 5.13[159].

TABLE 5.13 Lower Limits of Elemental Concentrations Measured Routinely Using X.R.F. to Analyse Soils and Rocks.

Element	Al	Si	Ti	V	Cr	Mn	Fe	Co	Ni	Cu	Zn
Lower Limit of Conc^{n} ($\mu g\ g^{-1}$) Measured in Sample	100	50	5	20	3	10	5	5	3	2	2

By increasing the counting period these limits can be lowered. The lower limit of detection (in $\mu g\ g^{-1}$) is given by the equation

$$\text{Lower Limit of Detection} = \frac{1}{m}\left(\frac{I_b}{T_b}\right)^{\frac{1}{2}}$$

where m is the counts per second per %, T_b is the counting time in seconds, and I_b is the peak minus background count-rate[157]. Correctly used, and with modern microprocessor facilities, precise analyses of many elements can be made in a short time. Another advantage of X.R.F. is that it is non-destructive.

An area of improvement in present day spectrometers is in the performance of the X-ray tube, particularly as regards power, stability and reliability. Many spectrometers have 3kW tubes that can be operated at 100 kV, and can therefore excite the K X-ray spectra of all elements except Th and U.

X-ray detectors have been improved by the use of semi-conductors, which are used as energy discriminators. The main advantage of semi-conductor detectors (Li doped Si or Ge, operated under vacuum at liquid nitrogen temperatures) is that they may be used with various sources of X-ray excitation, such as low power X-ray tubes, secondary X-ray targets, or radioisotopes. Another advantage is their ability to carry out multielement analyses simultaneously. However, the detector is of limited use for trace element analysis because of a low precision at the parts per million level. The scintillation and gas-flow proportional counters are likely to continue to be widely used for trace element analysis.

2. Atomic Absorption Spectroscopy

(i) *Introduction.* Atomic absorption spectroscopy can be used to analyse for about 70 elements. The limit of detection varies with the element but for most trace metals is generally in the range 0.1 - 1.0 μg g^{-1} in the original sample. In Table 5.14 the detection limits for Al, Si, and the first row transition metals are listed in μg ml^{-1}[159]. Also listed is the concentration, in μg g^{-1}, that this detection limit corresponds to, for a 0.2 g sample taken completely into solution and made up to 10 mls.

TABLE 5.14 Lower Limits of Elemental Concentrations Detected Using A.A.S. in the Analysis of Soil Solutions

Element	Al	Si	V	Cr	Mn	Fe	Co	Ni	Cu	Zn
Lower Limit of Detection (μg ml^{-1})	0.04	0.30	0.11	0.066	0.003	0.005	0.006	0.008	0.003	0.002
Corresponding Lower Limit of Detection (μg g^{-1})	2.0	15.0	5.5	3.3	0.15	0.25	0.30	0.04	0.15	0.10

These values of detection limit (μg g^{-1}) are generally an order of magnitude smaller than the corresponding values for the lower level of determination using X.R.F. (Table 5.13). The detection limit in A.A.S. can be effectively lowered by increasing the trace element concentration in the solution. Concentration techniques include evaporation, ion-exchange, co-precipitation[160] and solvent extraction[161].

Alternative means to lower the detection limit in A.A.S. are also possible by a change of instrumentation. Flameless A.A.S., such as the use of a carbon furnace, uses electro-

thermal techniques for heating and atomization in the place of a flame. Using flameless A.A.S. 2 - 20 μ dm^3 of the liquid sample, containing a few μg of a solid sample can be analysed with detection limits in the parts per billion range. The versatility of A.A.S. is evidenced by the voluminous number of publications citing A.A.S. usage in many diverse geological and earth science fields.

Atomic absorption spectroscopy is also a suitable means for the analysis of solutions obtained by selective extraction of certain chemical forms of elements from soil samples. In some respects the total elemental concentrations of soils is of limited use, compared with the chemical forms of the elements which can be selectively extracted. In this sense A.A.S. is a more useful analytical tool than X.R.F.

There are other features of the A.A.S. instrumentation that offer advantages over X.R.F. The cost of an A.A.S. unit is not high compared with the high capital cost of the X-ray equipment, and the level of operator skill required to use A.A.S. is not as great. The matrix effects in A.A.S. are also less of a problem and more easily controlled than those in X.R.F.

In A.A.S., the radiation source, usually a hollow cathode tube, is modulated, and the measuring device, a photo-multiplier, is set to select that modulation. Although multiple element tubes are sometimes used, problems can arise with the different volatilities of the element; also, the spectra are more complicated. Langmyhr[162] has described an electrodeless discharge lamp, which uses a radiofrequency to give an intense pure spectrum of very narrow line width, of the element which is placed in the resonant cavity. The use

of a continuous source[163], employing xenon arc and a tungsten filament, has advantages in reducing the number of hollow cathode lamps. It has been found however[163], that the sensitivity obtained with a continuous source is less than that of the normal hollow cathode tube. It is possible that laser sources may find use in A.A.S. instruments in the future.

RESULTS AND DISCUSSION - X.R.F. and A.A.S. COMPARISON

X-ray fluorescence was used to analyze the topo-sequence soils for the elements Ti, Cr, Mn, Fe, Ni, Cu and Zn, and the Waterton soils and concretions for Si, Al, Ti, Cr, Mn, Fe, Ni, Cu and Zn (Tables 5.15 and 5.16).

The level of detection achieved on the model of X.R.F. spectrometer used (PW 1540 Manual Vacuum Spectrometer) was poor compared to present day instruments. The detection limit was about 10 $\mu g\ g^{-1}$ for the transition elements analyzed, and 200 $\mu g\ g^{-1}$ for Al and Si. In Table 5.17 the uncertainties estimated for the experimental results obtained by X.R.F. are given. Also given in Table 5.17 are the uncertainties obtained from replicate analyses of a clay sample (Pod Ah, C horizon). Fourteen separate samples of this clay were decomposed by acid digestion, and the resulting solutions analyzed by A.A.S. Listed in Table 5.17 are the mean and standard deviation of fourteen experimentally determined concentrations for each element. Also listed is the mean and the standard error of the mean (S.E.M., $\frac{\sigma}{n}$) where σ is the standard deviation and n the number of cases. The S.E.M. indicates the error in the

TABLE 5.15 TOPOSEQUENCE

Analytical Data for Soils Using X-ray Fluorescence

SOIL AND HORIZON		Ti[a] (%)	Ti[b] (%)	Ti[c] (%)	Cr μg g^{-1}	Mn μg g^{-1}	Fe (%)	Ni μg g^{-1}	Cu μg g^{-1}	Zn μg g^{-1}
LFS	Ae	0.32	0.40	0.32	19	44	0.26	24	1	8
	Er	0.41	0.49	0.36	61	62	0.47	21	5	15
	Brs	0.73	0.87	0.57	41	77	0.62	14	3	35
	Bhrs	0.70	0.83	0.48	56	88	0.68	28	3	45
	Br	0.51	0.60	0.40	32	90	0.74	18	1	54
	Cr	0.35	0.43	0.31	26	224	1.37	25	1	74
CREST	E	0.25	0.31	0.22	16	29	0.33	7	1	0
	EB	0.41	0.49	0.31	25	47	1.41	9	1	0
	Bhs	0.57	0.67	0.41	54	75	2.62	16	9	49
	2Bs	0.54	0.65	0.39	38	102	2.51	22	13	75
	2Bw	0.48	0.58	0.35	33	156	2.35	19	14	72

a Determined by comparison with International Shale Standards

b Determined by comparison with International Rock Standards

c Determined colorimetrically.

TABLE 5.16 WATERTON SAMPLES

Analytical Data for Soils and Concretions Using X-ray Fluorescence

SOIL AND HORIZON		SiO_2	Al_2O_3	Ti[c]	Ti[d]	Ti[e]	Mn	Fe	Cr	Ni	Cu	Zn
		(%)							$\mu g\ g^{-1}$			
SOILS												
1	Brs	69.8	16.4	0.43	0.52	0.43	0.45	6.41	93	21	11	93
2	Br	69.6	18.6	0.45	0.54	0.47	0.20	5.34	75	41	14	84
3	Brs1	69.7	18.8	0.48	0.58	0.49	0.94	6.47	67	31	14	136
4	Brs2	71.9	17.6	0.45	0.54	0.49	1.03	5.70	64	36	4	150
CONCRETIONS												
1	Brs	57.6	11.6	0.37	0.45	0.34	6.12	12.4	58	70	6	188
2	Br	58.9	14.2	0.42	0.51	0.41	4.45	10.7	71	190	58	163
3	Brs1[a]	49.5	10.1	0.38	0.46	0.31	8.00	15.9	62	53	10	307
3	Brs1[b]	44.2	8.7	0.35	0.42	0.29	9.54	18.8	58	62	4	408
4	Brs2	61.8	11.5	0.40	0.48	0.34	7.54	12.9	75	91	26	318

a Concretion size: about 5 mm across.

b Concretion size: about 15 mm across.

c Ti determined by comparison with International Shale Standards.

d Ti determined by comparison with International Rock Standards.

e Ti determined colorimetrically.

TABLE 5.17 Uncertainty in Values Determined by X.R.F. and A.A.S.

	Al	Si	Ti[d]	V	Cr	Mn	Fe	Co	Ni	Cu	Zn
X.R.F.: Uncertainty[a] ($\mu g\ g^{-1}$)	$\pm 10^5$	$\pm 10^5$	±300	-	±10	±50	±500	-	±10	±10	±10
A.A.S.: Mean ± s.d.[b] ($\mu g\ g^{-1}$	-	-	7960±520	113±3	72±7	406±6	58950±1200	20±15	21±14	47±14	184±24
A.A.S.: Mean ± s.e.m.[c] ($\mu g\ g^{-1}$)	-	-	7960±140	113±3	72±2	406±2	58950±320	20±4	21±4	47±5	184±6

a Estimated uncertainty in experimental results.

b Mean of 14 analyses of one sample ± standard deviation.

c Mean of 14 analyses of one sample ± standard error of the mean.

d Ti determined colorimetrically.

mean, as opposed to the standard deviation which indicates the scatter of results about the mean. The standard error of the mean for the A.A.S. values, is in all cases less than the estimated uncertainty of the X.R.F. results (Table 5.17). It is also apparent from Table 5.17 that when the concentrations for Co, Ni, Cu and Zn are less than 50 $\mu g\ g^{-1}$, the uncertainties are relatively high whether determined by X.R.F. or A.A.S.

The reliability of A.A.S. results for Cu was checked by also determining Cu by a colorimetric method using diethyldithiocarbamate to complex the Cu in solution. The solutions analyzed were some solutions obtained after Na_2CO_3 fusions of known amounts of Cu were added to a platinum crucible. The results of these analyses, given in Table 5.18, show that there is a good agreement between A.A.S. and the colorimetric method, even though the recovery of added Cu is low.

The concentration of Ti obtained by X.R.F. was consistently higher than those obtained by the colorimetric method (Tables 5.15 and 5.16). The X.R.F. results for Ti were therefore also determined by making comparisons of the samples with three International Shale Standards, and the values obtained were closer to the colorimetric values than those determined with reference to the International Rock Standards. This suggests that the organic matter in the shales and soils reduces the mass absorption, and that the shale matrix is closer to that of the soil matrix. Although the concentrations of Ti differ when determined by X.R.F. and the colorimetric methods, the relative values are similar by both methods.

TABLE 5.18 Determination of Copper by A.A.S. and a Colorimetric Method.

µg Cu added/100 ml	RECOVERY (%)	
	A.A.S.	Cu-Diethyldithiocarbamate
0.100 mg	32	38
0.200 mg	24	27
0.061 mg	30	33
0.061 mg	29	33
Mean ± s.d.	29 ± 4	33 ± 5

The elements V and Co were not determined by X.R.F. due to serious spectral interference from the Ti Kβ and Fe Kβ lines respectively. The levels obtained for Mn and Zn by X.R.F. show reasonable agreement with the A.A.S. results (Table 5.6 and 5.8), more so in the concretions where the concentrations are higher. Good agreement for the Fe levels in the toposequence soils occurred when determined by X.R.F. and A.A.S., however in the Waterton soils and concretions (where the iron levels are higher), the Fe concentrations were consistently higher when determined by X.R.F. An enhancement similar to that of Ti could also be occurring for Fe when analyzed by X.R.F. Results for Ni are similar by both methods, but the X.R.F. results for Cu are quite low in comparison with the A.A.S. results.

A later model X.R.F. spectrometer, which was not available at the time of this study, coupled with improved correction capacity may considerably improve the X.R.F. data

for the samples analyzed, as well as providing data for V and Co. For this reason, analysis by X.R.F. was not pursued any further as, in terms of the instrument available, it was considered inferior to A.A.S.

CHAPTER 6

TRACE ELEMENTS IN AN IRON-PAN AND IRON-MANGANESE CONCRETIONS

The concentrations and chemical forms of trace elements in some iron-manganese concretions and an iron-pan have been obtained from elemental chemical analyses, electron microprobe and X-ray diffraction analyses.

A survey of the occurrence and properties of trace elements in soils and concretions has been given in Chapter 3. In this chapter, only selected work on trace elements in iron-manganese concretions and iron-pans will be discussed in relation to the present results.

RESULTS AND DISCUSSION

1. Introduction

The concretions studied in the present work were obtained from a shallow gully which has a very gentle gradient resulting in a slow flow of water. At times the soil is saturated. There is an accumulation of trace elements, especially Mn, at the lowest point of the gully[26]. The soil becomes waterlogged during the winter season, resulting in gleying, which causes a mobilization of trace elements, and their subsequent enrichment in the iron-manganese concretions.

The concretions were selected from profiles which had the highest proportion by weight (Table 6.1; although some Tables are included in the Chapter, most are collected in Appendix 1). In profile 3 the Brs1 and Brs2 horizons had 46 and 21% concretions respectively. Possible differences in

the concretions, due to size, were considered by examining two concretions of different size from the Brs1 horizon of profile 3. Since both concretions came from a sample obtained with a corer of 5 cm diameter, the maximum distance possible between them is 9.4 cm.

The iron-pan analyzed comes from the Bs horizon of the Ok profile (at a depth of 0.51 m) of the chronosequence of soils.

TABLE 6.1 WATERTON SOILS AND CONCRETIONS

Data for pH, Horizon Depths, Percentage of Concretion per Horizon by Weight, and Loss on Ignition Values,

Profile and Horizon	Soil(s) or Concretion(c)	pH(H_2O)	Horizon Depth	% Concretion per Horizon by weight	Weight Loss (%) on Ignition
1 Brs	s	5.9	5	8.3	6.3
	c[a]				4.3
2 Br	s	7.5	22	1.0	6.3
	c				5.5
3 Brs1	s	7.0	8	46.0	8.5
	c(medium)[b]				5.9
	c(large)[c]				6.6
3 Brs2	s	7.0	9	21.0	7.2
	c				5.4

[a] Unless specified concretions < 1.5cm in diameter

[b] Concretion 5 mm in diameter

[c] Concretion 15 mm in diameter

2. Iron-manganese concretion formation and morphology

Three types of nodule/concretion formations have been distinguished in Cambodian soils[164] - ferruginous (iron-

containing) nodules, ferruginous concretions, and iron-manganese concretions.

(i) *Ferruginous nodules.* Mitsuchi[164] found irregularly shaped ferruginous nodules (up to 3 cm in diameter) in lower soil horizons. These horizons were dominated by ferruginous mottles, which Mitsuchi suggested were the initial phase of nodule formation, resulting from the segregation of iron under alternate reducing and oxidizing conditions. The large amounts of quartz and kaolinite in the nodules - the major minerals in the surrounding soils - suggest that the nodules were formed by the ferric oxides cementing the soil matrix.

It was observed that below the zone of maximum nodule content, the nodule concentration fell off rapidly. This may be due to persistent moist conditions of the soil at the lower levels, which would inhibit dehydration and crystallization of the ferric oxides[164-166].

(ii) *Ferruginous concretions.* Concretions, as distinct from nodules, exhibit an iron-rich crust containing little, if any, quartz and soil grains, and have a concentric layering effect. The inner zone of the concretions does, however, contain soil grains cemented by ferruginous material. It appears that ferruginous nodules formed initially, and then acted as nuclei for concretion growth. The concretion crust is added to seasonally, through precipitation of ferric oxides from the soil solution as the soil dries out[164-166].

(iii) *Iron-manganese concretions.* Most iron-manganese assemblages are also coated with a ferruginous crust, and are therefore classified as concretions. The crust has concentric layering, while the inner zone - a manganiferous core contain-

ing many soil grains - does not. It is also likely that iron-manganese mottles are the initial stage of iron-manganese concretion formation[164-166]. The low resistance of Mn minerals to weathering, and the mobility of Mn, under weak reducing conditions, suggest that iron-manganese nodules would form before iron nodules.

In the present study, the diameters of the concretions ranged from 0.5 to 2.0 cm. They were unevenly shaped, with up to 3-4 hemispherical mounds protruding outwards from a larger central concretion.

Photographs of a thin section of a concretion (from the Brs1 horizon of profile 3), taken with transmitted and reflected light respectively (Figure 6.1), show predominantly black material, with less than 5% of the area of the sample being detrital quartz and feldspar grains. The average grain size is about 0.2 mm; the sizes range from silt to clay. The detrital grains are very angular.

The black areas in the photographs are mainly confined to roughly circular patches or zones, surrounded by red-brown material. However, patches of black material also extend throughout the red-brown substance. The red-brown, possibly microcrystalline material, appears to be a cementing matrix, while the black material, more towards the centre, incorporates the detrital grains. The black and red-brown patches were identified as mainly Mn and Fe containing regions, respectively, by electron microprobe analysis. This suggests an earlier stage of development of the black Mn containing regions, as compared with the ferruginous material. The larger concretions appear to be composed of separate Mn

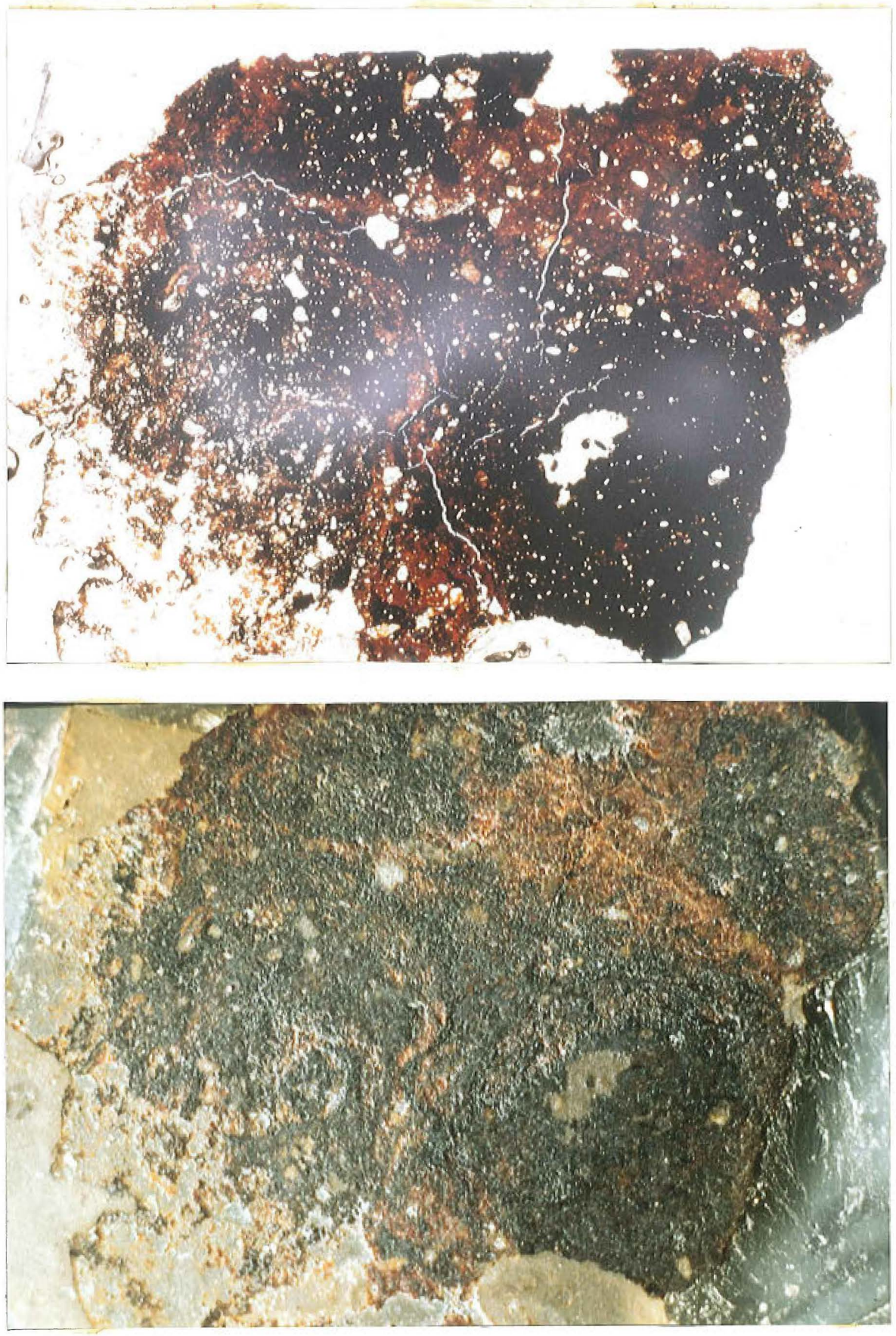

Figure 6.1. Photographs of a thin section of a concretion (3-Brs1,large) taken with transmitted light (top) and reflected light (bottom) respectively.

nodules, cemented together by the ferruginous material. The samples may therefore be called iron-manganese concretions on the basis of Mitsuchi's classification.

Cracks can be seen around some of the Mn (black) areas. These black nodule areas, which have presumably acted as nuclei of the concretions, may have been initially soft, or in the preliminary stages of hardening, when they were coated with ferruginous material. Contractions, at a later date, due to dehydration and crystallization, may have occurred in the nodule producing the cracks. The cracks would then provide pathways for the movement of soil water and the deposition of further material, such as iron oxides, within the concretion. Mitsuchi[164] demonstrated from electron microprobe analyses, that the coatings on the walls of cracks within concretions, were hydrated iron oxides.

3. Mineralogy

Goethite (FeOOH) was the only crystalline iron oxide detected by Schwertmann and Fanning[167] in concretions from a hydrosequence of Bavarian soils. On the basis of electron microprobe analyses, which showed an association between Ca and Mn regions, these workers suggested Mn is present as the mineral birnessite ($(Ca,Mg,Na_2K_2)_xMn(IV)Mn(II)(O,OH)_2$). Other Mn minerals have been identified in Australian soils and concretions; these include lithiophorite ($Li_2Al_8(Mn(II),Co,Ni)_2Mn(IV)_{10}O_{35}\cdot 14H_2O$), todorokite ($(Mn(II),Mg,Ca)Mn(IV)_6O_{13}\cdot 3\text{-}4\ H_2O$), and pyrolusite ($MnO_2$).

X-ray diffraction studies of some Cambodian soils[164] have demonstrated the presence of several Fe minerals, including goethite, hematite (Fe_2O_3), and maghemite (γFe_3O_4).

Silicon and Al were present in quartz and poorly crystalline kaolinite.

On the basis of X-ray diffraction studies, Sidhu et al.[166] found evidence for the presence of illite, quartz and feldspars, in concretions from some Northwest Indian soils. They did not find any evidence for the presence of crystalline Fe and Mn oxides, suggesting that these oxides are in an amorphous form. Similar results were obtained on some Russian podzols[165].

X-ray diffraction analysis was employed, in the present study, to determine the minerals present in concretion and iron-pan samples.

(i) *Results for concretions and surrounding soils.* In the concretions and surrounding soils from the 3-Brs1 and 3-Brs2 horizons, quartz (SiO_2), plagioclase feldspar ($NaAlSi_3O_8$) and illite ($K_xAl_4[Si_{1-x}Al_xO_{20}](OH)_4$) were the dominant crystalline minerals (Table 6.2). For the soil from the 3-Brs1 horizon (Table 6.3), the iron containing minerals, goethite and lepidocrocite (γ-FeOOH) were identified, while for the concretion, just lepidocrocite was identified.

Attempts were made to concentrate the minerals in the concretions. The iron minerals could not be concentrated using a magnet, or by density using the tetrabromoethane (density 2.95 g cm^{-3}). However, a twenty minute treatment of the sample with 40% HF, at room temperature, reduced the base line noise in the X-ray diffractogram, suggesting that poorly ordered material had been removed by the HF. The sample (3-Brs1) was then found to have the basal (0,0,1) spacing for the Mn mineral birnessite, as well as the lines for lepidocro-

TABLE 6.2 WATERTON SAMPLES

X-ray Diffraction Data for the Three Minerals, Quartz, Plagioclase Feldspar, and Illite, Found in Both Concretions and Soils

Quartz		Plagioclase Feldspar		Illite	
d(A)	I/I_1	d(A)	I/I_1	d(A)	I/I_1
4.25	20	6.39	10	9.90	10
3.34	100	5.91	3	4.46	100
2.46	7	5.58	3		
2.28	7	4.03	70		
2.24	3	3.85	10	2.59	100
2.13	4	3.78	30		
1.98	3	3.67	40		
1.82	10	3.51	10		
1.67	3	3.19	100		
1.66	1	2.97	20		
1.54	8	2.93	20		
		2.86	9		
		2.78	2		
		2.64	7		
		2.56	12		
		2.40	4		
		2.32	7		
		2.19	5		
		1.89	9		
		1.80	5		
		1.78	10		
		1.72	6		
		1.57	3		

Variety:		
α-Quartz(SiO_2)	Low Albite($NaAlSi_3O_8$)	Illite($k_xAl_4[Si_{1-x}Al_xO_{20}](OH)_4$)

TABLE 6.3 WATERTON SAMPLE (3-Brs1)

X-ray Diffraction Data Obtained for the Soil and Concretions from the 3-Brs1 Horizon

Soil or Concretion (c)	3-Brs1 (Soil)		3-Brs1 (c)		3-Brs1 (c) 20 minutes 40%HF		Mineral Species[a]
	d(A)	I/I_1	d(A)	I/I_1	d(A)	I/I_1	
					7.38	s[b]	Birn
					5.47	w	u
	6.26	w	6.26	w	6.26	w	Le
					5.81	100	F
	4.98	w					Go
	4.18	w					Go
					3.01	50	F
					2.90	60	F
	2.69	w					Go
					2.30	25	F,Birn
					2.04	20	F,Birn
	1.95	w	1.95	w	1.95	w	Le
					1.93	20	F
					1.76	32	F
					1.51	10	F

a u, unidentified; Go, goethite; Le, lepidocrocite; F, complex fluoride; Birn, Birnessite.

b s, strong; w, weak.

Quartz, feldspar and illite peaks are not included

cite found previously. The line corresponding to the basal spacing for birnessite (738 pm) is reasonably broad, reflecting a somewhat disordered crystal structure.

For the soil from the 3-Brs2 horizon (Table 6.4), the mineral goethite was also identified, as was a clay mineral from the smectite group. Upon treatment with glycerol, the basal line for the smectite changed from 1480 to 1770 pm, as normally occurs for smectite minerals. For the concretion in the 3-Brs2 horizon, the basal line for birnessite was also found. After treatment of the sample for 20 minutes with 40% HF, the basal line became more intense, indicating a concentration of the mineral in the residue. The mineral hematite was also identified. Whenever the HF treatment was used, the X-ray diffractogram was found to contain new lines which did not correspond to any Mn or Fe containing minerals. It is proposed that these lines are derived from a complex fluoride species formed by precipitation during the HF treatment. This is discussed more fully below. A summary of the minerals found is as follows;

	Concretion	Soil
Si:	quartz(SiO_2)	quartz(SiO_2)
Si/Al:	plagioclase($NaAlSi_3O_8$)	plagioclase($NaAlSi_3O_8$)
	illite ($K_xAl_4[Si_{1-x}Al_xO_{20}](OH)_4$)	illite ($K_xAl_4[Si_{1-x}Al_xO_{20}](OH)_4$)
Fe:	lepidocrocite(γ-Fe(III)OOH)	lepidocrocite(γ-Fe(III)OOH)
	hematite($Fe(III)_2O_3$)	goethite(Fe(III)OOH)
Mn:	birnessite($(Ca,Mg,Na_2K_2)_x$-Mn(IV)Mn(II)$(O,OH)_2$)	

(ii) *Results for iron-pan.* The X-ray diffraction pattern, for the iron-pan sample contained lines for quartz,

TABLE 6.4 WATERTON SAMPLE (3-Brs2)

X-ray Diffraction Data Obtained for the Soil and Concretions from the 3-Brs2 Horizon

Soil or Concretion (c)	3-Brs2 (Soil)		3-Brs2 (c)		3-Brs1 (c) 20 minutes 40%HF		Mineral Species[a]
	d(A)	I/I_1	d(A)	I/I_1	d(A)	I/I_1	
	17.7 (Glycerol)						Smec
	14.8	m[b]					Smec
			7.31	s	7.31	s	Birn
					6.61	w	u
					5.81	100	F
					5.47	w	u
	4.98	m					Go
	4.17	m					Go
					3.66	w	Hem
					3.01	50	F
					2.90	50	F
	2.69	m			2.69	m	Go,Hem
					2.51	w	Hem
					2.30	25	F,Birn
					2.04	20	F,Birn
					1.93	40	F
					1.76	60	F
					1.69	w	Hem
					1.51	10	F

[a] u, unidentified; Smec, smectite; F, complex fluoride; Go, goethite; Hem, hematite; Birn, birnessite.

[b] s, strong; m, medium, w, weak.

Quartz, feldspar and illite peaks are not included.

and the clay mineral kaolinite (6.5). After 20 and 40 minute treatments with HF, the quartz lines were still intense, indicating the highly ordered crystalline state of the quartz in this sample. Lines that can be ascribed to the titanium dioxide minerals, anatase and rutile, were also found after HF treatment. A number of new peaks probably correspond to complex fluorides. Campbell[20] also found anatase and rutile to be present in the clay fraction of the Br3 horizon of the Ok profile, which agrees with the present findings.

(iii) *Problems encountered in the concentration of minerals by hydrofluoric acid treatment.* Campbell[20] reported that treatment of a granite sample with 48% HF for more than two hours produced precipitates of complex fluorides (such as $Ca_{0.5}MgAlF_6$, $NaMgAlF_6$ and $KMgAlF_6$). Typical X-ray diffraction data (for $Ca_{0.5}MgAlF_6$) were;

d(nm)	0.582	0.303	0.291	0.251	0.231	0.205	0.193	0.178	0.170	0.151
I/I_1	100	54	86	7	29	24	30	63	5	21

Campbell concluded that the Mg^{2+} concentration in the solution was the limiting factor in the precipitation of the fluoride species. In the present study (Tables 6.3 and 6.4), the diffraction patterns for both concretions, after HF treatment, included a number of the lines, given above, for the complex fluoride species. In the present study, the fluorides were found to be present even after 20 minutes. This could reflect the poorly ordered nature of the samples, which would favour more rapid dissolution, and therefore enabling the solubility product of a fluoride species to be exceeded within a shorter time. The diffractogram data for the iron-pan (Table 6.5),

TABLE 6.5 OKARITO IRON-PAN

X-ray Diffraction Data Obtained for the Okarito Iron-pan

Fe-PAN		Fe-PAN/20 MIN 40%HF		Fe-PAN/40 MIN 40%HF		MINERAL SPECIES[a]
d(A)	I/I_1	d(A)	I/I_1	d(A)	I/I_1	
		9.89	s[b]	9.94	s	F
7.14	w					Kao
		4.96	w	4.98	w	F
4.45	m					Clay(110)
3.58	w					Kao
		3.50	m	3.52	m	Anat
3.45	s	3.47	m	3.47	m	u
						u
		3.25	m	3.25		Rut
3.02	w					u
2.95	w	2.95	w	2.95	m	u
				2.88	s	F
2.59	w			2.59	m	F
				2.52	m	F
				2.34	m	F
2.16	s					u
1.99	m	1.99	m	1.99	m	u
		1.69	w	1.69	w	Rut

[a] F, complex fluoride Taeniolite; Kao, kaolinite; Anat, anatase; u, unidentified; Rut, rutile.

[b] s, strong; m, medium, w, weak.

Quartz peaks are not included.

after HF treatment, has a number of new lines, coincident with a precipitated fluoride species, tentatively identified as taeniolite ($KLiMg_2Si_4O_{10}F_2$).

4. Chemical analysis

Over many studies it has been shown that the elemental chemical composition of concretions differs from that of the surrounding soil. The Al and Si content of the concretions is less than for the soil and generally, the larger the concretion, the lower is the silica content. On the other hand, concentrations of Mn and Fe[164-170] are higher than in the surrounding soil, and trace elements such as Co, Ni, Cu and Zn are enriched in the concretions. The accumulation of Co, Ni, Cu and Zn in concretions is said to be a result of the scavenging properties of the hydrous oxides of Mn and Fe for these trace elements[59,63,171]. However, such a statement is not an explanation. Concretionary matrices are important phases for influencing the concentration of trace elements in the soil solution. In one study[166], the concentrations of Mn, Co and Ni were found to increase with the size of the concretion, but for Fe conflicting results were obtained[165,166,168].

The chemical composition of concretions varies with their depth in the profile. A reason for this is that the iron and humus content of a soil often decrease with increasing depth, while the Mn content increases. A study of concretions from a strongly podzolized soil in Russia[165] showed that in the A2 horizon, Fe precipitation was dominant, while in the lower horizons, Mn compounds had formed, reaching a maximum of 13% in the lowest B horizon. The difference in

the behaviour of Fe and Mn in the soil profile is expected because Mn compounds are more soluble and mobile than Fe compounds[77]. Both pH and Eh values are higher in the lower part of soil profiles[165] than in the upper horizons, and therefore Fe(III) compounds precipitate, mainly in the upper horizons as concretions and mottles, while Mn(IV) containing materials are formed mainly in the lower horizons (Figures 3.3 and 3.4).

Studies on the spatial distribution of Mn and Fe in concretions have been carried out by several authors using electron microprobe analysis[71,167,168,172,173]. Point counting showed concretion crusts to be high in Fe and low in Mn, while for the core, the opposite trend was observed. The concentrations of Mn and Fe in some areas have been shown to lie between 50-60%. These results suggest separate deposition of Mn and Fe at these areas[172].

Chemical analyses were used in this work to determine the total elemental concentrations in concretions and an iron-pan, and their surrounding soils. In addition, the amounts of trace metals removed from the sample on treatment with two extraction reagents, ammonium oxalate and sodium pyrophosphate, were measured.

(i) *Total elemental analysis of concretions.* Hydrofluoric acid-perchloric acid digestions, followed by A.A.S. analysis, were used to determine the concentrations of V, Cr, Mn, Fe, Co, Ni, Cu and Zn (Table 5.8) in the concretions and the surrounding soils. Titanium was determined colorimetrically. Analytical data for Al and Si (and also Ti, Cr, Mn, Fe, Ni, Cu and Zn) was obtained by X.R.F. analysis (Table 5.16).

The concentrations of Al, Si, Ti and Cr were found to be higher in the soils than in the concretions, while for V, Mn, Fe, Co, Ni, Cu and Zn, higher concentrations occurred in the concretions. This information is summarized in Table 6.6, where the concretion to soil ratio for each element is given.

TABLE 6.6 . WATERTON SAMPLES

The Concretion to Soil Ratios of Elemental Concentrations Determined by the HF-$HClO_4$ A.A.S. Method

Profile and Horizon	Si	Al	Ti[a]	V	Cr	Mn	Fe	Co	Ni	Cu	Zn
1 Brs	0.83	0.71	0.79	0.87	0.56	14.5	1.95	7.8	—	1.8	2.4
2 Br	0.85	0.76	0.87	1.4	0.92	26.1	1.96	10.6	6.0	3.7	2.1
3 Brsl[b]	0.71	0.54	0.63	1.0	0.90	11.9	2.72	9.3	12.0	2.4	3.1
3 Brsl[c]	0.63	0.46	0.59	1.0	0.40	13.1	3.12	9.9	25.2	7.7	4.0
3 Brs2	0.86	0.65	0.69	1.3	1.2	7.44	2.27	5.3	2.1	3.1	3.0
Mean	0.78	0.62	0.71	1.11	0.80	14.6	2.4	8.4	11.3	3.7	2.9

[a] Ti determined colorimetrically

[b,c] Concretion sizes 5 and 15 mm in diameter respectively

The elements Mn and Co have been most strongly concentrated in the concretions compared with the surrounding soil. The mean concretion to soil ratios for Mn and Co are 14.6 and 8.4 respectively. The elements Fe, Ni, Cu and Zn are all enriched in the concretions, in most cases 2 to 4-fold. The concretion to soil ratios for Ni in the Brsl horizon are very high. This is probably due to the low Ni levels in the soil, which have a high associated experimental error, rather than due to a high Ni concentration in the concretion. The elements Si, Al, Ti and Cr all have lower concentrations in the concretions.

Vanadium concentrations in the soils and concretions were found to be similar.

From the analytical data, in Table 5.8 and 5.16, for two concretions of different size in the Brs1 horizon, it can be seen that the smaller concretion has higher concentrations of Si and Al, and lower concentrations of Mn, Fe and Zn. The levels of Ti, V, Cr, Co, Ni and Cu are not significantly different in the two concretions. These results may be explained by the greater proportion of soil particles (and hence higher concentrations of Al and Si) in the smaller concretion than in the larger.

In profile 3, the Brs2 horizon is below the Brs1 horizon. The concentration of Mn in the soil of the Brs2 horizon is greater than that of the Brs1 horizon (Table 5.8) as may be expected from the discussion earlier. However, the Mn concentration in the concretions is lower for the Brs2 horizon. The Fe concentration in the soils of the Brs1 and Brs2 horizons is similar, while in the concretions the Fe levels are lower in Brs2 horizon.

Possible reasons for the enrichment of the elements Mn, Fe, Co, Ni, Cu and Zn in the concretions, have been outlined in Chapter 3, and will be further discussed later in this chapter.

(ii) *Total elemental analysis of an iron-pan.*
Analytical data for the iron-pan (Bs horizon) and adjacent soils (Brs and C horizons) are given in Table 6.7. The Fe concentration is higher in the iron-pan than in the adjacent soils, while the Mn concentration is lower. The levels of the other elements are all low, and similar to those of the

TABLE 6.7 IRON-PAN (Bs Horizon, Ok Profile)
Analytical Data for Iron-pan and Adjacent Horizons

HORIZON	Ti (%)	V ($\mu g\ g^{-1}$)	Cr ($\mu g\ g^{-1}$)	Mn ($\mu g\ g^{-1}$)	Fe (%)	Co ($\mu g\ g^{-1}$)	Ni ($\mu g\ g^{-1}$)	Cu ($\mu g\ g^{-1}$)	Zn ($\mu g\ g^{-1}$)
Br3 (soil)	0.45	35	12	111	0.25	4	5	5	11
Bs (iron pan)	0.49	60	17	101	1.56	3	4	4	11
C (soil)	0.49	36	12	173	0.41	5	16	4	18

adjacent horizons. These results contrast with those found for the concretions. The most striking feature of the data is the 4 to 5-fold increase in the levels of Fe in the iron-pan, compared with the adjacent horizons. This is most likely due to the mobilization of Fe in the upper horizons under the gleying conditions of the Ok profile, and its movement down the profile, probably as organic complexes, to the pan. A notable feature of the pan is that the Fe to Mn ratio is 154, while in the concretions, this ratio is about 2. This can be attributed to greater loss of Mn from the Ok profile during weathering.

(iii) *The amount of trace elements extracted from soils and concretions*. Less than 2% of the total Si, Al, Fe, Mn and Cu content of the concretions, and about 10% of the Zn, were extracted with sodium pyrophosphate (Table 6.8). Considerably higher amounts were extracted by ammonium oxalate - 3 and 13% of the total Si and Al respectively, 60% of the Fe, 81% of the Zn, 45% of the Cu, and 95% of the Mn (Table 6.9). Ammonium oxalate is reputed to extract mainly non-crystalline material[174]. The high oxalate-extractable levels of Mn, Fe,

TABLE 6.8 WATERTON SAMPLES

The Amount of Trace Elements Extracted by Sodium Pyrophosphate, Expressed as a Concentration ($\mu g\ g^{-1}$) of the Sample, and as a Percentage of the Total Content of that Element in the Sample (in parentheses).

SOIL AND HORIZON	Si	Al	Fe	Mn	Cu	Zn
			($\mu g\ g^{-1}$)			
Soils						
1 Brs	3080(0.94)	21(0.02)	640(1.30)	127(3.3)	0(0)	2(2.2)
2 Br	3310(1.02)	300(0.40)	950(2.21)	108(7.7)	0(0)	2(2.7)
3 Brs1	2900(0.89)	186(0.35)	910(1.85)	103(1.7)	0(0)	7(5.1)
3 Brs2	3280(0.98)	194(0.42)	970(2.04)	67(0.75)	0(0)	65(44)
Mean	(0.97)	(0.30)	(1.02)	(5.1)	(0)	(13.5)
Concretions						
1 Brs	4260(1.58)	512(0.83)	1340(1.40)	34(0.06)	0(0)	26(11.9)
2 Br	4150(1.51)	33(0.04)	570(0.68)	5(0.01)	0(0)	18(11.3)
3 Brs1[a]	4400(1.90)	257(0.48)	1450(1.08)	21(0.03)	0(0)	41(9.6)
3 Brs1[b]	3810(1.85)	0(0)	1480(0.96)	9(0.01)	0(0)	49(7.6)
3 Brs2	4210(1.46)	32(0.05)	920(0.85)	4(0.01)	0(0)	42(9.4)
Mean	(1.66)	(0.28)	(0.99)	(0.02)	(0)	(10.0)

a,b Concretion sizes 5 and 15 mm in diameter respectively.

TABLE 6.9 WATERTON SAMPLES

The Amount of Trace Elements Extracted by Ammonium Oxalate, Expressed as a Concentration (%) of the Sample, and as a Percentage of the Total Content of that Element in the Sample (in parentheses).

SOIL AND HORIZON	Si	Al	Fe	Mn	Cu	Zn
			(%)		($\mu g\ g^{-1}$)	
Soils						
1 Brs	0.57(1.8)	0.60(6.9)	1.30(26.4)	0.30(78.9)	3(30.0)	69(75.8)
2 Br	0.77(2.4)	0.83(8.4)	1.33(30.9)	0.12(85.7)	6(26.1)	31(41.3)
3 Brs1	0.64(2.0)	0.68(6.8)	1.96(39.8)	0.62(100.0)	4(21.1)	95(69.3)
3 Brs2	0.64(1.9)	0.87(9.3)	1.73(36.3)	0.71(79.8)	4(21.1)	71(48.3)
Mean	0.66(2.0)	(7.9)	1.58(33.4)	0.44(86.1)	4.3(24.6)	67(58.7)
Concretions						
1 Brs	0.64(2.4)	1.08(17.6)	5.69(59.3)	4.86(88.0)	9(50.0)	171(78.4)
2 Br	0.64(2.3)	0.74(9.9)	3.79(45.0)	3.59(98.4)	57(67.0)	127(79.4)
3 Brs1[a]	0.87(3.8)	0.74(13.9)	9.27(69.2)	7.18(97.2)	21(46.7)	430(100)
3 Brs1[b]	0.81(3.0)	0.50(10.9)	10.4(67.5)	8.63(106.5)	11(7.5)	329(60.6)
3 Brs2	0.86(3.0)	0.74(12.2)	6.61(61.2)	5.53(83.5)	31(53.4)	393(88.1)
Mean	0.76(3.1)	(12.9)	7.15(60.4)	5.96(94.7)	26(44.9)	290(81.3)

a,b Concretion sizes 5 and 15 mm in diameter respectively.

Cu and Zn, particularly for the concretions, suggest that these elements are present in non-crystalline hydrous oxides. It is probable that the high levels of extractable Cu and Zn are due to these elements being liberated as the Mn and Fe hydrous oxides are dissolved by the ammonium oxalate. The low levels of oxalate-extractable Al and Si, in contrast, suggest these elements are present in mainly crystalline form.

The low levels of Si, Al, Mn, Fe and Cu extracted by sodium pyrophosphate, which is claimed to remove organic bound material[118], suggest that little of these elements, in the concretions, is present in an organic bound form. About 10% of the Zn in the concretions is associated with organic matter.

(iv) *The amount of trace elements extracted from the iron-pan.* Low levels of Si, Mn and Zn were extracted from the iron-pan with both ammonium oxalate and sodium pyrophosphate (Table 6.10). Comparable levels of Al (10% of the total Al) were extracted by both extractants. The proportion of total Fe extracted by ammonium oxalate was 56%, while 41% of the total Fe was extracted by sodium pyrophosphate.

Most of the non-crystalline Al and Fe in the iron-pan was extracted with ammonium oxalate. The levels of Al and Fe extracted by sodium pyrophosphate were similar to the levels extracted with oxalate and therefore, this Al and Fe is present as organic bound Fe and Al.

Levels of sodium pyrophosphate extractable Al and Fe in the iron-pan are higher than for the concretions, suggesting that organic material is more important in the formation of the iron-pan than the concretions. For the formation of

TABLE 6.10 IRON-PAN (Bs HORIZON, Ok PROFILE) Concentrations of Elements Extracted by Ammonium Oxalate and Sodium Pyrophosphate and as a Percentage of the Total Amount in the Sample (in parentheses).

Horizon	Mn	Fe	Zn	Al	Si
			($\mu g\ g^{-1}$)		
Ammonium oxalate extraction					
Br3	0(0)	60(2.4)	12(109)	1360(5.3)	0(0)
Bs	8(8)	8730(56.0)	8(73)	3660(14.2)	420(0.1)
C	0(0)	870(21.2)	13(72)	5830(18.3)	2130(0.5)
Sodium pyrophosphate extraction					
Brs	0(0)	0(0)	0(0)	1170(4.6)	10(0)
Bs	0(0)	6410(41.0)	11(100)	3620(14.1)	520(0.1)
C	0(0)	390(9.5)	0(0)	3240(10.2)	0(0)

iron-pans, which often occur in the B horizons of podzolized soils[18], it was initially thought that humic acids from the litter horizon dissolved Fe and Al sesquioxides from the A2 horizon[116,175]. McKeague showed that much of the Fe, extracted by ammonium oxalate, from the B horizons of podzols, was also extractable with sodium pyrophosphate, and was therefore organic bound[116]. However, podzolization can occur without any humic acids from the litter horizon dissolving in the water; if humic acids are dispersed from the litter, they are not able to solublize iron hydroxide films[2].

Mobilization of Al and Fe is probably achieved by some soluble organic compounds which the rain washes off living or recently dead leaves or vegetation. These compounds include polyphenols which, under acid conditions, can reduce ferric iron to form water soluble complexes with both ferrous and aluminium ions[176].

There is still uncertainty over the reasons for the precipitation of Fe and Al ions in the B horizons of podzols. Probably, initial deposition begins as the soil dries out in summer, resulting in an oxidation of the ferrous polyphenol compounds, forming ferric hydroxides[2]. Once deposition has started, it will continue more readily, since the ferrous polyphenols can be absorbed by the ferric oxide surface, and be oxidized[177], probably with the assistance of bacteria[178].

5. Electron microprobe analysis

One aspect of the present study of the concretions and the iron-pan, was to find any structural or analytical relationship between the various elements. An electron microprobe was used for this study, to determine directly the relationships between Mn and Fe and the other trace elements in the concretions and iron-pan.

(i) *Results of concretion study.*

(a) Point analysis. Approximately 30 to 40 points on each concretion sample were analyzed using an electron beam of 1 μm in diameter. In addition to counting on areas selected at random, a search was made for areas of high Mn and Fe. Effort was also made to ensure that the points analyzed were at widely separated positions on the sample and not from just one small area. The concentrations found, expressed as a percentage by weight composition (Table 6.11 to 6.13) ranged from <0.01 to 54% for Mn, from 0.2 to 47% for Fe, from 0.1 to 12% for Al, 0.1 to 45% for Si, and <0.01 to 32% for Ti. The concentrations of V, Co, Ni, Cu and Zn were all less than 1.2% and if the level of an element was <0.01% it was considered as not detectable (n.d.). For each concretion, correlation

coefficients (Table 6.11 to 6.13) were calculated for each pair of elements, using all the data. It is pertinent to qualify the use of correlation coefficients in the context of treatment of electron microprobe data. The Pearson correlation coefficients calculated for the present data provide a valid estimate of the association between two variables only if the data are approximately normally distributed[179]. Scattergrams, of microprobe data, for different pairs of elements showed that the data for the small Brs1 and the Brs2 concretion had an approximately normal distribution, but that for the larger Brs1 concretion, a logarithmic distribution was sometimes evident. An example of this is shown in Figure 6.2 which shows the variation of Mn concentrations with Zn concentrations. The cause of the non-normal distrib-

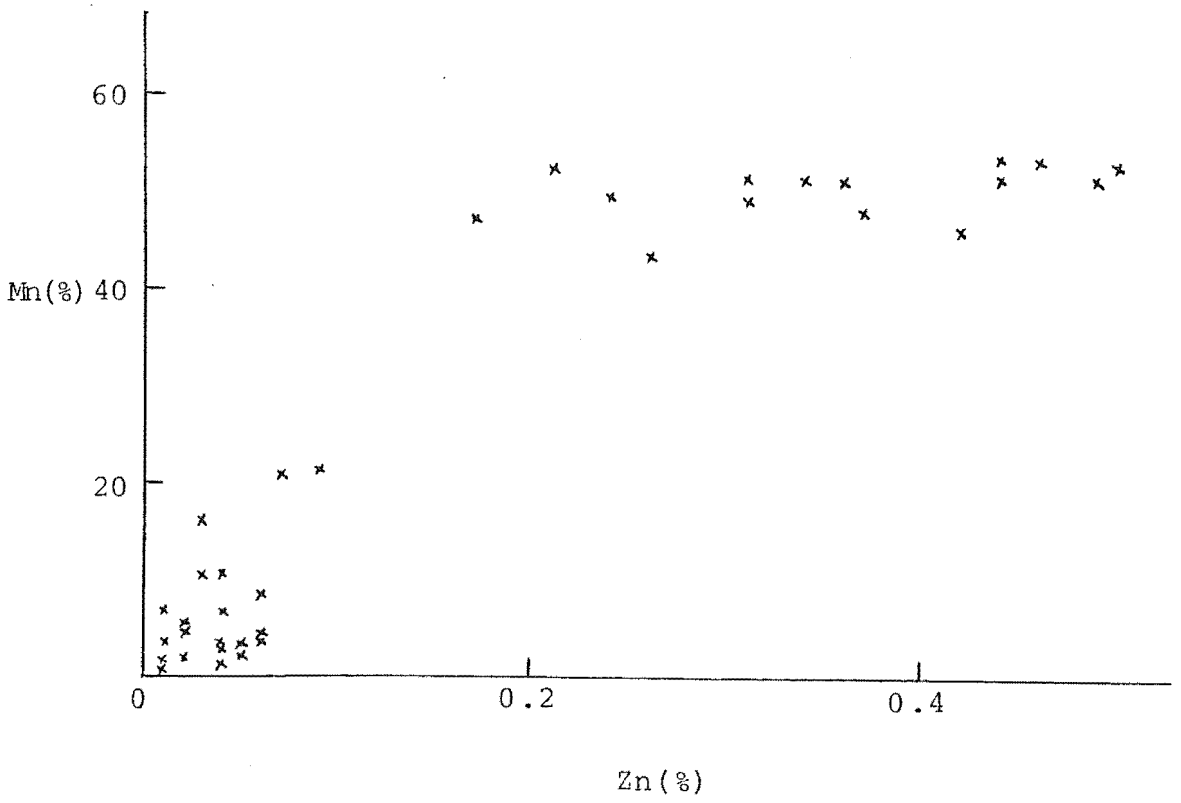

Figure 6.2. Scattergram of Mn and Zn concentrations for the Large 3-Brs1 Concretion.

ution is the non-random sampling procedure used in order to select areas of high Mn and high Fe concentrations. The high Zn concentrations which correspond to higher Mn concentrations are scattered widely, whereas at low Zn concentrations there is a closer grouping of points. The effect of this distribution is that,statistically, it behaves as two points rather than as a distribution of 40 points. This effect can be minimised by a logarithmic transformation of the data.

Calculation of correlation coefficients using log data was carried out (for the large Brsl concretion) on all pairs of elements with Mn and Fe.

A summary of significant correlation coefficients is given in Table 6.14. Most significant correlations (both positive and negative) were found for the large 3-Brsl concretion. The elements Si, Ti and Fe are all highly significantly correlated, while there is also a significant correlation between Al and Fe. There is a highly significant positive correlation between Mn and Co, Ni and Zn, and between Fe and V. The elements Mn, Co, Ni and Zn have significant negative correlations with Al, Si, Ti and Fe. These results suggest that the elements fall into two groups, namely Al, Si Ti, Fe, and Mn,Co,Ni and Zn.Copper does not correlate strongly with any of the other elements, and V correlated with Fe.

For the smaller concretion from the 3-Brsl horizon, similar though less pronounced correlations are found (Table 6.14), with Mn highly significantly correlated with Co and Zn, and in this case Fe significantly negatively correlated with Si. Silicon is also negatively correlated with Co.

For the third concretion, 3-Brs2, the pattern of

TABLE 6.14 CONCRETIONS

Summary of Significant Correlations Found From Electron Microprobe Data for Concretions

	POSITIVE CORRELATION COEFFICIENT		NEGATIVE CORRELATION COEFFICIENT	
	Significant[a]	Highly Significant[b]	Significant	High Significant
Sample 3-Brs1(Large)				
Al	Fe	Si,Ti	Zn	Mn,Ni
Si		Al,Ti,Fe	Co	Mn,Ni,Zn
Ti		Al,Si,Fe	Co	Mn,Ni,Zn
Mn		Co,Ni,Zn		Al,Si,Ti,V,Fe
Fe	Al	Si,Ti,V		Mn,Ni,Zn
Sample 3-Brs1(Small)				
Al			Ti	
Si			Fe,Co	
Ti		V,Ni	Al	
Mn		Co,Zn		
Fe			Si	
Sample 3-Brs2				
Al		Si		
Si		Al	Mn,Ni,Zn	
Ti		V	Co	
Mn		Ni,Cu,Zn		Fe
Fe			Ni	Mn,Zn

[a] Significant at 1% level

[b] High significant at 0.1% level

correlation coefficients resembles more closely that of the large 3-Brs1 concretion. The elements Al and Si are positively and highly significantly correlated, and Si is negatively correlated with Mn, Ni and Zn, as is Fe. Manganese is positively and highly significantly correlated with Ni, Cu and Zn.

As well as calculating correlation coefficients, the data for each concretion was analyzed to see if there was any

significant difference in the concentration of the elements with the type of area in which it was found. The areas selected were high Mn areas (concentration >25% Mn), high Fe areas (concentration >25% Fe), and low Mn and Fe areas. The cut-off between high and low areas is somewhat arbitrary, but does not greatly influence the overall relationships. The means and standard deviations for the concentrations of each element were calculated in the high Fe, high Mn and low Mn/Fe areas (Tables 6.11-6.13). The differences between the means for each element were then tested using the student's t test. The results are presented in Table 6.15, in terms of the probability that there is no significant difference between the means.

TABLE 6.15 Probability that there is no Significant Difference between the Means of the Various Elements in High Mn and High Fe Areas

SAMPLE	PROBABILITY			
	<0.001	<0.01	<0.02	0.2
Large concretion 3-Brs1				
Elements with highest concentration in high Mn areas	Ni,Zn	Co		Cu
Elements with highest concentration in high Fe areas	Si,Ti,V		Al	
Small concretion 3-Brs1				
Elements with highest concentration in high Mn areas	Zn			Co
Elements with highest concentration in high Fe areas				
Concretion 3-Brs2				
Elements with highest concentration in high Mn areas	Zn	Ni		Cu
Elements with highest concentration in high Fe areas				V

Enrichment within the various areas of the concretion can be seen from the ratio of the concentration of an element in the concretion to the concentration in the surrounding soil (Table 6.16). Data from the chemical analysis of bulk concretions is also included in this Table.

(i) Large concretion, 3-Brs1 horizon. For the elements Al, Si, Ti and V, the mean values (Table 6.11) are higher in the high Fe areas, and are significantly different to the mean levels found in the high Mn areas (Table 6.15), suggesting that there are more soil particles associated with the Fe areas. In the low Mn/Fe areas, the levels of Al, Si and Ti are, as expected, even higher (Table 6.16). There is no enrichment of Al, Si and Ti in the concretion as all the concretion to soil concentration ratios are <1. For V in high Fe areas, the concretion to soil concentration ratio is 4 times the concretion to soil ratio of the bulk concretion, indicating a significant enrichment of V in these areas.

The concentrations of Co, Ni, Cu and Zn are higher in Mn rich areas and the mean concentration for each element is significantly different to the mean in the high Fe areas (Table 6.15). For these elements, the greatest enrichment occurs in the Mn areas of the concretion, as indicated by the concretion to soil concentration ratios (Table 6.16), which are also much greater than the concretion to soil ratio for the bulk concretion values. Except for Zn, the concretion to soil ratios are greater in the Fe areas than the ratio for the bulk concretion, indicating that Co, Ni and Cu are also enriched, but to a lesser extent, in the high Fe areas.

The enrichment of Zn in the high Mn areas is nearly as

TABLE 6.16 WATERTON CONCRETIONS

Enrichment of Elements within the Various Areas of the Concretions, and in the Bulk Concretion, compared with the Surrounding Soils

CONCRETION TO SOIL CONCENTRATION RATIO

Concretion	3-Brs1 (small)				3-Brs2				3-Brs1 (large)			
Area	High Mn	High Fe	Low Mn/Fe	Bulk concretion[a]	High Mn	High Fe	Low Mn/Fe	Bulk Concretion	High Mn	High Fe	Low Mn/Fe	Bulk Concretion
Al	0.55	0.46	0.64	0.46	0.37	0.42	0.68	0.65	0.12	0.27	0.57	0.54
Si	0.50	0.45	0.75	0.63	0.25	0.26	0.56	0.85	0.02	0.27	0.39	0.71
Ti	2.1	2.6	8.71	0.59	3.8	1.2	7.3	0.69	0.04	0.27	0.65	0.63
V	1.5	4.0	4.9	1.0	2.3	3.5	5.5	1.3	1.1	4.4	2.0	1.0
Mn	-	5.2	9.2	13.1	-	7.2	5.4	7.4	-	5.5	10.4	11.9
Fe	1.0	-	0.97	3.1	0.98	-	2.3	2.3	0.47	-	1.8	2.7
Co	36.2	19.2	9.2	8.8	15.4	17.1	5.4	5.3	30.0	11.5	3.8	9.3
Ni	5.5	3.5	3.5	1.7	28.0	8.0	4.0	2.1	19.4	3.2	-	2.0
Cu	8.9	8.4	6.3	7.7	18.9	11.1	9.0	3.1	15.8	5.3	-	2.4
Zn	8.8	3.1	2.2	4.0	17.7	4.4	2.0	3.0	25.5	2.6	6.6	3.1

	High Mn/Fe	Low Mn/Fe	High Mn/Fe	Low Mn/Fe	High Mn/Fe	Low Mn/Fe
Al	0.51	0.64	0.39	0.68	0.20	0.57
Si	0.48	0.75	0.25	0.56	0.14	0.39
Ti	2.3	8.7	2.5	7.3	0.15	0.65

[a] From Tables 5.8 and 5.16

great as for Co, and taking into account that there is over 4 times as much Zn in the soil than Co, it could be claimed that Zn is the more strongly enriched of the four elements Co, Ni, Cu and Zn. Of the elements enriched in the high Mn areas, Cu is the least enriched, and while Cu is higher in Mn areas than the Fe areas, the significance of this difference is not great ($p < 0.2$). This is portrayed diagramatically in the distribution histogram for Cu in the high Mn and Fe areas (Figure 6.3). A similar histogram for Zn shows clearly the distinct enrichment of Zn in the high Mn areas.

The levels of Fe in the Mn rich areas are less than in the surrounding soil, but for Mn, in the Fe rich areas, an enrichment factor of 5-6 occurs (Table 6.16). In the low Mn/Fe areas, the concretion to soil ratios for both Mn and Fe are similar to that obtained for the bulk concretion ratio.

(2) Small concretion, 3-Brsl horizon. This concretion is different in some respects to the larger sample from the same horizon. The levels of Al and Si, even in the Mn and Fe rich areas, are quite high, and as a consequence, the Mn and Fe levels are significantly lower than in the large concretion (Table 6.12). From the concretion to soil concentration ratios (Table 6.16), it can be seen that the Si content of areas low in Mn and Fe in the concretion is 75% of the levels in the soil, while for Al, 64% of the level in the soil. Even in the high Mn and Fe areas, the levels of Si and Al are approximately 50% of the soil levels. Therefore, the smaller concretion has a greater proportion of soil particles, a fact which supports the suggestion that the soil particles act as nuclei for concretion formation and therefore, there will be

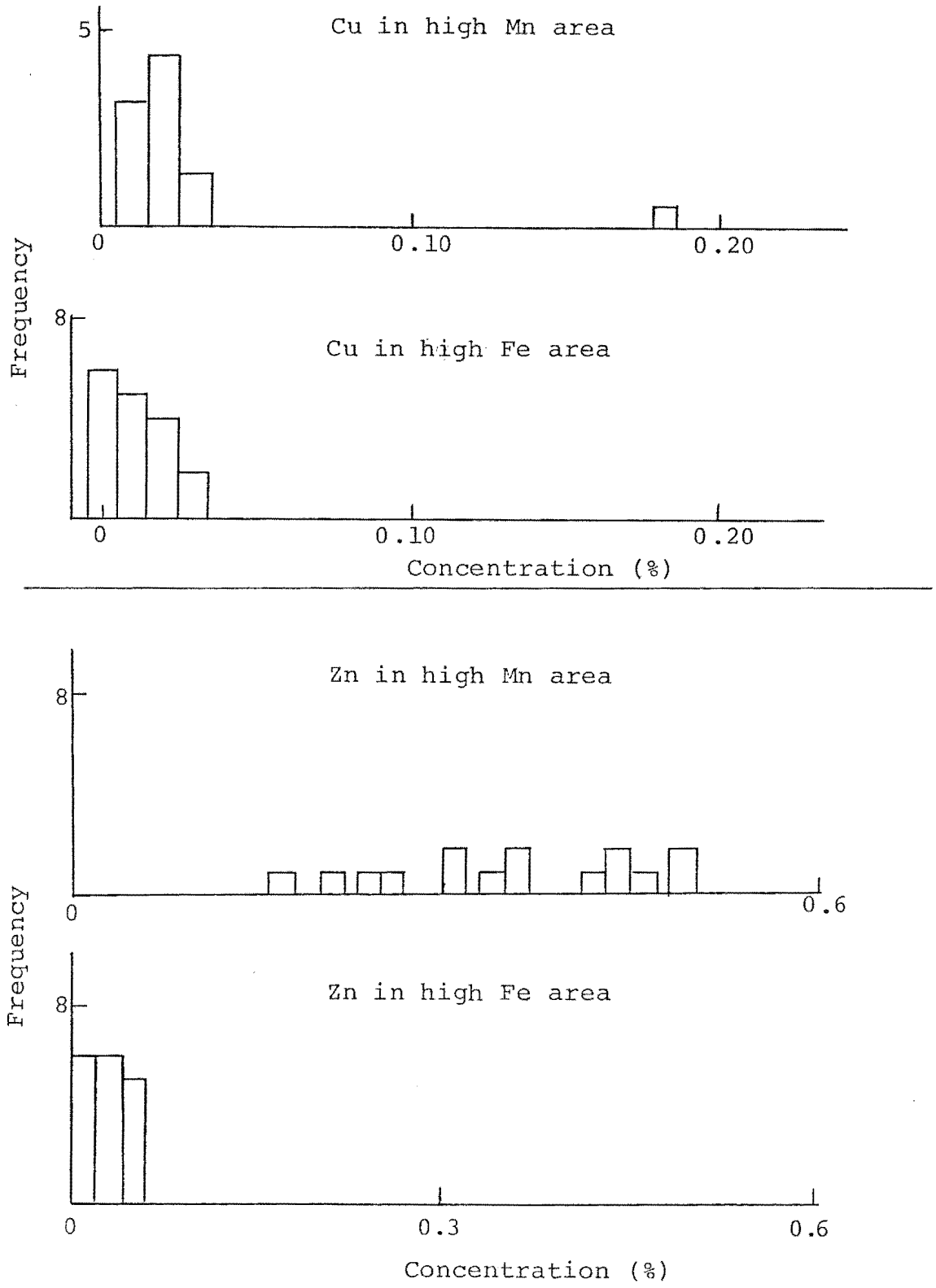

Figure 6.3. Distribution histograms for Cu and Zn in large concretion, 3-Brs1.

a bigger proportion in small concretions.

In this concretion the levels of Ti are as high as 20 to 30% at some areas. In general, the highest Ti levels coincide with areas of low Mn and Fe. The high Ti spots (>5% Ti) are associated with the highest values of V; the difference in the mean V concentrations in the low and high Ti areas is highly significant ($p < 0.001$). There is also a highly significant positive correlation coefficient (0.955) between Ti and V for this sample (Table 6.12). There is no significant correlation of Ti with Fe, suggesting that the titanium does not occur as the mineral ilmenite ($FeTiO_3$).

Only Co and Zn have significant concentration differences between high Mn and high Fe areas (Table 6.16). Nickel and Cu are equally distributed between the Mn and Fe areas. The differences between the two concretions (from the 3-Brs1 horizon) highlight the problems of comparing results from different samples. The differences may be related to size, and hence the age of the concretions. If this is the case, then the fact that the levels of iron in the Mn rich areas are higher in the small concretion (5.0% as compared with 2.3%) could suggest that in the early stages of concretion formation, both Mn and Fe deposits are important, while at a later stage the elements become more segregated.

(3) Concretion from the 3-Brs2 horizon. This concretion appears, from the microprobe point analysis, to be intermediate in its formation, to the small and large 3-Brs1 concretions - this is borne out by its size which is 9 mm in diameter. The levels of Al and Si are also high in this concretion (Table 6.13) - the Al and Si contents of areas low in Mn and

Fe are 56% and 68% of the levels in the surrounding soils, respectively (Table 6.16).

At the same spots the levels of Ti are quite high (4.4 - 14%), and as for the small concretion these correlate with high V levels. The fact that the V levels are significantly different ($p < 0.10$) between high Mn and high Fe areas (Table 6.15) tends to support the contention that the Brs2 concretion is at an intermediate stage of development between the small and large 3-Brs1 concretions; the large Brs1 concretion shows a highly significant difference for V between the high Mn and high Fe areas, while no difference occurs for the small Brs1 concretion (Table 6.15).

Nickel, Cu and Zn are significantly enriched in the Mn areas of the 3-Brs2 concretion (Tables 6.15 and 6.16). It is interesting to note that in this concretion, Co does not have a greater enrichment in the high Mn area; in fact, it is marginally more enriched in the high Fe areas.

Hence, on the basis of the point analyses, what appeared to be three similar concretions have some marked differences. This may also be seen by considering the enrichment of the elements in a particular area compared with the enrichment in the bulk concretion (Table 6.17).

Regression analysis of the concentrations of Mn versus Co, for each concretion, produced lines of similar slope, suggesting that although there may be differences between the concretions, there are similar variations in the concentrations of Mn and Co in all three concretions. Similar results were obtained for regression analyses of concentrations of Mn and Zn, Fe and Co, and Fe and Zn.

TABLE 6.17 WATERTON CONCRETIONS

Enrichment Factors[a] of Elements in Different Areas of the Concretions, Compared with their Concentrations in the Bulk Concretions

ENRICHMENT FACTORS FOR CONCRETIONS

Concretion	3-Brs1 (small)			3-Brs2			3-Brs (large)		
Area	High Mn	High Fe	Low Mn/Fe	High Mn	High Fe	Low Mn/Fe	High Mn	High Fe	Low Mn/Fe
Al	1.2	1.0	1.4	0.6	0.6	1.0	0.2	0.5	1.1
Si	0.8	0.8	1.2	0.3	0.3	0.7	0.03	0.4	0.6
Ti	3.6	4.3	14.8	5.5	1.8	11.0	0.07	0.4	1.0
V	1.5	4.0	4.9	1.8	2.7	0.9	1.1	4.3	2.0
Co	4.1	2.2	1.0	2.9	3.3	1.0	3.2	1.2	0.4
Ni	3.2	1.4	1.4	13.5	3.8	1.9	9.7	1.6	-
Cu	1.1	1.1	0.8	6.2	3.6	2.9	6.7	2.2	-
Zn	2.2	0.8	0.6	5.8	1.5	0.7	8.2	0.8	2.1
		High Mn/Fe	Low Mn/Fe		High Mn/Fe	Low Mn/Fe		High Mn/Fe	Low Mn/Fe
Al		1.1	1.4		0.6	1.0		0.4	1.1
Si		0.8	1.2		0.3	0.7		0.2	0.6
Ti		4.0	14.8		7.3	10.6		0.2	1.0

[a] Enrichment factor = concentration of element in certain area/concentration in bulk concretion.

The differences could possibly be dependent on the sample and the sampling points. However, in each case, the section analyzed was a slice through the concretion, to give maximum surface area, and a representative cross-section. The section areas analyzed were approximately 20 mm^2 (3-Brs1 small), 64 mm^2 (3-Brs2), and 112 mm^2 (3-Brs1 large). In view of the number of points analyzed, the consistency of the results for any one concretion, and the effort made to select points from different positions on the slice, it seems unlikely that the differences are due to sampling, though it cannot be excluded.

(b) Line analysis. Point analysis yields information on elemental concentrations at points, while a line analysis gives information along a line, providing qualitative assessment of interelemental relationships.

A line analysis for the elements Al, Si, Mn, Fe and Co in the 3-Brs1 (large) concretion is shown in Figure 6.4. The result, presented as a plot of concentration against distance along the line, indicates that there is a definite segregation of Al and Si from Mn and Fe, and of Mn and Fe from each other. This result lends support to the method used in the previous section of separating the data into high Mn and high Fe areas. The segregation corresponds to deposition of Mn and Fe hydrous oxides, at different times, and entrapping Al and Si containing minerals. The line scan for Co (Figure 6.4) illustrates a close association of Co and Mn along the line analyzed, in agreement with the point analyses results.

(c) Photographic analysis. A photographic record of an oscilloscope display of the elemental distribution in two

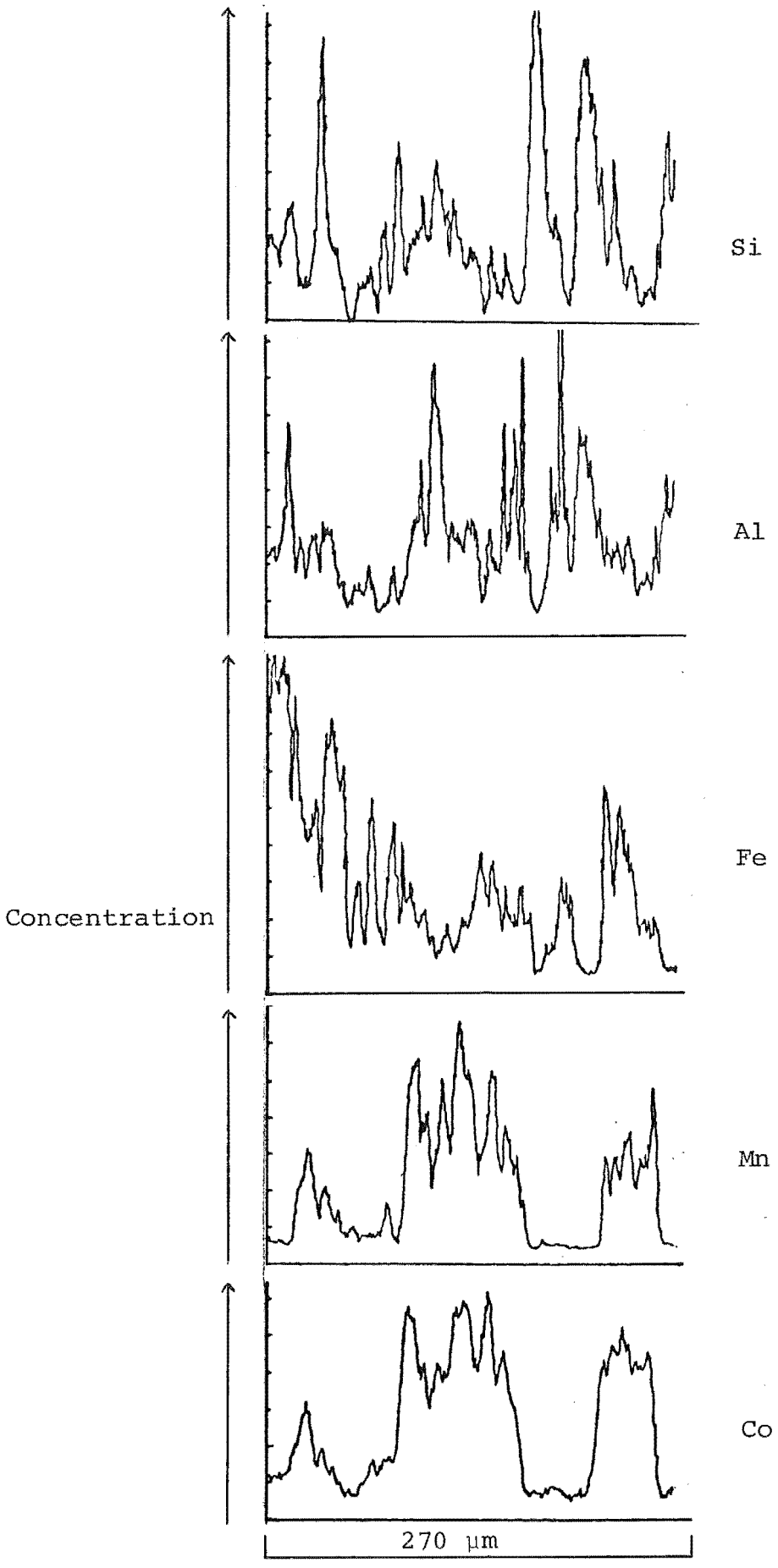

Figure 6.4. A line analysis for the elements Si, Al, Fe, Mn and Co in the 3-Brs1 (large) concretion.

dimensions was obtained. The photographs in Figure 6.5 are for the distribution of Al, Si, Mn and Fe in an area of approximately 2300 μm^2 on the concretion sample 3-Brs2. The other trace elements were too low in concentration to be detected by this method. A secondary electron image (S.E.I.) showing the surface features of the same area is also given. In the photographs, a greater concentration of white dots corresponds to a greater concentration of the element. The photographs show that Al and Si are distributed over the entire area except for two diagonal regions. Manganese and Fe, however, are less evenly distributed, and in the case of Mn, mainly concentrated in the regions of low Al and Si concentrations - that is in the two diagonal regions. The Fe in the area photographed is more evenly distributed than Mn, though it also shows elevated levels in the vicinity of the two diagonal regions observed for Mn. It is apparent from the photographs that the high concentrations of Mn lie adjacent to areas of high Fe, but are not coincident with them. This confirms the suggestion that the deposition of Mn and Fe oxides occurred at different times.

(ii) *Results of the iron-pan study.*

(a) Point analysis. Twenty three and 33 separate points on two samples of the Ok iron-pan were analyzed using an electron microprobe. Both random point counting and searches for areas high in Ti, Mn and Fe were carried out.

The highest levels (as a percentage composition by weight) obtained in the areas analyzed (Tables 6.18 and 6.19) were 16% (Al), 47% (Si), 41% (Ti), 3.2% (Mn) and 37% (Fe). The levels found for Co, Ni, Cu and Zn were in almost all

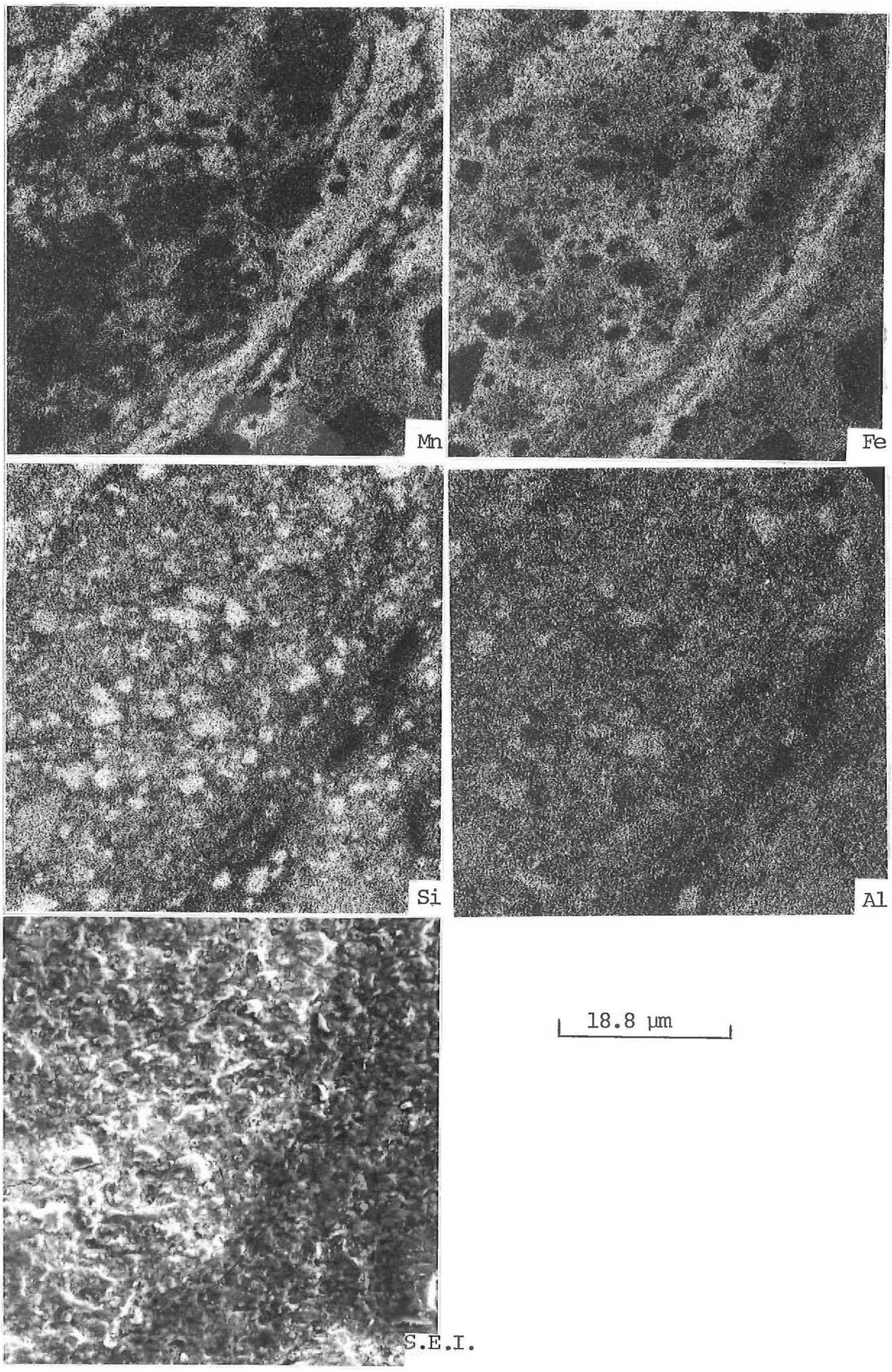

Figure 6.5. Concretion (3-Brs2). Photographs showing the secondary electron image (S.E.I.,surface features), and the distribution of the elements Mn, Fe, Si and Al in a section of the concretion.

cases <0.10%, and often <0.01% - the level which was taken as the limit of detection.

The correlation coefficients (Tables 6.18 and 6.19) were calculated for each pair of elements for each sample. Listed in Table 6.20 is a summary of significant correlations found for the iron-pan samples. In sample 1, Al and Si are positively correlated, while both are negatively correlated with both Ti and Mn. There is a highly significant positive correlation between Ti and Mn, and Mn is also significantly correlated with both Cu and Zn. Iron is negatively correlated with Si.

In sample 2, Al and Si are negatively correlated with Ti, V, Mn, Co, Ni, Cu and Zn; Ti and Mn are again highly significantly correlated, and both are correlated with V, Co, Ni, Cu and Zn (0.1% level). Iron is significantly correlated with Co and Zn.

The analytical results suggest that the iron-pan consists of two distinct phases - an aluminosilicate phase and a Ti-Mn phase. It is the latter area where the trace elements are enriched.

The data for each iron-pan sample was also analyzed as for the concretions, to see if the elements were related in a significant way, to the areas analyzed. The areas in this case were classified as low Ti and Fe, high Ti and Fe, high Ti, and high Fe, and the analytical data given in Tables 6.18 and 6.19 is grouped in this way.

The means and standard deviations for the concentrations of each element were calculated for the various groupings shown in Table 6.21. The differences between the means were

TABLE 6.20 IRON-PAN

Summary of Significant Correlations Found for Iron-pan using Electron Microprobe Analysis

	POSITIVE CORRELATION COEFFICIENT		NEGATIVE CORRELATION COEFFICIENT	
	Significant	Highly Significant	Significant	Highly Significant
Sample 1				
Al	Si			Ti,Mn
Si	Al		Ti	Mn,Fe
Ti		Mn	Si	Al
Mn	Cu,Zn	Ti		Al,Si
Fe				Si
Sample 2				
Al			Co,Ni,Cu	Ti,V,Mn,Zn
Si			Co	Ti,V,Mn,Fe,Ni,Cu,Zn
Ti		V,Mn,Co,Ni,Cu,Zn		Al,Si
Mn		Ti,V,Co,Ni,Cu,Zn		Al,Si
Fe	Co,Zn			Si

[a] Significant at 1% level

[b] Highly significant at 0.1% level

then tested using the student's t test. The results are listed in Table 6.21, in terms of the probability that there is no significant difference between the means. Also listed in Table 6.21 is the iron-pan to surrounding soil concentration ratio for each element.

It can be seen from Table 6.21 that Al and Si occur mainly in the areas of low Ti and Fe, and to a lesser extent in the high Fe only areas. One point analyzed in sample 2 contained 47.2% Si - this spot must have been practically a pure quartz grain.

The remaining elements, V, Mn, Co, Ni, Cu and Zn, display the same pattern. The levels in the high Ti/Fe areas

TABLE 6.21 OKARITO IRON-PAN

Probability that there is no Difference Between the Means of the Various Elements in Various Areas of the Iron-pan, as determined by Students' t Test, and the Iron-pan to Soil Concentration Ratio

Element	Area of Concretion	PROBABILITY		IRON-PAN TO SOIL CONCENTRATION RATIO		
		Sample 1	Sample 2	Sample 1	Sample 2	Bulk iron-pan
Al	Low Ti/Fe	<0.001	<0.001	3.18	2.46	-
	High Ti; High Ti/Fe			0.20	0.25	-
	High Fe	<0.001	<0.001	2.13	2.32	-
	High Ti; High Ti/Fe			0.20	0.25	-
Si	Low Ti/Fe	<0.001	<0.001	0.63	0.46	-
	High Ti/Fe			0.03	0.04	-
	High Fe	<0.02	<0.001	0.11	0.27	-
	High Ti/Fe			0.03	0.04	-
V	High Ti/Fe; High Ti	<0.10	<0.001	60	31.4	1.7
	Low Ti/Fe; High Fe			-	5.7	-
Mn	High Ti/Fe; High Ti	<0.001	<0.001	142	113	0.71
	Low Ti/Fe; High Fe			-	0.92	-
Co	High Ti/Fe; High Ti	<0.2	0.01	20	72	0.60
	Low Ti/Fe; High Fe			-	26	-
Ni	High Ti/Fe; High Ti	>0.2	<0.002	80	24	0.40
	Low Ti/Fe; High Fe			-	6	-
Cu	High Ti/Fe; High Ti	<0.02	<0.02	20	74	0.80
	Low Ti/Fe; High Fe			-	28	-
Zn	High Ti/Fe; High Ti	<0.10	<0.001	27	36	0.70
	Low Ti/Fe; High Fe			-	10.7	-

and the high Ti only areas were significantly different, and higher compared with the levels in the low Ti/Fe and Fe only areas. Since these elements are at low to not detectable levels in the areas with just high Fe (for example Zn - in the high Fe only area, the mean concentration is 0.02%, while in the high Ti/Fe area, the mean concentration is 0.06% (Table 6.21)), this suggests the elements Co, Ni, Cu and Zn are enriched in the iron-pan because of the enrichment of Mn in the high Ti/Fe and high Ti areas (Mn is enriched 113 times in the iron-pan sample 2 in these areas compared with surrounding soil). However, because of the relatively high Fe concentrations in the high Ti/Fe areas, the effect of Fe in these circumstances cannot be ruled out.

The elements V, Mn, Co, Ni, Cu and Zn are all higher in concentration in the iron-pan relative to the surrounding soil, in the areas of high Ti/Fe, and also in the areas of low Ti/Fe in the second iron-pan sample. This may be seen from the iron-pan to soil concentration ratios in Table 6.21, which range from 6 for Ni in sample 2 to 142 for Mn in sample 1. The fact that these elements (except V) are not enriched in the pan on the basis of bulk analysis (Table 6.21) is quite different to the iron-manganese concretions.

(b) Photographic analysis. The photographs in Figure 6.6 are of an area 2300 μm^2, in sample 2 of the iron-pan. A particle, which is easily distinguishable in the secondary electron image (S.E.I.), is seen to contain predominantly Ti, Fe and Mn. The distribution of Si is high in all areas except for the high Ti and Fe areas, and while the Al distribution is similar to that of Si, it is reduced and not as uniform

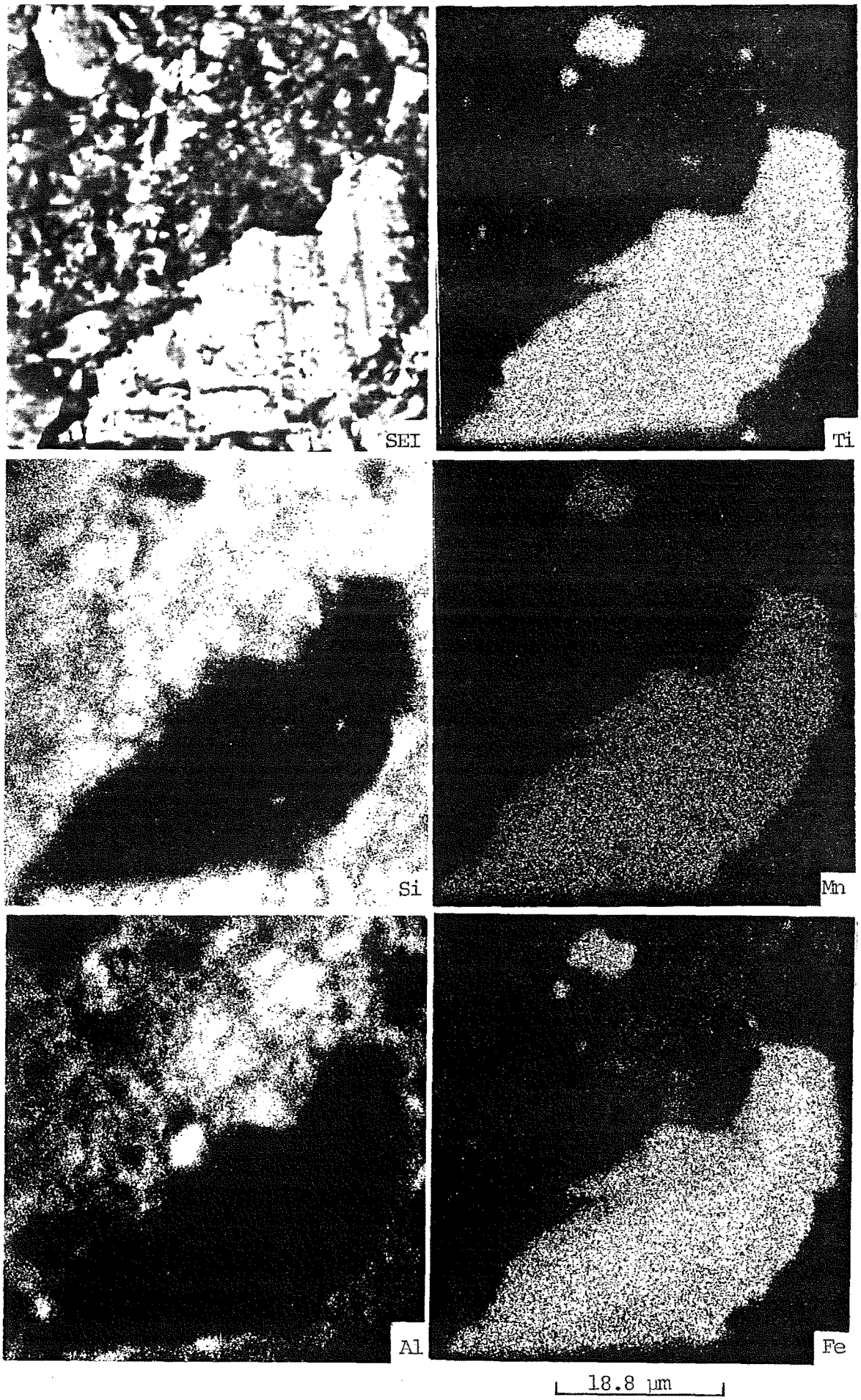

Figure 6.6. Iron-pan. Photographs showing the secondary electron image (S.E.I.,surface features), and the distribution of elements Mn,Fe,Ti,Si and Al in a section of the iron-pan (sample 2).

as for Si. The exposure times for Si, Ti and Fe were 10 minutes, and for Al and Mn, 30 minutes.

6. Discussion of possible reasons for the observed inter-element associations

The interelement correlations found from the electron microprobe analysis of concretions and an iron-pan, and the analysis of the data in selected areas of high Mn, Fe or Ti, show that the trace elements Co, Ni, Cu and Zn are enriched primarily in the high Mn areas and, to a lesser extent, in the Fe rich areas. Therefore, it is of interest to search for reasons for the enrichment of the trace elements in the Mn and Fe areas, and why their enrichment is greater in the Mn areas. Possible contributing factors are (i) sorption, (ii) ionic replacement, (iii) crystal field energies, and (iv) lattice energies. While each of these will be considered in turn, it is very likely that each, to some extent, contributes to the enrichment process.

The oxidation states of Mn and Fe in the concretions are of importance when considering the enrichment of trace elements. The Mn and Fe containing minerals identified in the concretions were goethite (Fe(III)OOH), lepidocrocite (γ-Fe(III)OOH), hematite ($Fe(III)_2O_3$), and birnessite ($(Ca,Mg,Na_2,K_2)_xMn(IV)Mn(II)(O,OH)_2$). In these minerals, Fe is in the trivalent oxidation state, while Mn occurs in the divalent and tetravalent states. It is also likely that Fe could be present in the divalent state in some of the poorly ordered oxyhydroxides.

As was pointed out in Chapter 3 of this work, several authors have claimed that Co is concentrated by Fe(III) oxides,

even though it is now generally accepted that Co is most significantly associated with Mn(IV) oxides. Burns[74] attempted to explain the observed Fe-Co correlations in soil concretions in terms of Mn-Co correlations by suggesting that the δ-MnO_2 phase is epatiaxially intergrown with $FeOOH.nH_2O$. McKenzie[173], in an electron microprobe study of soil concretions, found that Co and Ni were, in all samples studied, significantly correlated with Mn, and while Zn was correlated with Mn in half the samples, no correlations were observed between Cu and Mn. McKenzie also found significant negative correlations of Fe with Co and Ni, and in some cases, with Zn.

It should be pointed out that explanations based on correlation coefficients can be misleading. Although negative correlations were obtained between Fe and elements such as Co, Ni and Zn, the results of the present study indicate that enrichment does occur in the high Fe areas, but more so in the high Mn areas.

(i) *Sorption.* The results of the present study can be interpreted assuming the primary process involved is sorption. It is known from the ammonium oxalate extractions and the general lack of well defined X-ray diffraction patterns for the concretions and iron-pan samples, that a large proportion of the Mn and Fe species is poorly ordered. The ammonium oxalate extractions indicate that 95% of the Mn in the concretions is in an unordered amorphous state, as is 60% of the Fe. Such non-crystalline species have large surface areas available for the sorption of trace elements. These results suggest that there is a greater proportion of Mn sorption surface than for Fe.

A general mechanism for the sorption of metal ions on oxides and hydrous oxides is the exchange of protons bound to the oxide surface with cations, according to the equilibria;

$$M^{n+} + x(-AOH) \rightleftharpoons M(-AO)_x^{(n-x)+} + xH^+ ,$$

where M is the metal ion sorbed, and (-AOH) and (-AO) are the sites on the oxide surface[85].

It has been reported[85,171] that when Na^+ or Ca^{2+} ions (10^{-3} mol dm^{-3}) were sorbed on to δ-MnO_2, H^+ ions were released into the solution, but that no detectable manganese was found in the solution. However, when Co, Ni, Cu or Zn ions were sorbed[85,171] both H^+ and Mn^{2+} ions were found in solution, and that Co displaced more manganese than did the other ions. The reason given for the greater release of Mn^{2+} by Co^{2+} ions was attributed to its oxidation to Co^{3+} by Mn(III) or Mn(IV), and incorporation into the oxide structure[74,85,171].

Several workers[66,87,171,180] have shown that trace element cations are sorbed onto the surfaces of the Mn and Fe hydrous oxides. However, since the zero point of charge for Mn oxides occurs around a pH of 2.0-4.0, the surface will be negatively charged at the pH values of most soils[180]. In contrast, the hydrous oxides of Fe usually have a zero point of charge in the pH range 6.8-8.0, and so in many soils, these oxides are positively charged, or near neutral[37]. The concretions studied in this work (3-Brs1 and 3-Brs2 horizons) came from horizons with a pH of 7.0, and so the Mn oxides will be negatively charged, and Fe oxides probably near neutral. Hence, the cations will be preferentially attracted to and sorbed by the Mn oxides. It is suggested that this is prob-

ably the main reason why the trace metals are more strongly enriched in the high Mn areas, in the present samples.

Murray et al.[180] studied the sorption of Ni(II), Cu(II) and Co(II) on δ-MnO_2. They found that while the extent of Ni(II) sorption at around pH 4 is similar to that of the group II ions, Cu(II), and especially Co(II), sorb much more strongly. Also, although Na^+ and K^+ can be desorbed by lowering the pH to that of the zero point charge, Ni(II), Cu(II) and especially Co(II) were not desorbed, even from positively charged surfaces. Such behaviour, they claim, can only be explained by the existence of a relatively large specific adsorption potential, ϕ_+, of an ion;

$$\Gamma_+ = 2rC \exp\left(\frac{-z_+ e(\psi_\delta + \phi_+)}{kT}\right),$$

where Γ_+ is the adsorption density in the Stern layer, r is the radius of the adsorbed ion, C its equilibrium concentration, and ψ_δ the surface potential. They calculated the specific sorption potentials for Co, Ni and Cu, obtaining a value of -7.9 kJ mol^{-1} for Ni(II) and Cu(II) and a higher value of around -21 kJ mol^{-1} for Co(II). They also proposed that the high specific sorption potential of Co may be due to a surface oxidation of Co(II) to Co(III), leading to an increase in its specific sorption potential.

Morgan and Stumm[37] explained the high sorption capacity of δ-MnO_2 for metal ions as due either to complex formation or ion exchange. They suggested that strongly hydrolyzable metal ions (Co, Ni, Cu and Zn) can be sorbed on δ-MnO_2 to a greater extent than can weakly hydrolyzable metal ions (group II ions). While sorption can explain the greater enrichment in the Mn phases

over Fe, this is probably the initial step only, and further processes are involved in the incorporation of the metal ions into the hydrous oxides structure.

(ii) *Ionic replacement.* As indicated above manganese is present as both Mn(II) and Mn(IV), while iron is likely to be present mainly as Fe(III), but possibly also as Fe(II) (especially at the stage where iron builds onto the concretion). In the soil solution Co, Ni, Cu and Zn probably exist mainly in the divalent hydrated metal ion form. Since ionic potentials (charge/radius) for the divalent ion forms of Mn, Fe, Co, Ni, Cu and Zn are similar ($2.6\text{-}2.8 \times 10^{-2}$ pm^{-1}), simple ion exchange and isomorphous replacement between one metal and another can take place. Because of the greater sorption potential of hydrous Mn oxides for trace metal ions, there would be more opportunity for ion exchange and isomorphous replacement, leading to greater incorporation of trace metal ions into the hydrous Mn oxides.

The divalent metal ions (ionic radii in Table 6.22) could also replace Mn(III) and Fe(III) ions (difference in radii $<\pm 15\%$[181]), but they could not replace Mn(IV) ions. However, replacement of the trivalent ions (Mn(III) and Fe(III)) by divalent ions would not be favourable on a charge basis. If isomorphous replacement of the host ions by the divalent trace metal ions of Co, Ni, Cu and Zn was a determining factor in enrichment, then minerals containing Fe(III) would be favoured over minerals containing Mn(IV). However, Co(III) (low spin state) (53 pm) could replace Mn(IV) ions (54 pm) (except for the unfavourable charge), and provided a mechanism for oxidation exists, this could be important in explaining

the strong Co enrichment in the Mn phases compared with Ni(II), Cu(II) and Zn(II). However, it would seem that arguments based just on ionic size do not readily explain the enrichment of Ni, Cu and especially Zn in the high Mn areas of the concretions, nor why the hydrous Mn oxides are able to concentrate trace metals more than the hydrous Fe oxides.

(iii) *Crystal field energies.* Glasby[83] claims that crystal field theory has a limited role in the interpretation of trace element fractionation in sedimentary processes. This is said to be due to the fact that precipitation from aqueous solution is unlikely to change the crystal field stabilization energy of an ion, except where there is a change in oxidation state[87]. In Chapter 3, three processes achieving gains in crystal field stabilization energy were outlined to explain the enrichment of cobalt: 1) Oxidation of Co(II) by Mn(III), 2) oxidation of Co(II) by Fe(III), and 3) oxidation of Co(II) by Mn(IV). The changes in free energy and CFSE for these processes are summarized below;

MECHANISM		ΔG(kJ mol^{-1})	ΔCFSE (kJ mol^{-1})
$Co(II)_{aq} + Mn(III)_s$	$Co(III)_s + Mn(II)_{aq}$	+32	+311
$Co(II)_{aq} + Fe(III)_s$	$Co(III)_s + Fe(II)_{aq}$	+103	+512
$2Co(II)_{aq} + Mn(IV)_s$	$2Co(III)_s + Mn(II)_{aq}$	-60	+132

Oxidation of Co(II) by Mn(IV) is seen to be the favoured thermodynamic process. Supporting evidence for this oxidation is reported by Murray and Dillard[89], who found that Co(III) was present on the surfaces of δ-MnO_2, after initial sorption of Co(II) ions; no evidence was found for Mn(III) ions.

While Co is certainly strongly enriched in the Mn and

Fe areas of the concretions, and this may be interpreted in terms of a gain in C.F.S.E., the explanation is inadequate to explain the enrichment of Cu(II), Ni(II) and Zn(II) in the high Mn and Fe areas in the concretions. In each of these cases there would be a net loss of crystal field stabilization energy on substitution for Mn(IV) ions.

(iv) *Lattice energies.* Crystal field energies account for around 10% of the stabilization energy in crystalline solids and so the lattice energy is the more important factor. All the minerals identified in the concretions of this study, hematite, goethite, lepidocrocite and birnessite, have the metal ions surrounded by an octahedral environment of O or OH groups[74,155]. An approximate estimate of the order of lattice energies for the various trace metal ions in the octahedral cavities of the Mn and Fe hydrous oxides can be made assuming that the replacement of divalent Co, Ni, Cu and Zn in the structure does not change the overall structure, or if it does the change is minor. This is reasonable since the proportion of trace metals included in the structure compared with the Mn and Fe ions, is very low (<0.3%).

The approximation to the Born-Landé equation for lattice energy, U, as developed by Kapustinskii[154] was used for the estimations;

$$U = \frac{N_A A e^2 \nu \quad Z_+ Z_-}{4\pi\varepsilon_o \; 2 \; (r_- + r_+)} \cdot (1 - \frac{1}{n}),$$

where Z_+ and Z_- are the changes of the cation and anion, r_+ and r_- are the ionic radii for octahedral coordination, ν is the number of ions in the simplest stoichiometric molecule, A is the Madelung constant, and n is a constant, with a value

of 9. The values given in Table 6.22 are in terms of A and ν.

TABLE 6.22 Calculation of Lattice Energy Using the Kapustinskii Equation

Element	Mn	Mn	Mn	Fe	Fe	Co	Co	Ni	Cu	Zn
Oxidation state	II	III	IV	II	III	II	III	II	II	II
Ionic radii(pm)[a]	80	66	54	76	64	74	53[b]	72	72	74
Lattice energy (A. ν kJ mol^{-1})	-1123	-1798	-2546	-1143	-1816	-1154	-1825	-1165	-1165	-1154

[a] Ionic radius of O^{2-} is 140 pm

[b] Co(III) is the low spin state

It is seen from the data in Table 6.22 that the structures with the greatest lattice energy contain the Mn(IV) ions, followed by Fe(III) and Co(III) ions. All the divalent ions result in lower lattice energies. It does not seem, therefore, that lattice energy considerations by themselves explain the enrichment of the divalent metal ions in the Mn and Fe phases of the concretions. The Co(III) ion appears to be the most likely to be incorporated into such a structure especially if it replaces Mn(II) or Mn(III). However, to do so the Co(II) ion has to be oxidised.

The oxidation potential for the oxidation of Co(II);

$$Co^{2+}_{(aq)} \rightarrow Co^{3+}_{(aq)} + e ,$$

is -1.82 V; however, this potential is less in the presence of coordinating agents. For example, in basic media, the potential is -0.17 V;

$$Co(OH)_{2(s)} + OH^- \rightarrow CoO(OH)_{(s)} + H_2O + e,$$

and for the ammine complexes the potential is -0.1 V. Some means of stabilizing the Co(III) oxidation state is necessary if this is to be an important factor because water rapidly reduces the uncomplexed Co(III) ion. The oxidation is also likely to be catalysed by metal ions. Therefore, assuming the energy of oxidation is not critical, the problem resolves to one of exchange of metal ions in the lattice and a consequential change in the lattice energy. Because of the high lattice energy associated with the Mn(IV) ion, it would seem unlikely that this ion is the oxidizing agent, unless reduction of it proceeded no further than to Mn(III).

In summary, it appears that there is no adequate single explanation for the enrichment of the trace metals in the high Mn and Fe areas, particularly in the Mn areas, other than an initial sorption process. It could well be that the incorporation of metal ions into the concretions is then simple occlusion, that is the trace metal is entrapped by further precipitation of Fe and Mn oxides. The similarity in the ionic radii of the ions being considered and those of Mn(II) and Fe(II)(the forms existing in solution) would mean that as far as growth of the solid phases (that is precipitation and occlusion) is concerned, the various metal ions are indistinguishable. Therefore, it is suggested that a possible process is sorption, which would be most favourable for the Mn phases, followed by occlusion. As regards the especially high enrichment of Co, it would appear that some oxidation process is necessary to account for it. However, as the results indicate, Zn is also strongly enriched, and an oxidation process is not applicable here. Also, Zn is the largest of the divalent

metal ions and could be expected to be the least strongly sorbed. However, the levels of Zn are greater in the soil than Co, Ni or Cu, and its strong enrichment may be a feature of its higher concentration pushing the sorption equilibrium reaction (p.198) to the right.

(v) *Enrichment of vanadium in concretions and iron-pan.* It can be seen from Tables 6.14 and 6.20 that V is highly significantly correlated with Fe in the large 3-Brsl concretion, and that in the two other concretions and the iron-pan, Ti is highly significantly correlated with V. In Table 6.17, it was also shown that V is enriched in high Fe areas compared with high Mn areas.

The existence of such minerals as karelianite (V_2O_3), which is iso-structural with hematite (Fe_2O_3, corundum structure[155]), and montroseite (V,Fe)OOH, which is iso-structural with goethite (FeOOH), and the similarity of the cell sizes of these iso-structural minerals, suggest that V is most likely present in the structure of most soil iron oxides[181,182]. Since goethite and hematite are present in the concretion samples, it is likely that Fe and V are associated as just described.

Goldschmidt[181] states that V is sometimes found in titanium minerals, such as rutile, especially in such minerals as are connected with ferromagnesian magmas. A similar association of Ti and V may be occurring in the samples of the present study.

CHAPTER 7

EXPERIMENTAL METHODS

In this chapter, the soil surveys covering the study areas are reported, and soil sampling procedures are outlined. Physical and chemical methods employed in the analyses are given, along with the details and background theory of the various instrumental techniques.

FIELD WORK

1. Previous surveys

(i) *Chronosequence and biosequence.* The only published survey of the soils of the Inangahua Depression is the reconnaissance mapping of the South Island of New Zealand[183] (at a scale of 1:253,440).

In 1965 a report and map (at a scale of 1:63,360) of the soils in an area of 2000 ha surrounding Reefton was prepared by Kear[184]. Most of the terrace land and some of the flanking hills and steeplands in the lower valleys of the Waitahu River were covered in this survey.

During 1972,a soil survey of 44,000 ha of terrace and hill country soil in the Inangahua Valley between Reefton and the Inangahua Junction was undertaken (at a scale of 1:63,360). The results of the survey are presented in a report[121] which has a restricted distribution.

The chronosequence and biosequence soils have also been studied previously by Campbell[20], who investigated the effect of different soil forming factors on soil properties such as

the total major element concentrations, mineralogy and cation exchange properties.

(ii) *Toposequence*. The only survey of the soils in the Waimakariri Catchment is the General Survey of the Soils of the South Island of New Zealand[185] (at a scale of 1:253,440).

Young[25] has investigated the toposequence soil with a view to seeing how the topography of the landscape affected soil variability and soil formation.

(iii) *Waterton soils*. Two surveys by the New Zealand Soil Bureau have covered the Irwell area. One survey contains a description of the soils of pastoral and cropping lands of Canterbury and North Otago, as mapped in a reconnaissance soil survey (at a scale of 1:63,360). This survey covers 1,075,601 ha of the Eastern part of the central South Island of New Zealand.

The second survey[186] covers 50,674 ha (with a scale of 1:31,680) and is confined to an area about 32 km south of Christchurch, New Zealand.

The Waterton soils were also the subject of a study looking at the effect of topography, and consequent water-logging, on soil chemistry and iron-manganese concretion formation[26].

2. Sampling

Once the sampling sites were chosen, contamination from foreign sources was carefully avoided. No evidence suggesting contamination was observed, and no obvious discontinuities were found in the analytical results.

The chronosequence, biosequence, and toposequence soils were all sampled without regard to the volume and weight of the sample. The chronosequence had earlier[20] been

sampled by taking and weighing all the soil in the horizons within a given volume. The Waterton soils were sampled[187] down to the underlying shingle using a corer. All the samples collected were stored in plastic bags.

Profile descriptions, which were made during or soon after sampling, are given in appendix 2.

ANALYTICAL PROCEDURES

1. Sample preparation

Half of each sample was weighed, air dried and re-weighed. For the chronosequence soils, the amount of inorganic and organic material in the soil was calculated for each horizon. The remaining sample was resealed in a plastic bag and stored under field moist conditions.

The air dried samples were crushed, but not powdered, with a steel rolling pin and passed through a 2 mm sieve. If the quantity of material >2 mm was less than 1% by weight it was discarded, otherwise it was kept for analysis. The horizons which had significant amounts of material >2 mm were the deepest horizons of the Ha, Io, Ah and Ku profiles of the chronosequence.

2. Physical procedures

(i) *Soil pH.* A suspension of soil (<2 mm) in distilled water (1:2.5) was stirred thoroughly and left overnight. The solution was again thoroughly stirred and the pH measured, using a glass-calomel electrode. The pH meter was calibrated, using potassium hydrogen phthalate (10.21 g dm^{-3}, pH 4.0 at $20^{o}C$), and sodium tetraborate (3.81 g dm^{-3}, pH 9.2 at $20^{o}C$).

(ii) *Dry matter and loss on ignition.* The amount of dry matter was obtained by heating 5 g samples of air dried soil in a porcelain crucible overnight at 105°C. Weight loss on ignition was obtained by igniting a weighed sample of dry matter to 380°C in a muffle furnace for 16 hours, cooling, and reweighing. Sand, silt and clay fractions were treated in the same way.

(iii) *Particle size fractionation.* Twenty gram samples of soil (<2 mm) were placed in 100 ml polyethylene centrifuge tubes, with distilled water up to a level of 10 cm above the soil. The stoppered tubes were shaken for 15 minutes on an end to end shaker, and then on a mechanical vibrator to ensure complete dispersion of soil aggregates.

The samples were then centrifuged at 500 r.p.m. for 10 minutes to settle the sand and silt particles, and the supernatant suspension of clay particles was siphoned off. This process was repeated 5-7 times until the supernatant liquid was clear. After the 3rd and 5th treatments, a dispersing agent, sodium hexametaphosphate, was added to the centrifuge tubes at the rate of 10 ml (of a 4% solution) per litre of water. The 4th and 6th shaking were extended to 25 minutes to ensure complete dispersion.

The clay size particles (<2 μm) were flocculated with NaCl and centrifuged at 2000 rpm. The clear supernatant above the settled clay was discarded. The clay was then resuspended in distilled water, hand shaken in the centrifuge tubes, and spun down again; if the solution was clear it was discarded. This process was repeated, with fresh distilled water, until the centrifuged solutions were not clear, indic-

ating that the excess NaCl had been removed from the clay and peptization was occurring. A few drops of saturated NaCl solution were then added, and the clays spun down for a final time. The wet clays were treated with ethanol to give a 4% ethanol-clay mixture, which was then freeze-dried[188].

The sand and silt mixtures were transferred to a centrifuge tube, water was added to 10 cm above soil particles, and the tubes were hand shaken. After the 4.68 minutes (20°C) necessary for sand sized particles to fall 10 cm, the silt in the suspension was siphoned off. This process was repeated 5-7 times until the supernatant was clear. The silt-water mixture was centrifuged at 500 rpm for 10 minutes, by which time the particles had settled out, and the clear supernatant liquid was discarded. The silts were freeze dried while the sand fractions were oven dried.

The separation gives sand, silt and clay fractions conforming approximately to the Internation Size Classifications, namely sand 2-0.020 mm, silt 0.020-0.002 mm, and clay <0.002 mm (<2 μm).

The fractionation of some chronosequence and biosequence soils was carried out twice. In some cases there was evidence that an incomplete dispersion of the soil aggregates was obtained in the first fractionation, probably due to inadequate shaking and agitation. In the second fractionation, samples completely dispersed. Unless stated otherwise, all analytical results refer to samples from the second fractionation.

3. Chemical procedures

(i) *Standard solutions.* A multiple element standard

solution was made using ANALAR grade salts containing V, (NH_4VO_3); Cr, ($K_2Cr_2O_7$); Mn, ($MnSO_4.H_2O$); Co, ($CoSO_4.7H_2O$); Ni, ($(NH_4)_2SO_4.NiSO_4.6H_2O$); Cu, ($CuSO_4.5H_2O$) and Zn ($ZnSO_4.7H_2O$). All solutions were made up to the same concentration of 1000 μg ml^{-1} of the element in 1M HCl. A separate standard solution was prepared for Fe using ANALAR grade $NH_4Fe(SO_4)_2.12H_2O$.

A standard Ti solution was prepared from ANALAR grade $K_2TiO(C_2O_4).2H_2O$ by heating the compound in a kjeldahl flask with 100 ml of concentrated H_2SO_4 and 8 g of $(NH_4)_2SO_4$. The mixture was heated slowly and boiled for 10 minutes. The solution was then diluted to give a Ti concentration of 500 μg ml^{-1}.

A standard solution containing Al and Si was prepared using B.D.H. Atomic Absorption Spectrophotometric Standard Solutions. The concentration of each element was 400 μg ml^{-1}.

(ii) *Evaluation of soil decomposition methods.* Two techniques were used to evaluate the different soil decomposition methods, a) a method similar to standard additions, and b) the analysis of International Rock Standards. The procedures are outlined below, followed by a description of the soil decomposition methods used. A summary of the decomposition methods used, the soils analyzed by each method, and the elements studied by the evaluation methods is given in Table 7.1.

(a) The method of standard additions. Two separate standard addition type experiments were carried out using the spiking technique for the elements V, Cr, Mn, Co, Ni, Cu and Zn. One spiking series, denoted by Sp, did not involve a soil component, while in the other series So, a clay sample

TABLE 7.1 Summary of Soil Decomposition Methods and Their Evaluation

Decomposition Method	Samples Analysed	Evaluation Method	
		Standard Addition	Int. Rock Standards
$HF-HClO_4$	Chronosequence soils	V,Cr,Mn, Co,Ni,Cu	Ti,V,Cr,Mn, Fe,Co,Ni,Cu
	Biosequence soils	Zn	Zn
	Toposequence soils	"	"
	Waterton soils and concretions	"	"
$LiBO_2$	Toposequence soils	V,Cr,Mn, Co,Ni,Cu	Ti,V,Cr,Mn, Fe,Co,Ni,Cu
	Waterton soils and concretions	Zn	Zn
Na_2CO_3	Toposequence soils	Mn,Co,Cu, Zn	Mn,Fe,Co,Cu, Zn
	Waterton soils and concretions[a]	"	"

[a] Results from Budhia[26]

was used. The spiking was arranged so that the amount of each element added was 0, 1.0, 2.0, 3.0 and 4.0 $\mu g\ ml^{-1}$ in the final solution. This range spans the likely concentrations of the elements in the solutions obtained from the soils studied.

(b) Analysis of International Rock Standards. All three soil decomposition methods (Table 7.1) were used on duplicate samples of the International Rock Standards AGV-1 (an andesite), G-2 (a granite) and BCR-1 (a basalt). The solutions were analyzed for Ti, V, Cr, Mn, Fe, Co, Ni, Cu and Zn, and the results compared with the preferred values in the literature[156].

(ii) *Decomposition methods.*

(a) Hydrofluoric acid-perchloric acid digestion. This method was used to decompose the various fractions of

the chronosequence, biosequence, toposequence and Waterton soils, and concretions.

A finely ground weighed sample (0.2 g) was place in a 30 ml platinum crucible. The crucible was then heated over a bunsen burner to just below red heat in order to remove the greater part of the organic matter. After cooling, the sample was moistened with a few drops of water, and then HF (6 ml, 40%) and $HClO_4$ (0.5 ml, 60%) added. The crucible was heated on a sand conductor to about 200-230^{o}C until the fuming of $HClO_4$ had ceased, by which time all the HF and SiF_4 had been removed. Hydrochloric acid (5 ml, 3M) was then added and the crucible gently heated. The solution was transferred to a volumetric flask; the crucible was further treated with HCl (5 ml, 3M), which was also added to the flask.

(b) Lithium metaborate fusion. This method was used to decompose the toposequence and Waterton soils, and concretions.

A finely ground sample (0.4 g) was mixed well with 1.5g of $LiBO_2$ in a platinum crucible, and quietly fused, initially for 1-2 minutes, over a bunsen burner. Stronger heating was then applied to the open crucible until the melt was clear (about 10 minutes). The melt was swirled up the side of the crucible walls before cooling, to assist subsequent dissolution. Cold distilled water (10 ml) and HCl (10 ml, 3M) were added to the crucible, which was stirred magnetically, to dissolve the melt. The solution was then transferred to a standard flask and made up with a La^{3+} solution so that the final concentration was 2% in La^{3+}. Lanthanum is used as a releasing agent.

(c) Sodium carbonate fusion[28]. This method was used to decompose the toposequence and Waterton soils, and concretions.

About 1 g of finely ground soil was ignited to just below red heat in a platinum crucible, and then mixed with 5g of anhydrous Na_2CO_3. A 1 g layer of Na_2CO_3 was then spread over the mixture. The crucible was partly covered and gently heated initially, and strongly heated with a meker burner for 30 minutes.

The cooled crucible was covered with distilled water in a beaker and heated on a steam bath until the melt had disintegrated. The crucible and lid were removed and rinsed, then treated with HCl (5 ml, 6M), which contained a little ethanol. A soil containing manganese oxides gives manganates on fusion, which in the presence of HCl will liberate chlorine which can attack the platinum. The addition of ethanol prevents this by reducing the Mn species to Mn(II).

The solution from the melt was then acidified with HCl (10 ml, 11M) and $HClO_4$ (10 ml, 60%). The washings from the lid and crucible were also added to the solution, which was evaporated to fuming. A further 15 minutes heating was used to dehydrate the silica. Hydrochloric acid (25 ml, 1M) was added, and the silica was removed by filtering, with thorough washings using hot HCl (1M). The filtrate was then concentrated to the required volume.

As mentioned above in the evaluation of the decomposition methods, the Na_2CO_3 fusion method was evaluated by the method of standard additions. Two spiking experiments, each using a clay samples and denoted So were carried out. In the

first case the filtered silica was washed with 1M HCl, and this experiment is denoted So (1M HCl). Secondly, the silica was collected using glass fibre filter paper and washed with 6M HCl. This experiment is designated So (6M HCl)(Table 5.2).

For these two standard addition experiments, the silica filtered off in each case was dissolved by HF-$HClO_4$ digestion and the resulting solutions analyzed.

(iv) *Extraction methods*. Oxalate and pyrophosphate extractions were carried out on whole soils of the chronosequence, biosequence, toposequence and Waterton soils, and concretions. The Waterton soils and concretions were ground to <53 μm while all the other samples were <2 mm in size.

(a) Ammonium oxalate extraction[110]. An ammonium oxalate solution (50 ml, 0.2M), adjusted to a pH = 3.0 with a saturated oxalic acid solution, was added to polyethylene centrifuge tubes containing 1 g of soil. The centrifuge tubes were tightly stoppered and shaken for 4 hours in darkness on a reciprocating shaker. A 'superfloc' solution (0.3 ml, 0.2%) was then added to each tube, which was hand shaken and centrifuged at 2500 r.p.m. The supernatant liquid was decanted into clean dry polypropylene bottles.

(b) Sodium pyrophosphate extraction[118]. A 1 g soil sample was added to a sodium pyrophosphate solution (100 ml, 0.1M) in clean polypropylene bottles, which were shaken for 16 hours on an end-over-end shaker. 'Superfloc' (0.3 ml, 0.2%) was added to each bottle, which after hand shaking, was ultra-centrifuged for 10 minutes. The supernatant solution was stored as before.

In all the chemical procedures listed above, replicate blank samples were carried through each procedure.

The regions of the electromagnetic spectrum and the various types of spectroscopy used in analytical techniques are shown in Figure 7.1. The nuclear, atomic (electronic) and molecular transitions which absorb or emit radiation are also shown.

1. Absorption of electromagnetic radiation by matter

(i) *Introduction.* When electromagnetic radiation travels through a transparent layer of matter, certain frequencies are selectively removed by an absorption process. In

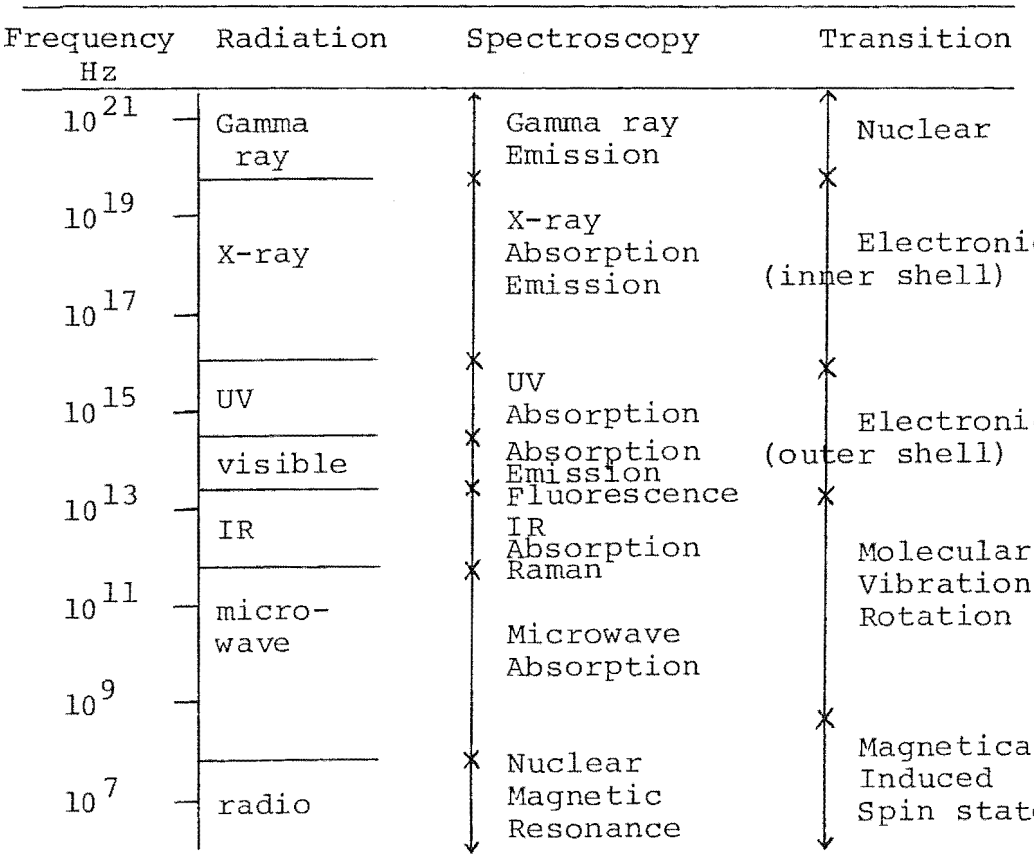

Figure 7.1. Electromagnetic spectrum and spectroscopy[189]

such cases the radiant energy is transferred to the atoms and molecules in the sample, thereby raising them in energy from the lowest ground states to the higher energy states.

Excited atoms and molecules return to their ground states after 10^{-8} - 10^{-9} s, usually with the release of energy as heat. Sometimes the excited species may undergo a photochemical reaction which absorbs the excitation energy, while at other times, radiation is re-emitted in the form of fluorescence or phosphorescence.

There are a number of discrete quantized energy levels in atoms, molecules and ions. When the energy of a photon and the energy difference between the ground state and one of the excited states of an atom or molecule is the same, absorption of radiation occurs. Because these energy differences are unique for each species, absorption studies can lead to the identification of the components of a sample. For this purpose, an absorption spectra - a plot of absorbance as a function of wavelength - is determined experimentally.

The shape of an absorption spectra depends on the complexity, the physical state and the environment of the absorbing species. There are two main types of absorption, namely atomic absorption and molecular absorption.

(ii) *Atomic absorption.* When a polychromatic beam of visible and ultraviolet radiation travels through a medium such as a monatomic gas, there is an absorption of a number of frequencies corresponding to the possible energy states of the atoms.

Visible and ultraviolet radiation is of appropriate energy to cause transitions of the outermost or bonding electrons. X-rays, on the other hand, are of a high energy, as can be seen in Figure 7.1, and can cause transitions involving inner electrons. Atomic absorption spectra are composed of a

number of narrow bands.

(iii) *Molecular absorption.* Absorption of ultraviolet-visible radiation by polyatomic molecules is a more complex process because the number of possible energy states is increased, and line broadening occurs due to the population vibrational and rotational energy states. Therefore molecular spectra are usually characterised by absorption bands that span a range of wavelengths.

(iv) *Measurement of the absorbed radiation.* Since the lifetime of the excited species is short (10^{-8} - 10^{-9} s), the concentration of such species at any instant is normally negligible. Consequently, absorption experiments have the advantage of creating only a minimal disturbance of the system under study.

(v) *Beer's Law.* Beer's Law is a relationship governing the absorption of all types of electromagnetic radiation. It applies to solutions, gases and solids. Beer's Law is

$$\log \frac{P_o}{P_t} = abc = A.$$

The logarithmic term is called the absorbance, denoted A, while P_o and P_t refer to the power of the incident and transmitted radiation respectively. The symbol, a, is called the molar absorptivity when the concentration, c, is given in terms of moles of absorber per litre, and the path length, b, is given in centimetres.

Neither P_o nor P_t can be measured easily in the laboratory since the solution to be studied must be in some sort of container. Interaction between the walls and the radiation is unavoidable, resulting in a lower value of P_t at each surface

due to reflection or absorption. A loss in radiant power can occur also because of scattering by large molecules in the solution. These diminutions of radiant power can be allowed for. The power of the transmitted beam emerging from the sample is compared with the power of the transmitted beam emerging from an identical cell containing the same solvent or matrix. The true solution absorbance is then approximated by the experimental absorbance

$$A \simeq \log \frac{P_{matrix}}{P_{sample}} \simeq \log \frac{P_o}{P_t}$$

2. Atomic absorption spectroscopy (A.A.S.)

(i) *Introduction.* Atomic absorption spectroscopy (A.A.S.) involves the study of the absorption of radiant energy (in the visible and ultraviolet regions) by atoms in the gaseous state. In A.A.S. the analyte must be reduced to the elemental state, varporized and transported into the beam of radiation from the source. This is achieved by aspirating the sample, as a fine mist,into a suitable flame. The flame is therefore analogous to the cell in conventional absorption spectroscopy.

(ii) *Interferences in A.A.S.* Several types of interference arise in A.A.S. They are a) spectral interference, b) ionization interference, and c) chemical interference.

(a) Spectral interference. Spectral interference occurs when a resonant line of one element, from a hollow cathode tube, is also absorbed by a second element in the flame. For example, the Co line at 253.649 nm interferes in the determination of Hg using the 253.652 nm line[179].

A more common form of spectral interference, encountered

in the present work, is molecular absorption. When solutions of high salt content are aspirated into a flame or vaporized in a carbon furnace, a significant concentration of molecular species can get into the light path. Molecular electronic absorption may occur, leading to interference if the molecular absorption bands extend over the absorption line of the analyte.

Molecular absorption was initially thought to be due to light scattering by salt particles[190]. Quite often though, light scattering is negligible compared with molecular absorption. An example of molecular absorption, and the removal of its effect, was encountered in the present work. The Na_2CO_3 fusions produced a high level of sodium salts in solution; molecular absorption processes considerably enhanced the absorption signal from both standard and sample (the matrix of the standards was matched with that of the samples) for Co and Ni, and to a lesser extent for Zn. This interference was countered in two ways. Firstly, blank solutions, with a matrix matched to the samples and standards, were used for background correction. Secondly, a deuterium lamp background correction was used. The deuterium arc lamp produces a continuum in the 200-300 nm spectral region. A rotating chopper allows energy from the hollow cathode lamp, and the deuterium lamp, to pass through the sampling cell alternatively. The undesired background absorption affects both signals in the same manner. Since the analyte element absorbs very narrow wavelength bands, it absorbs significant energy from the hollow cathode line source, but relatively nothing is absorbed from the deuterium arc continuum. The two absorptions

are subtracted electronically and the effect of background absorption is removed.

In the analysis of silicates and soils, in general, molecular absorption interference must be corrected, since solutions may contain high concentrations of K, Na, Mg, Ca, Al or Fe. The importance of this molecular absorption was illustrated by Fletcher[163] when he determined Co, Ni, Cu and Zn in solutions containing salts.

(b) Ionization interference. During the period of several milliseconds following the vaporization of a sample in a flame, many processes can occur: solvent evaporation, melting and vaporization of minute solid particles, chemical decomposition of particles and gaseous molecules, excitation and ionization of the gaseous species, recombination of the atomic vapour to form oxides, hydroxides and other molecular species, and condensation of gaseous species to form solid particles.

The distribution of analyte atoms in a flame is influenced by some or all of these processes. Anything that changes the ground state population of the analyte element is a type of interference. Ionization interference results from the ionization of an analyte atom in the flame (for example $Al \rightleftharpoons Al^{3+} + 3e$). Ionization of the analyte is prevented by flooding the flame with electrons from a more readily ionized element (commonly K or Cs) which pushes the above reaction to the left.

(c) Chemical interference. Various types of chemical interference can occur, several of which had to be compensated for in the present study. Species of a number of elements

(including Mn, Ni, Cu and Zn) are poorly dissociated into free ground state atoms by a low temperature (1900°C) air-propane flame. Hence the higher temperature air-acetylene flame (2100°C) was favoured. Air-acetylene flames can also be used in the analysis of Fe and Co.

An air-acetylene flame can be used in the analysis of Cr, as long as no Fe is present in the sample, and the fuel to oxidant ratio is adjusted to give a fuel rich mixture. The fuel rich flame (with limited oxygen) reduces the formation of the oxides of Cr, and thereby maintains a high ground state population of atoms. However, iron is always present in soils and solid particles consisting of Cr atoms dispersed in a matrix of Fe atoms remains after evaporation of the solvent in the flame. The volatility of such particles is low, and this will reduce the ground state Cr atoms population, depressing the Cr signal. This was overcome in the present work by using the hotter (2700°C) nitrous oxide-acetylene flame.

Elements that form particularly stable oxides, for example Al, Ti, Si, V and Cr, also require the hotter flame. In addition to using a hotter flame for the analysis of stable species, a releasing agent may be added to the solutions. A releasing agent is a material added which forms a more stable species than the analyte thereby releasing it. This has already been discussed (p.126) in relation to the influence of Al on the analysis of V and Cr.

3. X-ray methods

In this section some of the theoretical aspects of the emission, the absorption and the diffraction of X-radiation

(10 - 2500 pm) will be examined, as will some of the theory pertaining to X-ray fluorescence.

(i) *Emission line spectra.* X-rays can be obtained in 3 ways: 1) by striking a metal target with a beam of high energy electrons, 2) by bombarding a material with a primary beam of X-rays so as to produce a beam of fluorescent X-rays, and 3) by using a radioactive source which emits X-rays.

X-ray sources emit both a continuous and a line spectrum. It is the line spectrum which is of importance in analytical determinations using X-ray fluorescence and X-ray diffraction.

An example of a line spectrum, superimposed on a continuous spectrum is shown in Figure 7.2. For example, the

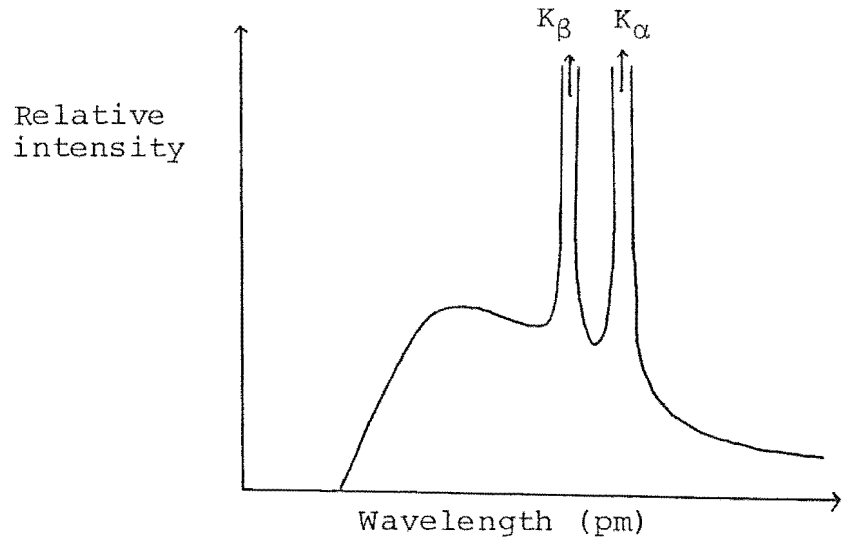

Figure 7.2. Characteristic line spectra

line spectrum from a Cu target has intense lines at wavelengths 139 and 154 pm[192]. Other weaker Cu lines occur in the 1200 - 1600 pm region.

The lower wavelength lines are called the K series (Kα and Kβ), while the weaker lines constitute the L series.

Elements with atomic numbers less than 23 emit only a K series of lines.

Electronic transitions involving the innermost atomic orbitals produce the X-ray line spectrum. When the higher energy electrons from the cathode remove electrons from the orbitals closest to the nucleus of the target atom (the orbital of principal quantum number n = 1), the highest energy K series of lines are produced. The collisions produce excited ions which lose their excitation energy as electrons undergo transitions from the outer orbitals to the vacated orbital.

The L series of X-ray lines result when an electron is lost from the atomic orbital of principal quantum number n = 2. This can be caused either by ejection by an electron from the cathode, or by the transition of an L electron (n = 2) to the K (n = 1) orbital. The L series of lines are then produced as a consequence of electronic transitions to relax the excited atom.

Because X-ray line spectra result from electronic transitions involving the innermost orbitals, the wavelengths of the line spectra are independent of the form of chemical combination of elements other than those with low relative atomic weight (atomic number < 20).

(ii) *Absorption of X-rays*[189,193]. X-rays travelling through matter are attenuated by an amount dependent on the thickness and the density of the absorbing material. X-rays of different frequencies are attentuated by different amounts by the same absorber. The main cause of the attentuation of X-rays is photoelectric absorption.

When a beam of X-rays of radiant power P_o travels through matter of thickness x cm, and has a transmitted intensity P_t, the absorption of the X-rays is described by Beer's Law

$$\ln \frac{P_o}{P_t} = \mu_l x$$

where μ_l is the linear absorption coefficient, which is characteristic of the element and the number of atoms in the path of the beam. Beer's Law can also be written

$$\ln \frac{P_o}{P_t} = \mu \rho x$$

where ρ is the density of the sample, and μ is the mass absorption coefficient, a quantity that is independent of the physical and chemical state of the element.

The mass absorption coefficient has two components - a scattering component and a photoelectric component. The photoelectric absorption is the dominant component, and the mass absorption can be approximated by it. It has been determined experimentally that the mass absorption coefficient for an element conforms to the relationship

$$\mu = KNZ^4\lambda^3A^{-1}$$

where N is Avogadro's number, A is the relative atomic weight of the element, Z its atomic number, and λ is the wavelength of the radiation. K is a constant for all elements. It can be seen from this relationship that μ is a function only of the wavelength of the absorbed radiation and the atomic number of the absorbing element.

Mass absorption coefficients are additive, and contribute according to the amount of each element in a sample,

i.e.

$$\mu_m = F_1\mu_1 + F_2\mu_2 + \ldots$$

where μ_m is the mass absorption coefficient of a sample, F_1, F_2, ... are the mass fractions of each element 1, 2, ... and μ_1, μ_2, ... represent the mass absorption coefficients for each of the elements.

(iii) *Diffraction of X-rays*[159,193-195]. A consequence of the three-dimensional periodicity of a crystal structure is that it is possible to consider a crystal as made up of numerous sets of parallel planes. Each set of parallel planes are equally spaced and contains identical atomic arrangements. For diffraction to occur the wavelength of the X-rays must be of the same order of magnitude as the interatomic distances.

When an X-ray beam impinges on a crystal surface at an angle σ, some of the radiation is scattered by the surface layer of atoms (Figure 7.3). The unscattered beam penetrates

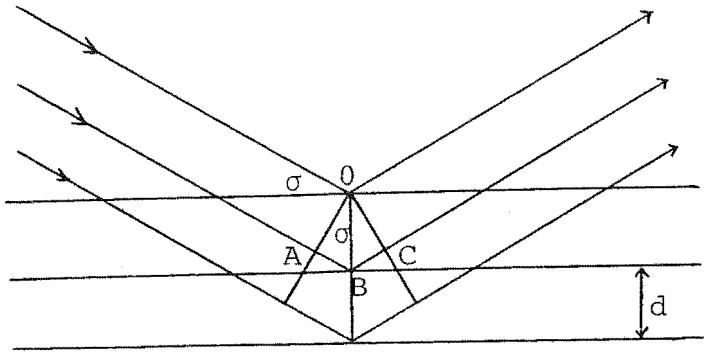

Figure 7.3. Diffraction of X-rays by a crystal.

to the second layer of atoms where there is more scattering, with the remaining X-ray beam passing to the third layer and so on. The overall effect of this scattering from the periodic crystal structure is a diffraction of the X-ray beam.

The Braggs developed a treatment of the scattering of X-rays by a crystal, based on the equivalence of the scatter-

ing of X-rays from a set of planes and a reflection from successive planes.

Since there are large numbers of parallel planes involved in the scattering of X-rays, reflections from successive planes will interfere with each other. There will be constructive interference only when the difference in path length between rays from successive planes is equal to a whole number of wavelengths. This is illustrated in Figure 7.3 where X-rays, of wavelength λ, are incident at an angle σ, on a set of planes of spacing d. The ray striking the second plane travels a distance AB + BC further than the ray striking the first plane. These two rays will be in phase when AB + BC = n , where n is an integer. Since AB and BC both equal d sinσ then

$$2d \sin\sigma = n\lambda$$

which is the Bragg equation.

4. X-ray fluorescence

(i) *Introduction*. The absorption of X-rays produces electronically excited ions that return to their ground state by transitions involving electrons from higher energy levels. For example, when a Mn atom absorbs radiation of wavelengths of shorter than 190 pm[192], an excited ion with a vacant K shell is produced. After 10^{-8} - 10^{-9} s the ion returns to its ground state by the emission of X-rays (fluorescence). The wavelength of the fluorescent lines are always slightly greater than the wavelength of the corresponding absorption edge, since absorption requires ionization, while emission involves transitions of an electron from a higher energy level within

the atom.

(ii) *Interelement effects*. In X-ray fluorescence analysis,careful consideration must be given to interelement effects on the intensity of the X-ray fluorescence. Interelement effects arise from 1) interference from the spectra of the various elements, 2) X-ray absorption by the matrix, and 3) X-ray enhancement.

In most cases spectral interference can be overcome by using another spectral line of the element, or by selection of different instrumental settings, such as the dispersion crystal used, the counter, the collimator, and the pulse height discriminator. The Ti Kβ fluorescence which occurs at the same energy as the V Kα fluorescence, is an example of spectral interference.

Interference by absorption or enhancement of the X-ray fluorescence signal is more widespread. Samples inevitably absorb some X-rays because the primary X-ray beam penetrates the sample to a finite depth. The extent of the absorption, both primary and secondary, is proportional to the mass absorption coefficient, at the wavelength concerned, which is derived from the sum of the products of the individual absorption coefficients of the elements and the mass fraction of the corresponding element.

Enhancement occurs when fluorescent X-rays generated in the sample from matrix elements, are then absorbed by the analyte element, producing an increased emission from the element.

Absorption and enhancement interferences can be compensated for mathematically, by equations relating the elemental fluorescent intensity to the mass absorption coeff-

icient and the fluorescent yield. An iterative procedure is then used in which successive approximations of the concentration are calculated.

Matrix effects can be corrected for by using the method of standard additions, where a known amount of the analyte is added to the sample, its concentration being obtained from the measured countrates before and after the addition. Another method, not so relevant for trace element analysis is dilution of the sample by fusion with sodium tetraborate producing a glass[196]. If the samples are sufficiently diluted, effects due to variations in absorption coefficients may be overcome. The addition of a heavy absorber (La) during dilution suppresses the matrix effects. While dilution suppresses the matrix effect it also reduces the sensitivity, and so it is necessary to compromise between these two.

Fusion of a sample into a glass is effective in eliminating sample heterogeneity. However, in the analysis of silicates, homogeneity can be obtained by grinding the sample in a tungsten-carbide mill. Also, grinding of both samples and standards ensures a constant particle size, which eliminates particle size effects.

Brenner et al.[197] achieved acceptable accuracy in the analysis of silicate rocks for Ti, Mn, Fe, Co, Ni, Cu and Zn. They analyzed the material as loose powders or pellets, and found no bias due to grain size effects, nor did they find absorption or enhancement of radiation by other elements.

5. Electron microprobe analysis

The electron microprobe uses an electron-optical

system to focus an electron beam onto an area of about 1 μm in diameter. A Bragg spectrometer is used to select the characteristic X-radiation produced by the element hit by the electrons. The X-ray intensity is measured with a proportional counter. The slowing down of the electrons in the beam by the specimen also produces a continuous X-ray spectrum which constitutes a background, over and above which the characteristic X-ray lines are superimposed.

For quantitative work, the net intensity (peak minus background) of the characteristic line of each element is measured and compared with the intensity generated with the same incident electron current in a standard of known composition. Concentrations and intensities conform to the relationship

$$\text{specimen} = \text{standard} \times \frac{I_{\text{specimen}}}{I_{\text{standard}}} \times f$$

where f is a product of 3 seperate factors which take into account the differences in efficiency of X-ray generation in the specimen and the standard (called the generation factor), the differences in the absorption of the emerging X-rays (the absorption factor), and the enhancement of the measured characteristic radiation by secondary excition (the fluorescence factor). The f factor was calculated using a computer program, MAGIC IV[198], which was employed to calculate the percentage concentrations of the elements in the sample.

EXPERIMENTAL METHODS FOR THE INSTRUMENTAL TECHNIQUES

1. Atomic absorption spectroscopy

(i) *Analysis of decomposition solutions.* In the

present study, A.A.S. was employed to determine the concentrations of V, Cr,Mn,Fe,Co,Ni, Cu and Zn in solutions resulting from the decomposition of soil samples, using a Varian Techtron A.A.5 Spectrometer, with a Varian Techtron BC-6 background corrector. The intensity of the deuterium continuum lamp (required for background correction) was maintained constant throughout a set of measurements. A Varian Model 63 Carbon Rod Atomizer was used for the flameless A.A.S. determination of Co, Ni, Cu and Zn in the silica obtained from the soil decomposition solutions after Na_2CO_3 fusion.

(ii) *Interferences encountered in A.A.S.* Many kinds of interference can take place in A.A.S. and need to be corrected.

Several interference effects were investigated in the present study and corrections made. A list of the interferences encountered, and means to suppress them, is given in Table 7.2.

The sodium present in the solution from the Na_2CO_3 fusions caused a 30% enhancement to the Co and Ni signals, and a smaller enhancement of the Cu and Zn signals. The use of a background corrector together with a solution blank obtained from a Na_2CO_3 fusion, was used to correct for this enhancement. The enhancement was probably caused by molecular electronic absorption.

No interference due to trivalent Al or Fe was found in the signals from Mn, Fe, Co, Ni, Cu and Zn, when using an air-acetylene (A-A) flame to vaporize solutions from the $HF-HClO_4$ digestion solutions. However, signals from Ti, V and Cr were all strongly affected by Al or Fe. Since the Ti signal showed a strong interference from both Al and Fe it was not deter-

TABLE 7.2 Interference Encountered in A.A.S. Analysis and Their Suppression

Element Analyzed	Method	Flame	Interference	Removal of Interference
Ti	$HF-HClO_4$	A-A[a]	Fe,Al depression	Used colorimetric method of analysis
V	$HF-HClO_4$	A-A	Fe depression	Used N-A flame, and 200 µg Al ml^{-1}
V,Cr	$LiBO_2$	A-A	Fe depression	Used N-A flame, 2% La solution, and 200 µg Al ml^{-1}
Cr	$HF-HClO_4$	A-A	Fe depression	Used N-A flame, and 200 µg Al ml^{-1}
Mn,Fe,Co, Ni,Cu,Zn	$HF-HClO_4$ $LiBO_2$	A-A	-	-
Co,Ni	Na_2CO_3	A-A	30% Enhancement due to Na	Background correction
Cu,Zn	Na_2CO_3	A-A	Slight enhancement due to Na	Background correction
Al	Oxalate, Pyrophosphate	N-A[b]	Ionization of Al	1000 µg Cs ml^{-1}
Mn,Fe,Cu,Zn	Oxalate, Pyrophosphate	A-A	-	-
Si	Oxalate Pyrophosphate	N-A	-	-

[a] A-A = Air-acetylene

[b] N-A = Nitrous oxide-acetylene

mined by A.A.S. In a nitrous oxide-acetylene (N-A) flame, the V signal is strongly depressed by Fe. This interference was overcome by adding Al (200 μg ml^{-1}) to all the standard and blank solutions, to act as a releasing agent (see p.126). The solutions resulting from the soil decompositions did not require addition of Al, as sufficient was present in the soil. The depression of the Cr signal caused by Fe was overcome by use of a N-A flame.

For solutions from the $LiBO_2$ fusions both V and Cr were analyzed with a N-A flame, with Al(III), added and in a 2% La solution (as releasing agent).

As silicon is present in the $LiBO_2$ fusion solutions, its effect on elemental response in A.A.S. was investigated. No effect was detected within the range of Si in the sample solutions.

(iii) *A.A.S. analysis of the extraction solutions.* The oxalate and pyrophosphate extraction solutions were analyzed by A.A.S. for Si, Al, Mn, Fe, Cu and Zn. When analyzing for Al, the solutions and standards were made up to 1000 μg Cs(III) ml^{-1} to prevent the depression of the Al signal as a result of ionization.

All standard solutions used for the A.A.S. analysis of the oxalate extracted solutions also contained 0.1M ammonium oxalate. The pyrophosphate extracted solutions were treated similarly and the standard solutions were all 0.05M in sodium pyrophosphate. Three separate standard solutions were used in the A.A.S. analysis, one containing Mn, Cu and Zn, one containing only Fe and the third with Si and Al.

Silicon and aluminium were analyzed using a N-A flame, while Mn, Fe, Cu and Zn were all analyzed using an A-A flame

(Table 7.2).

2. X-ray diffraction

(i) *Introduction.* X-ray diffraction is used for the identification of crystalline compounds. The method is based on the fact that a X.R.D. pattern is unique for a certain crystalline structure. If a match can be found between the X.R.D. pattern of a sample and that of a previously determined structure, chemical identity may be suggested.

(ii) *Sample preparation and analysis.* The samples were prepared by grinding about 0.2 g of sample in an agate pestle and mortar, mixing with a few drops of ethanol, then transferring the suspension to a glass slide.

A Phillips PW 1010 generator, together with a PW 1050 Norelco Diffractometer, employing a Cu target tube (50 kV, 20 mA, 154.18 pm) was used to obtain the diffraction patterns for the Waterton soils and concretions, and the Ok Fe pan. The high iron content of the concretions increased the overall background on the diffractogram due to iron fluorescence produced by the Cu radiation.

3. X-ray fluorescence

(i) *Standards for analysis.* The standards used were the International Rock Standards U.S.G.S. G-2 (a granite), W-1 (a diabase), AGV-1 (an andesite), BCR-1 (a basalt) and GSP-1 (a granodiorite). For Ti analysis, 3 Shale standards KnC-ShP-1, SCO-1 and SGR-1 were used.

The major matrix effect in X.R.F. is the mass absorption of the X-rays. The counts for the samples and standards were therefore corrected for mass absorption, and the best calibration line for the set of standards was determined from a least

squares fit.

(ii) *Sample preparation and analysis.* Samples were oven dried at 105°C and ground in a tungsten-carbide mill to <53 μm. Discs were prepared by mixing 2 g of milled sample with 0.2 g methyl cellulose, which acts as a binder. The mixtures were then pressed into briquettes for analysis. Some discs were also prepared by pressing a 2 g sample, without binder, using a borax base for support.

A Philips PW 1010 generator, coupled with a PW 1540 Manual Vacuum Spectrum, with a Cu target tube, was employed for the X.R.F. analysis. Operating parameters are given in Table 7.3.

X.R.F. analysis was used to determine Si, Al, Ti, Cr, Mn, Fe, Ni, Cu and Zn in the Waterton soils and concretions, and Ti, Cr, Mn, Fe, Ni, Cu and Zn in the toposequence soils.

TABLE 7.3 Operating Parameters for X-ray Fluorescence

Element	Line Analyzed	Crystal	Collimator	Atmosphere	kV/mA	Counter
Ti	Kα	LiF(200)	Fine	Vacuum	36/36	Flow
Cr	Kα	LiF(200)	Coarse	Vacuum	36/36	Flow
Mn	Kα	LiF(200)	Fine	Vacuum	36/36	Flow
Fe	Kα	LiF(200)	Fine	Air	36/36	Scintillation
Ni	Kα	LiF(200)	Fine	Air	36/36	Scintillation
Cu	Kα	LiF(200)	Fine	Air	36/36	Scintillation
Zn	Kα	LiF(200)	Fine	Air	36/36	Scintillation
Al	Kα	T.L.A.P.[a]	Fine	Vacuum	36/36	Flow
Si	Kα	T.L.A.P.	Fine	Vacuum	36/36	Flow

[a] Thallium acid phthalate crystal

4. Electron microprobe analysis

(i) *Sample preparation.* The samples studied by electron microprobe analysis were an Fe pan from the chronosequence Ok profile, and the Waterton concretions. Since a smooth polished surface is required, the samples had to be first impregnated with an epoxy resin. A vacuum impregnation system[199] was used to obtain efficient impregnation of the sample.

The vacuum sample chamber contained 6 open-end glass tubes (10 x 15 mm), into each of which one sample was placed. These sample tubes were mounted on a circular table so that a dropping funnel containing the epoxy resin could be rotated from one sample to the next.

The sample chamber was pumped down to about 10^{-3} torr, and the samples were allowed to outgas for up to 15 hours prior to impregnation. Araldite M (a special impregnating resin) was mixed with the hardener HY 956 in a 5:1 ratio. The Araldite mixture was introduced to a dropping funnel on the top of the vacuum chamber. The chamber was isolated from the pump and the Araldite mixture was outgassed for 10 minutes. The sample chamber and the dropping funnel were then brought to the same pressure, and after aligning the funnel over a sample tube, Araldite was run into the tube to cover the sample. When opened to the atmosphere pressure, and pressurized with nitrogen in a bomb to 1380 kPa, the Araldite was forced into the samples.

After 12 hours the resin had hardened, and the samples were cut into 1 mm thick slices and re-impregnated. The samples were then polished using 400 and 600 carborundum powders, P600 and P1200 carborundum papers, a Buehler Textmet

synthetic cloth with pure tin oxide powder, and finally buffed with a soft cloth dusted with a little tin oxide. All samples were then vacuum carbon coated using a Polaron E500 instrument.

(ii) *Analysis*. The electron microprobe used was a JEOL JSM 35 with a JEOL wavelength spectrometer. Operating conditions are given in Table 7.4. Standards were polished samples of the metals, and were vacuum carbon coated. The elements analyzed were Ti, V, Mn, Fe, Co, Ni, Cu, Zn, Si and Al.

Three methods were used to gather data on the samples. Firstly, point counting at sites selected either at random or at points of high concentration for certain elements. For both standards and samples, counts were accumulated for 30 s on the peak and also the background. A computer program, MAGIC IV[198], which corrects for backscattering, ionization-penetration, absorption and fluorescence, was used to calculate the weight percentages of the elements analyzed. The program assigns oxygen concentrations assuming the following metal ion oxidation states: Al(III), Si(IV), O(II), Ti(IV), V(III), Mn(IV), Fe(III), Co(II), Ni(II), Cu(II) and Zn(II).

Secondly, a line scanning technique was used. This involved traversing the specimen under a stationary beam. A line scan is carried out at a set wavelength, so each element

TABLE 7.4 Electron Microprobe Operating Parameters

X-Ray Take-Off Angle	35^{o}
X-Ray Detector	Gas flow proportional counter
Accelerating Voltage	25 kV
Beam current	$1\text{-}2 \times 10^{-7}$A
Analysing crystal for Ti,V,Mn,Fe,Co,Ni,Cu,Zn	LiF
Analysing crystal for Si,Al	RAP (Rubidium hydrogen phthalate)

was scanned separately by varying the wavelength. Graphical methods were then used to compare variations in elemental concentrations across a sample.

The third technique used was electron beam scanning. The focussed beam was swept, in a regular way, across a square area of a sample, while a synchronous oscilloscope display indicated the two-dimensional intensity distribution of back-scattered electrons for a characteristic X-radiation. Photographs of the oscilloscope display provide a permanent record of textural features and phase relations (backscattered electrons), and the relative enrichment of a particular element (characteristic X-radiation) throughout the area. A comparison of photographs taken during electron beam scanning enables interelemental relationships to be recognised at a glance, provided that the element is present in sufficient concentration, not to be obscured by the background radiation.

For the Ok Fe pan, two samples were analyzed, while three concretions from horizons of the Waterton soils were studied.

5. Colorimetric analysis

(i) *Titanium*. Tiron[200], disodium 1,2-dihydroxybenzene 2,5-disulphonate was used for the determination of Ti in the sample solutions. Tiron reacts with Ti giving a species with a yellow colour, the intensity of which relates to the concentration of Ti.

Ten millilitres of a buffer solution (equal volumes of 1M acetic acid and 1M sodium acetate, adjusted to pH 4.7) was diluted threefold. Tiron (5 ml, 4% W/V) and an aliquot of

the sample were added and the solution made to volume. To a portion of this solution about 5 mg of sodium dithionite was added. The absorbance at 400 nm was recorded after 10 minutes, on a Varian U.V.-Visible Spectrometer Superscan 3.

(ii) *Copper*[28]. In the evaluation of the Na_2CO_3 method of decomposition, it was found that added Cu (as well as Co, Ni and Zn) could not be completely recovered. A.A.S. was used for these analyses. It was decided to analyze the same solutions for Cu by a colorimetric analysis using diethyldithiocarbamate.

In the colorimetric analysis the cupric ion reacts with sodium diethyldithiocarbamate to form a complex which is soluble in CCl_4. Addition of a citrate -EDTA mixture prevents interference from Fe and Mn. A sample solution was added to a separatory funnel, to which was added 25 ml of the citrate-EDTA mixture (200 g ammonium citrate and 50 g disodium, ethylenedinitrilotetraacetate dm^{-3} of water, with the pH adjusted to 8.5 with NH_4OH). The carbamate solution (3 ml, 1%) and CCl_4 (10 ml) were added and the solution was agitated. The CCl_4 layer was transferred to a centrifuge tube, and a further 5 ml of CCl_4 was added to the original aqueous solution. The CCl_4 layer was then centrifuged at 1200 rpm for 5 minutes.

Suitable standards were prepared in a similar manner, and the intensity of the Cu complex absorption measured at both 440 nm and 500 nm, using a Varian Techtron U.V.-Visible Spectrometer Model 635.

6. Correlation analyses

Correlation analyses were carried out separately on the

analytical data obtained for the soil samples by HF digestion followed by A.A.S. analysis, and by electron microprobe analysis of concretions and an Fe pan. The computer program[191], (S.P.S.S. -The Statistical Package for Social Scientists) was used to produce correlation coefficients and the level of significance. The program was run on a computer (Burroughs B6700) at the University of Canterbury.

CHAPTER 8

TRACE ELEMENT ANALYSES IN SOILS

The analysis of trace elements in the soil sequences and iron-manganese concretions of this work has raised some questions pertaining to such studies. Although attempts were made to answer these questions, further attention is required to fully resolve the issues. In this Chapter a summary of the problem areas is given, which may prove useful for future work.

The problems originate in the complexity of the soil system, which has physical, chemical and biological properties, and in attempting to interpret analytical data mainly in terms of soil chemistry.

THE SAMPLE, SAMPLING AND SAMPLE TREATMENT

One of the shortcomings of any study of trace elements in soils is the need to take samples from the field into a laboratory for analysis. This can result in changes occurring to the soil sample. For example, air drying of soil and greater penetration of oxygen from the atmosphere, can lead to oxidation of iron and manganese oxides, and a change in microbial populations. In such a way, the sample is changed from what it was originally in the field - not in the content of trace metals, but in their form.

The first problems encountered in soil studies are obtaining a sample and deciding on the type of sampling procedure to use. In this work, changes in trace elements in soil

sequences were to be studied in relation to soil forming factors. In previous studies[20,25], sites were selected for similar purposes, and so comparable sites, adjacent to those of the previous studies, were selected. Care was taken nevertheless, to avoid the influence of other factors as much as is possible, which would complicate the present study's aim. Sampling randomly would mean that many different soil forming factors would have had an effect on the soil samples, and that therefore the information derived from the analysis of such samples may be of a more general nature, and more applicable to a soil survey, rather than the study of the effect of one soil forming factor.

The question of sampling is also relevant in the concretion study. The three concretions analyzed in detail did have many similarities between them in terms of trace element concentrations, however,there were also differences between them, even though two of the concretions were only centimetres apart in the ground.

The separation of a soil into various particle sizes is a common practice in soil analysis. While a necessary process in order to simplify any analysis the size designations are arbitrary, and the separation process itself can lead to changes in the soil, such as comminution of particles which can obscure the boundaries between the particle sizes, especially for silt and clay. It would appear therefore, that any comparative studies of soils in terms of particle size groupings is subject to some uncertainty in the amounts of each particle size obtained.

RESULTS

The analysis of soil material can pose questions as to the accuracy of the data obtained. No standard soil samples were available for confirming the accuracy of experimental methods, and although standard rock samples were available, there are considerable differences between soils and rocks. Various decomposition techniques and instrumental methods were used in an attempt to assess the accuracy of the results, and although some factor (unknown) may be operating to prevent accurate data, the data should at least be precise and suitable for comparative purposes.

The presentation of such voluminous data has been a concern, both from the point of view of compactness, and being able to analyze the data meaningfully. In the chronosequence, the data for the various soils was presented on a volume basis as well as on a mass basis, in order to be able to compare different soils. More attention in the future should be directed at comparisons of different soils from different places as analyzed by various workers, as it is likely that the treatments employed in the present work are in some respects inadequate. Attempts should be made to describe the variables in soils in measurable terms, in order to relate them quantitatively, and thus to eventually achieve a soil chemistry description of wide usefulness.

The interpretation of the data from the extraction methods remains very generalized. Many extraction solutions can be used and one of the difficulties in interpreting the data obtained is that it depends on the concentration of the extractant used, the time and vigour of the extraction method,

temperature, particle size, etc. The different properties of different soils often makes comparisons difficult, and it is likely that comparisons will be more valid with soils of the same type. A second major shortcoming of extraction type work is that laboratory experiments are performed under conditions completely different to field conditions, thereby making it difficult to interpret laboratory results in terms of field conditions.

The final problem area, as far as results are concerned, is the statistical treatment of so much data. Care is required in the choice of statistical tests to be used, and it is essential to confirm the results of such analyses with results of other analyses. For example, the correlation coefficient is widely used, but as was pointed out in Chapter 6, indiscriminate deductions from such parameters can be misleading.

CHOICE OF ELEMENTS TO STUDY

It is apparent from this and other studies that a multi-element study is essential because of interelemental effects, especially as can be seen in the iron-manganese concretions. With this in mind it is important which elements are studied. In the present work, the first row transition metals, many of which are essential trace elements for plants, were selected for study. By selecting the entire first row of elements, it was envisaged that having elements related by periodic changes may prove of value and interest in such a study. The results have shown that the elements of the left and right sides of the first row of transition metals have different soil

chemistry. The most abundant trace elements - manganese and iron - which are in the centre of the period, display chemical properties typical of both the left and right hand sides of the period. As a consequence, the soil chemistry of the trace elements, which is strongly influenced by manganese and iron, becomes quite complex.

FUTURE WORK

This study has highlighted some of the shortcomings of soil studies, and these could constitute areas for future work. Besides this, the present study has produced data on trace elements in soil sequences and iron-manganese concretions which can be explained in terms of the environment they occur in. Such information can be of value in agricultural practices, and a knowledge of trace elements may lead to a forecasting of the trace element status of soils as a source of micronutrient elements for plants and animals.

REFERENCES

1 J.F. Hodgson, Advances in Agronomy, 15, 119 (1963).

2 E.W. Russell, Soil Conditions and Plant Growth, 10th Ed., Longman Gp. Limited, London (1973).

3 F.E. Bear, Chemistry of the Soil, 2nd Ed., Reinhold Pub. Corp. N.Y. (1967).

4 T.C. Broyer, C.M. Johnston et al., Pl. Soil, 8, 337 (1957).

5 S.L. Tisdale and W.L. Nelson, Soil Fertility and Fertilizers, 3rd Ed., MacMillan Pub. Co. Inc., N.Y. (1975).

6 H.O. Buckman and N.C. Brady, The Nature and Properties of Soils, 7th Ed., MacMillan Pub. Co. Inc., N.Y. (1970).

7 B.D. Soane and D.H. Saunder, Soil Sci., 88, 322 (1959).

8 H.H. Le Riche and A.H. Weir, J. Soil Sci., 14, 225 (1963).

9 R.M. Taylor and R.M. McKenzie, Aust. J. Soil Res., 4, 29 (1966).

10 H.M. Reisenauer, A.A. Tabikh and P.R. Stout, Soil Sci. Soc. Amer. Proc., 26, 23 (1962).

11 D.J. Swaine and R.L. Mitchell, J. Soil Sci., 11, 347 (1960).

12 R.L. Mitchell, Scot. Agric., 34, 139 (1954).

13 H. Jenny, Soil Sci., 61, 375 (1946).

14 H. Jenny, Factors of Soil Formation, McGraw-Hill, N.Y. (1941).

15 H. Jenny, Ecology, 39, 5 (1958).

16 J.D. Raeside, N.Z. Soil News, 6, 168 (1966).

17 A.A. Rode, The Soil Forming Process and Soil Evolution, Israel Program for Scientific Translations, Jerusalem (1961).

18 N.H. Taylor and I.J. Pohlen, Soil Survey Method, N.Z. D.S.I.R., Soil Bureau Bull., 25 (1970).

19 F.A.O. - UNESCO. Soil Map of the World, Volume 1, Legend. UNESCO Printing Press, Paris (1974).

20 A.S. Campbell, Ph.D. Thesis, Lincoln College, University of Canterbury, New Zealand.

21 R.P. Suggate, Bull. Geol. Surv. N.Z., 56, 1 (1957).

22 R.P. Suggate, Bull. Geol. Surv. N.Z., 77, 1 (1965).

23. R.P. Suggate and N.T. Moar, N.Z.J. Geol. Geophys., 13, 742 (1970).

24 S. Nathan and N.T. Moar, J. R. Soc. N.Z., 3, 409 (1973).

25 A.W. Young, Pers. Comm. (1981).

26 D.M. Budhia, M.Sc. Thesis, University of Canterbury, New Zealand (1978).

27 H.D. Foth and L.M. Turk, Fundamentals of Soil Science, 5th Ed., John Wiley and Sons Inc. N.Y. (1972).

28 P.R. Hesse, A Textbook of Soil Chemical Analysis. John Murray, London (1971).

29 C.A. Black, Methods of Soil Analysis, Part 2, American Society of Agronomy Inc., Madison, U.S.A. (1965).

30 R.K. Schofield and A.W. Taylor, J. Soil Sci., 6, 137 (1955).

31 B.W. Bache, J. Soil Sci., 21, 28 (1970).

32 G.K. Voigt, Forest Science, 6, 2 (1960).

33 P.L. Gersper and N. Holowaychuk, Soil Sci. Soc. Amer. Proc., 34, 786 (1970).

34 I.S. Kaurichev, Ye. M. Nozdrunova and R.P. Yevseyeva, Soviet Soil Sci., 1, 547 (1969).

35 C.R. Hursh and M.D. Hoover, Soil Sci. Soc. Amer. Proc., 6, 414 (1941).

36 W.H. Huang and W.D. Keller, Am. Miner., 55, 2076 (1970).

37 W. Stumm and J.J. Morgan, Aquatic Chemistry, John Wiley and Sons Inc., N.Y. (1970).

38 T.W. Walker, In Experimental Pedology, E.G. Hallsworth and D.V. Crawford, Butterworths, London (1965).

39 Jackson, Soil Chemical Analysis, Constable, London (1958).

40 C.J. Schollenberger, Soil Sci., 24, 65 (1927).

41 J.M. Bremner and D.S. Jenkinson, J. Soil Sci., 11, 394 (1960).

42 D.F. Ball, J. Soil Sci., 15, 84 (1964).

43 P.J. Zinke, Ecology, 43, 130 (1962).

44 E. Barkoff, Arbeiten Maalaloust Aikak, 32, 179 (1960).

45 A.P. Edwards and J.M. Bremner, J. Soil Sci., 18, 47 (1967).

46 D.T. Pritchard, J. Soil Sci., 25, 34 (1974).

47 A.P. Edwards and J.M. Bremner, J. Soil Sci., 18, 64 (1967).

48 V.J. Kilmer and L.T. Alexander, Soil Sci., 68, 15 (1949).

49 W.W. Emerson, J. Soil Sci., 22, 50 (1971).

50 R.L. Mitchell and J.C. Burridge, Phil. Trans. Royal Soc. London, B288, 15 (1979).

51 K. Norrish, In Trace Elements in Soil-Plant-Animal Systems, Editors D.J.D. Nicholas and A.R. Egan, Academic Press Inc. (1975).

52 R.L. Mitchell, Bull. Geol. Soc. Am., 83, 1069 (1972).

53 R.M. McKenzie, Aust. J. Soil Res., 8, 97 (1970).

54 M.L. Berrow, M.J. Wilson and G.A. Reaves, Geoderma, 21, 89 (1978).

55 J.R. Butler, Geochim. Cosmochim. Acta, 4, 157 (1953).

56 B.A. Goodman and M.V. Cheshire, Geochim. Cosmochim. Acta, 39, 1711 (1975).

57 D.H. Yaalon, C. Jungreis and H. Koyumdjisky, Geoderma, 7, 71 (1972).

58 R.L. Mitchell, In Chemistry of the Soil, Editor F.E. Bear, 2nd Ed, Reinhold, N.Y., 320 (1964).

59 C.W. Childs, Geoderma, 13, 141 (1975).

60 A. Andersson, Swedish J. Agric. Res., 9, 7 (1979).

61 M.J. Dudas and S. Pawluk, Can. J. Soil Sci., 60, 763 (1980).

62 A. Andersson, Swedish J. Agric. Res., 7, 79 (1977).

63 E.A. Jenne, Adv. Chem. Ser., 73, 337 (1968).

64 T.T. Chao and P.K. Theobald, Econ. Geol., 71, 1560 (1976).

65 J.L. Means, D.A. Crerar, M.P. Borcsik and J.O. Duguid, Geochim. Cosmochim. Acta., 42, 1763 (1978).

66 R.M. Taylor, R.M. McKenzie and K. Norrish, Aust. J. Soil Res., 2, 235 (1964).

67 H.H. Le Riche, Geoderma, 9, 43 (1973).

68 M.L. White, Econ. Geol., 52, 645 (1957).

69 S.K. Ng and C. Bloomfield, Geochim. Cosmochim. Acta, 24 206 (1961).

70 C.H. Van der Weijden, Chem. Geol., 18, 65 (1976).

71 R.G. Burns and D.W. Fuerstenau, Am. Miner., 51, 895 (1966).

72 R.G. McLaren and D.V. Crawford, J. Soil Sci., 24, 443 (1973).

73 J.F. Collins and S.W. Buol, Soil Sci., 110, 111 (1970).

74 R.G. Burns, Geochim. Cosmochim. Acta, 40, 95 (1976).

75 S.N. Adams, J.L. Honeysett, K.G. Tiller and K. Norrish, Aust. J. Soil Res., 7, 29 (1969).

76 C.W. Childs and D.M. Leslie, Soil Sci., 123, 369 (1977).

77 K.B. Krauskopf. Geochim. Cosmochim. Acta, 12, 61 (1957).

78 A.O. Summers and S. Silver, Ann. Rev. Microbiol., 32, 637 (1978).

79 C. Douka, Soil Biol. Biochem., 9, 89 (1977).

80 H.L. Ehrlich, Appl. Microbiol., 11, 15 (1963).

81 J.W. Murray, Geochim. Cosmochim. Acta, 39, 635 (1975).

82 R.M. McKenzie, Aust. J. Soil Res., 5, 235 (1967).

83 G.P. Glasby, Geoderma, 13, 363 (1975).

84 R.M. McKenzie, Geoderma, 13, 369 (1975).

85 P. Loganathan and R.G. Burau, Geochim. Cosmochim. Acta, 37, 1277 (1973).

86 R.M. Garrels and C.L. Christ, Solutions, Minerals and Equilibria, Harper and Row, N.Y., and John Weatherhill Inc., N.Y. (1965).

87 R.G. Burns, Mineralogical Applications of Crystal Field Theory, Cambridge University Press (1970).

88 B.N. Figgis, Introduction to Ligand Fields, Interscience, N.Y. (1966).

89 J.W. Murray and J.G. Dillard, Geochim. Cosmochim. Acta, 43, 781 (1979).

90 M. Schnitzer and S.U. Khan, Humic Substances in the Environment, Marcel Dekker Inc., N.Y. (1972).

91 J.F. Hodgson, H.R. Geering and W.A. Norvell, Soil Sci. Soc. Amer. Proc., 29, 665 (1965).

92 J.F. Hodgson, W.L. Lindsay and J.F. Trierweiler, Soil Sci. Soc. Amer. Proc., 30, 723 (1966).

93 H.R. Geering, J.F. Hodgson and C. Sdano, Soil Sci. Soc. Amer. Proc., 33, 81 (1969).

94 F.J. Stevenson and M.S. Ardakani, In Micronutrients in Agriculture, Editors, J.J. Mortvedt, P.M. Giordano and W.L. Lindsay, Soil Sci. Soc. Amer. Proc., Inc., Wisconsin (1972).

95 S.U. Khan, Soil Sci. Soc. Amer. Proc., 33, 851 (1969).

96 M. Schnitzer and S.I.M. Skinner, Soil Sci, 96, 181 (1963).

97 M. Schnitzer, Soil Sci. Soc. Amer. Proc., 33, 75 (1969).

98 R.A. Rosell and K.L. Babcock, In Isotopes and Radiation in Soil Organic Studies. International Atomic Energy Agency, Vienna (1968).

99 Y. Takai and T. Kamura, Folia Microbioligica, 11, 304 (1966).

100 F.T. Turner and W.H. Patrick, Int. Congr. Soil Sci. Trans. 9th, Adelaide, 4, 53 (1968).

101 F.N. Ponnamperuma, Adv. Agron., 24, 29 (1972).

102 F.N. Ponnamperuma, E.M. Tianco and T. Loy, Soil Sci., 103, 374 (1967).

103 F.N. Ponnamperuma, E.M. Tianco and T. Loy, Soil Sci., 108, 48 (1969).

104 D.H. Yaalon, I. Bremner and H. Koyumdjisky, Geoderma, 12, 233 (1974).

105 J.L. Sims and W.H. Patrick, Soil Sci. Soc. Amer. Proc., 42, 258 (1978).

106 M.J. Conry and P. Ryan, Irish J. Agric. Res., 4, 61 (1965).

107 N.S. Kee and C. Bloomfield, Plant Soil, 16, 108 (1962).

108 C.N. Reddy and W.H. Patrick, Soil Sci. Soc. Amer. Proc., 41, 729 (1977).

109 R.L. Malcolm and R.J. McCracken, Soil Sci, Soc. Amer. Proc., 32, 834 (1968).

110 J.A. McKeague and J.H. Day, Can. J. Soil Sci., 46, 13 (1966).

111 O.P. Mehra and M.L. Jackson, Clays and Clay Minerals 7, 317 (1960).

112 A.S. De Endredy, Clay Minerals Bull., 29,209 (1963).

113 L.N. Aleksandrova, Soviet Soil Sci., 2, 190 (1960).

114 P.J. Viro, Soil Sci., 79, 459 (1955).

115 J.I. Wear and C.E. Evans, Soil Sci. Soc. Amer. Proc., 32, 543 (1968).

116 J.A. McKeague, J.E. Brydon and N.M. Miles, Int. Sci. Soc. Amer. Proc., 35, 33 (1971).

117 C.L. Bascomb, J. Soil Sci., 19, 251 (1968).

118 J.A. McKeague, Can. J. Soil Sci., 47, 95 (1967).

119 D.P. Franzmeier, B.F. Hajek and C.H. Simonson, Soil Sci. Soc. Amer. Proc., 29, 737 (1965).

120 F. De Coninck, Geoderma, 24, 101 (1980).

121 G. Mew and J.A. Adams, Soils of the Inangahua Depression, South Island. N.Z. Soil Bureau Report (Restricted distribution) (1972).

122 C.E. Marshall, Soil Sci. Soc. Amer. Proc., 5, 100 (1941).

123 H.H. Le Riche, Rep. Welsh Soils Disc. Group, 9, 17 (1968).

124 M.D. Sudom and R.J. St. Arnaud, Can. J. Soil Sci., 51, 385 (1971).

125 D.L. Mokma, M.L. Jackson, J.K. Syers and P.R. Stevens, N.Z. J. Sci., 16, 769 (1973).

126 P.F. Pratt and G.R. Bradford, Soil Sci. Soc. Amer. Proc., 22, 399 (1958).

127 K. Boratynski, E. Roszyk, S. Roszyk and M. Zietecka, Roczniki Gleboznawcze T. XXV, Dodatek, Warszawa, 25, 67 (1974).

128 S. Terashima, Chishitsu Chosasho Geppo, 29, 401 (1978).

130 P.G. Jeffery, Chemical Methods of Rock Analysis, 2nd Ed., Pergamon Press, Oxford (1975).

131 A.F. Bosch, R.F. Bosch and V. Hernandez, Quim. Anal., 30, 399 (1976).

132 B.G. Russell, J.D. Spangenberg and T.W. Steele, Talanta, 16, 487 (1969).

133 Z. Sulcek, P. Povondra and J. Dolezal, Critical Reviews in Analytical Chemistry, 6, 255 (1977).

134 J.C. Van Loon and C.M. Parissis, Analyst, 94, 1057 (1969).

135 S.H. Omang, Anal. Chim. Acta, 46, 225 (1969).

136 N.H. Suhr and C.O. Ingamells, Anal. Chem., 38, 730 (1966).

137 J.H. Medlin, N.H. Suhr and J.B. Bodkin, Atomic Absorption Newsletter, 8, 25 (1969).

138 F. Barredo and L. Diez, Talanta, 23, 859 (1976).

139 I.A. Voinovitch, Bull. Liaison Lab. Pont Chaussees, 79, 81 (1975).

140 E. Jeanroy, Analuysis, 2, 703 (1974).

141 J. Saavedra, A.G. Sanchez and S.R. Perez, Chem. Geol., 13, 135 (1974).

142 F.J. Langmyhr, Anal. Chim. Acta, 39, 516 (1967).

143 B. Bernas, Anal. Chem., 40, 1682 (1968).

144 F.J. Langmyhr and P.E. Paus, Anal. Chim. Acta, 43, 397 (1968).

145 R. Sanzolone, T. Chao and G. Grenshaw, Anal. Chim. Acta, 105, 247 (1979).

146 F. Al-Kufaishi, Bull Coll. Sci. Univ. Baghdad, 16, 339 (1975).

147 D.E. Buckley and R.E. Cranston, Chem. Geol., 7, 273 (1971).

148 G.F. Smith, Analyst, 80, 16 (1955).

149 A.N. Finn and J.F. Klekotka, J. Res. Natl. Bur. Std., 4, 809 (1930).

150 J.A. Maxwell, Rock and Mineral Analysis, Interscience Pub., N.Y. (1968).

151 J.J. La Brecque, Chem. Geol., 26, 321 (1979).

152 F.J. Langmyhr and S. Sveen, Anal. Chim. Acta, 32, 1 (1965).

153 M.C. Ball and A.H. Norbury, Physical Data for Inorganic Chemists, Longman, London (1974).

154 W.E. Dasent, Inorganic Energetics, Penguin Books, England (1970).

155 A.F. Wells, Structural Inorganic Chemistry, Clarendon Press, Oxford (1962).

156 S. Abbey, X-Ray Spectrometry, 7, 99 (1978).

157 J. Zussman, Physical Methods in Determinative Mineralogy, 2nd Ed., Academic Press (1977).

158 S.D. Weaver, Pers. Comm. (1982).

159 Varian Techtron, Analytical Methods for Flame Spectroscopy, Manual.

160 T. Joyner and J.S. Finley, Atomic Absorption Newsletter, 5, 4 (1966).

161 E.A. Jenne, J.W. Ball and C. Simpson, J. Environ. Qual., 3, 281 (1974).

162 F.J. Langmyhr, Abst. Fifth Int. Conf. on Atomic Spectroscopy, Melbourne, A, 23 (1975).

163 K. Fletcher, Econ. Geol., 65, 588 (1970).

164 M. Mitsuchi, Soil Sci. Pt. Nutr., 22, 409 (1976).

165 T.A. Sokolova and R.N. Polteva, Int. Congr. Soil Sci. Trans., 9th, Adelaide, 4, 459 (1968).

166 P.S. Sidhu, J.L. Sehgal, M.K. Sinha and N.S. Randhawa, Geoderma, 18, 241 (1977).

167 U. Schwertmann and D.S. Fanning, Soil Sci. Soc. Amer. Proc., 40, 731 (1976).

168 W.P. Phillippe, R.L. Blevins, R.I. Barnhisel and H.H. Bailey, Soil Sci. Soc. Amer. Proc., 36, 171 (1972).

169 F.R. Zaydel'man and A.K. Ogleznev, Soviet Soil Sci., 3, 619 (1971).

170 M. Drosdoff and C.C. Nikiforoff, Soil Sci., 49, 333 (1940).

171 R.M. McKenzie, Geoderma, 8, 29 (1972).

172 R.M. McKenzie, Technical Memorandum 16/74, C.S.I.R.O., Division of Soils, Adelaide (1974).

173 R.M. McKenzie, Aust. J. Soil Res., 13, 177 (1975).

174 S. Pawluk, Can. J. Soil Sci., 52, 119 (1972).

175 J.A. McKeague, M. Schnitzer and P.K. Heringa, Can. J. Soil Sci., 47, 23 (1967).

176 C. Bloomfield, J. Soil Sci., 4, 5 (1953).

177 C. Bloomfield, J. Soil Sci., 6, 284 (1955).

178 D.V. Crawford, Trans. 6th Int. Congr. Soil Sci., C, 197 (1956).

179 R.D. Reeves and R.R. Brooks, Trace Element Analysis of Geological Materials, John Wiley and Sons (1978).

180 D.J. Murray, T.W. Healy and D.W. Fuerstenau, Adv. Chem. Ser., 79, 74 (1968).

181 V.M. Goldschmidt, Geochemistry, Clarendon Press, Oxford (1954).

182 R.M. Taylor and J.B. Giles, J. Soil Sci., 21, 203 (1970).

183 Soils of New Zealand, N.Z. Soil Bur. Bull., 26, 1 (1968).

184 B.S. Kear, H.S. Gibbs and R.B. Miller, N.Z. Soil Bur. Bull., 14 (1967).

185 General Survey of the Soils of the South Island, New Zealand, Soil Bur. Bull., 27 (1968).

186 W.T. Ward, C.S. Harris and H.P. Schapper, N.Z. Soil Bur. Bull., 21 (1964).

187 A.W. Sheat, M.Sc. Thesis, University of Canterbury, New Zealand (1977).

188 K.W. Perrott, Geoderma, 17, 219 (1977).

189 D.A. Skoog and D.M. West, Principles of Instrumental Analysis, Holt, Rinehart and Winston Inc., N.Y. (1971).

190 B.R. Culver and T. Surles, Anal. Chem., 47, 920 (1975).

191 Burroughs B6700 S.P.S.S.: Statistical Package for the Social Sciences, User's Manual, Davis, California (1972).

192 C.R.C. Handbook of Chemistry and Physics, 60th Ed., C.R.C. Press, Florida (1979).

193 R. Jenkins and J.L. De Vries, Practical X-Ray Spectrometry, Eindhoven, The Netherlands (1967).

194 D.E. Sands, Introduction to Crystallography, W.A. Benjamin Inc., N.Y. (1969).

195 W.J. Moore, Physical Chemistry, 5th Ed., Longman, London (1972).

196 J.E. Townsend, Appl. Spectrosc., 17, 37 (1963).

197 I.B. Brenner, L. Argov and H. Eldad, Appl. Spectrosc., 29, 423 (1975).

198 J.W. Colby, Magic IV. A computer program for quantitative electron microprobe analysis. Bell Telephone Lab. Inc., Allenton, Pennsylvania (1967).

199 K. Norrish, Pers. Comm. (1978).

200 J.H. Toe and A.R. Armstrong, Anal. Chem., 19 100 (1947).